Fondazione IRCCS Policlinico San Matteo

UNIVERSITÀ DI PAVIA

Fondazione IRCCS Policlinico San Matteo
Università degli Studi di Pavia
May 8th, 2023

Chronic Lymphocytic Leukemia: A Journey from basic immunology to target therapies

Paolo Ghia

-

B cell Neoplasia Unit and
Strategic Research Program in CLL

OSPEDALE SAN RAFFAELE

UNIVERSITÀ VITA-SALUTE SAN RAFFAELE
UniSR
QUID EST HOMO?

Disclosures: Paolo Ghia

Company name	Research support	Employee	Consultant	Stockholder	Speakers bureau	Advisory board	Other
AstraZeneca	x		x			x	
AbbVie	x		x			x	
MSD			x			x	
BeiGene			x			x	
BMS	x		x			x	
Janssen	x		x			x	
Lilly/Loxo			x			x	
Roche			x			x	

From immunology to target therapy

CLL240

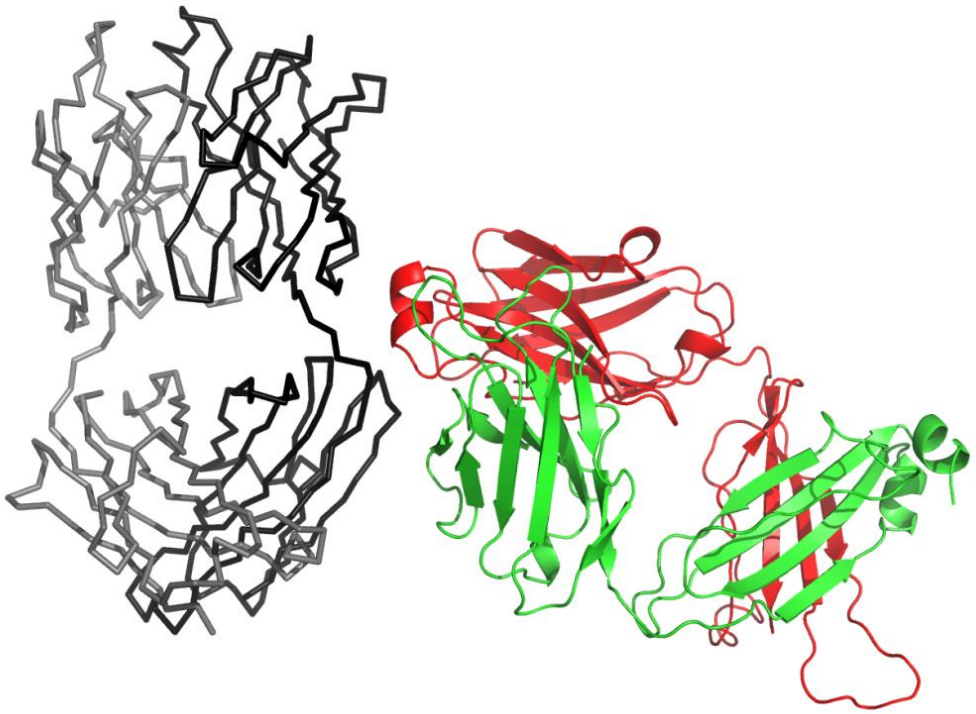

A

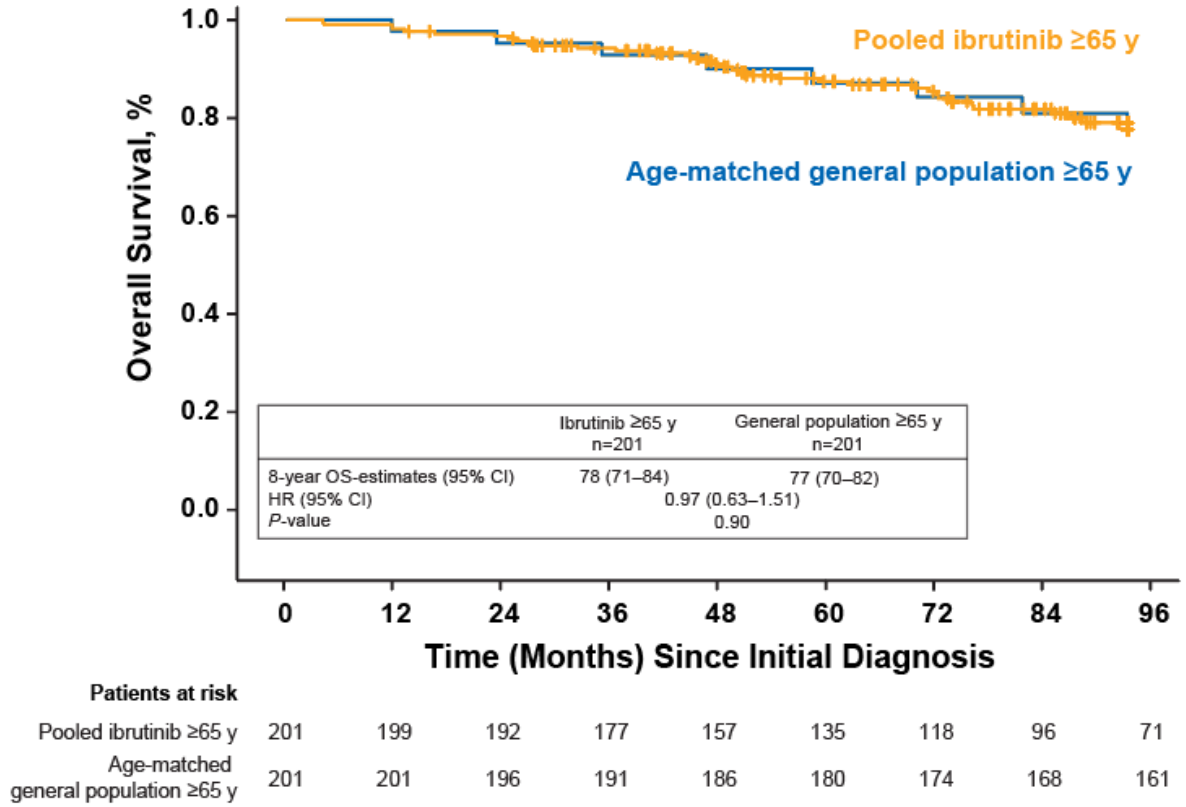

Median follow-up of 6.8 years

Minici C, Gounari M et al, Nature Comm 2017

Ghia et al., ASH 2022 (New Orleans)

A long path to CLL

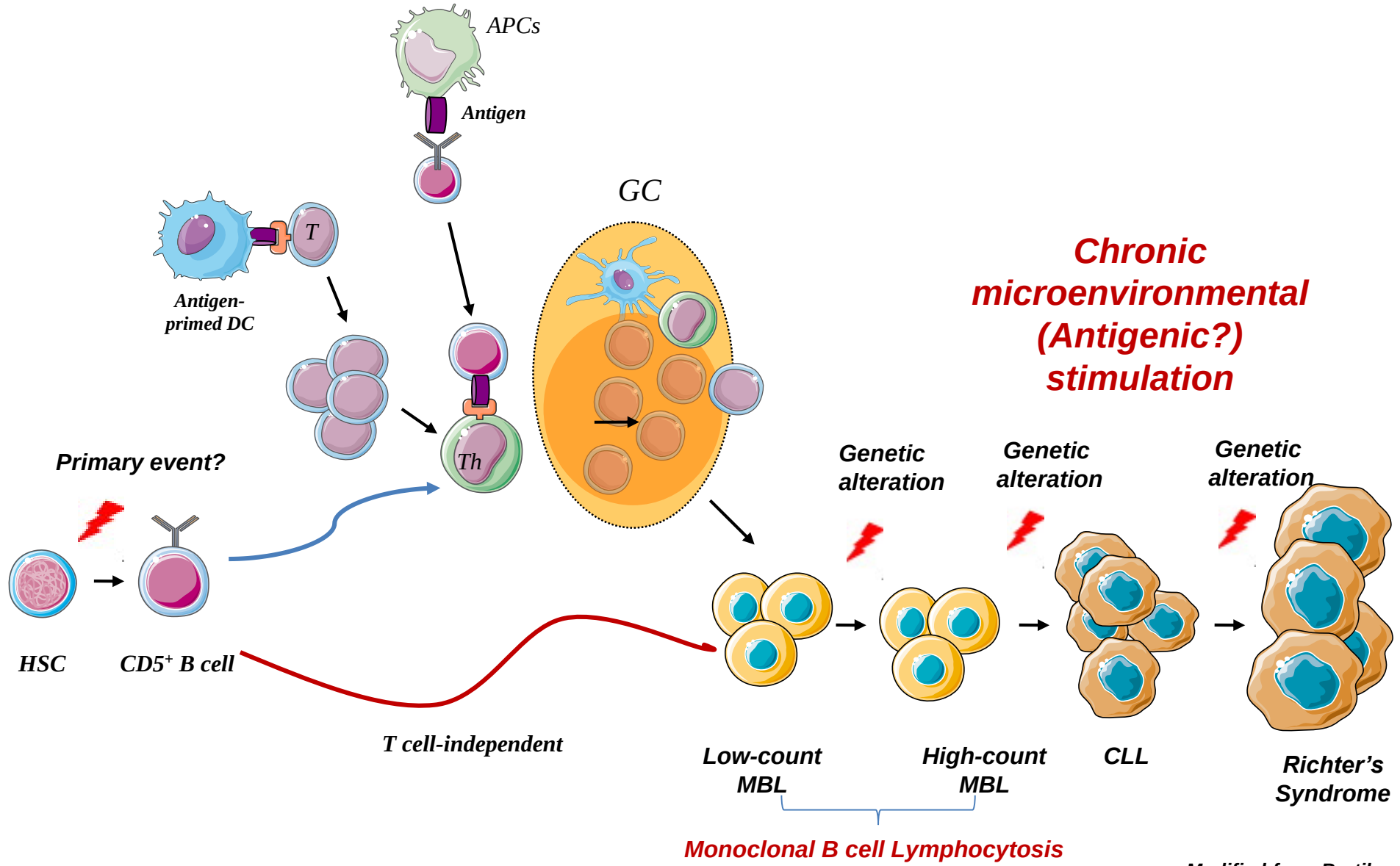

Modified from Bertilaccio et al., Leukemia 2013

Genetic aberrations in the pathogenesis of CLL

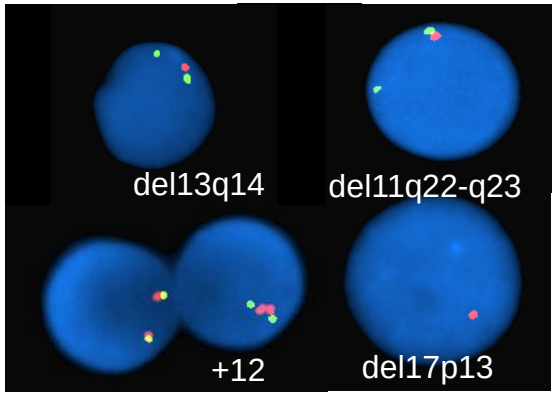

Aberration	Incidence (%)	Median OS (mo)
17p del	3-7	32
11q del	11-25	79
+12	10-16	114
Normal	18-22	111
13q del	33-44	133

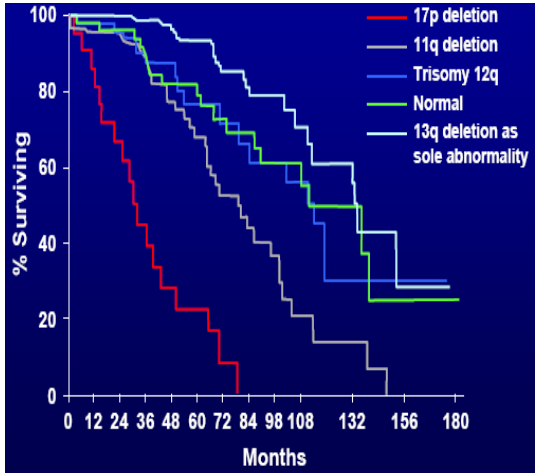

Döhner, New Engl J Med 2000

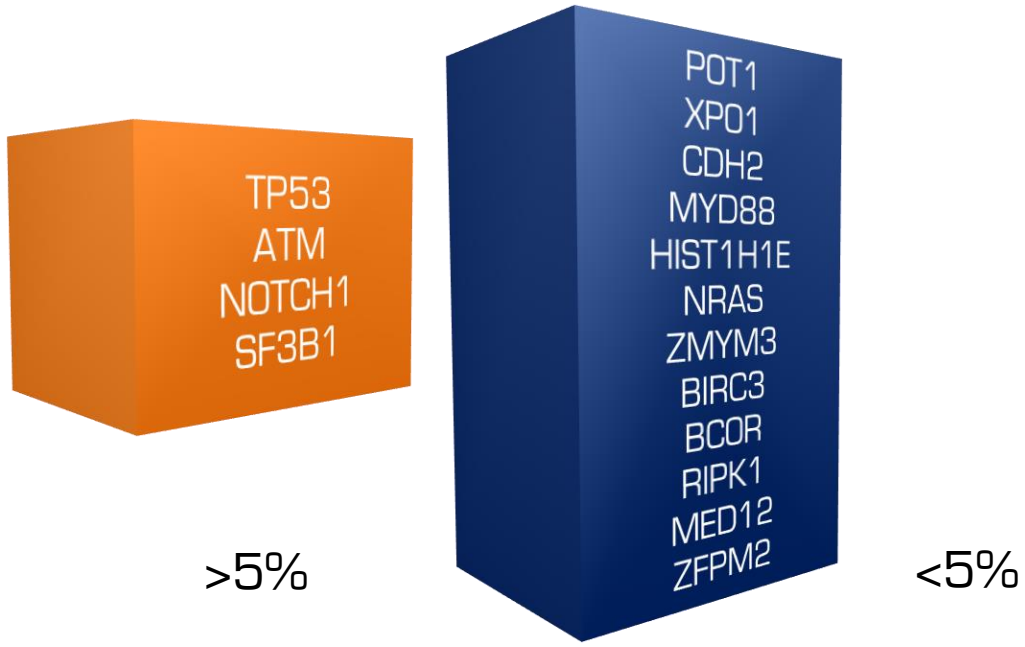

Fabbri, J Exp Med 2011; Puente, Nature 2011; Rossi, Blood 2011 & 2012; Quesada, Nat Genet 2011; Wang, NEngl J Med 2011, Puente, Nature 2015

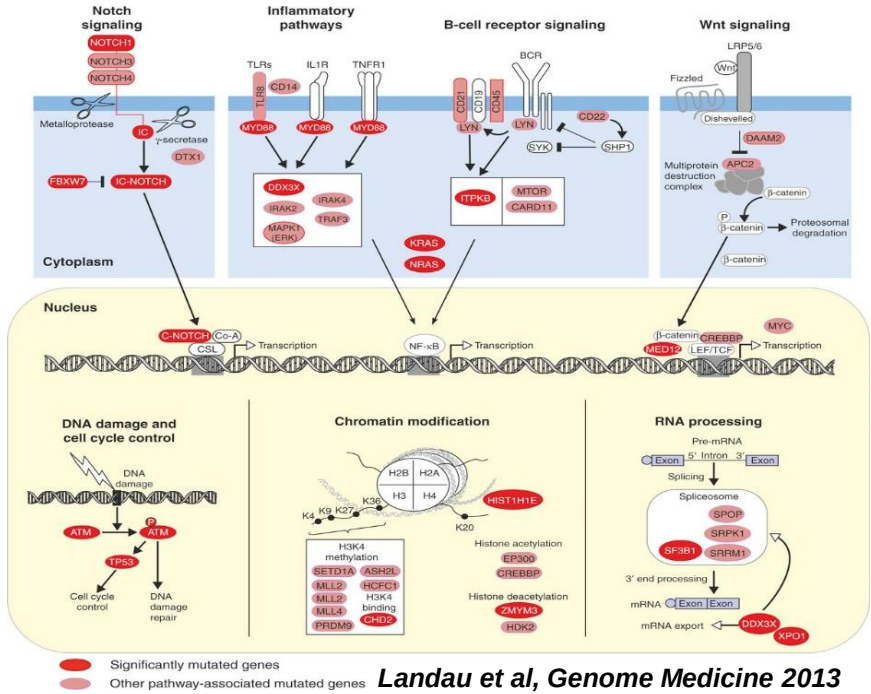

Landau et al, Genome Medicine 2013

LC-MBL, HC-MBL, Ultrastable CLL have similar genetic complexity

Somatic variants

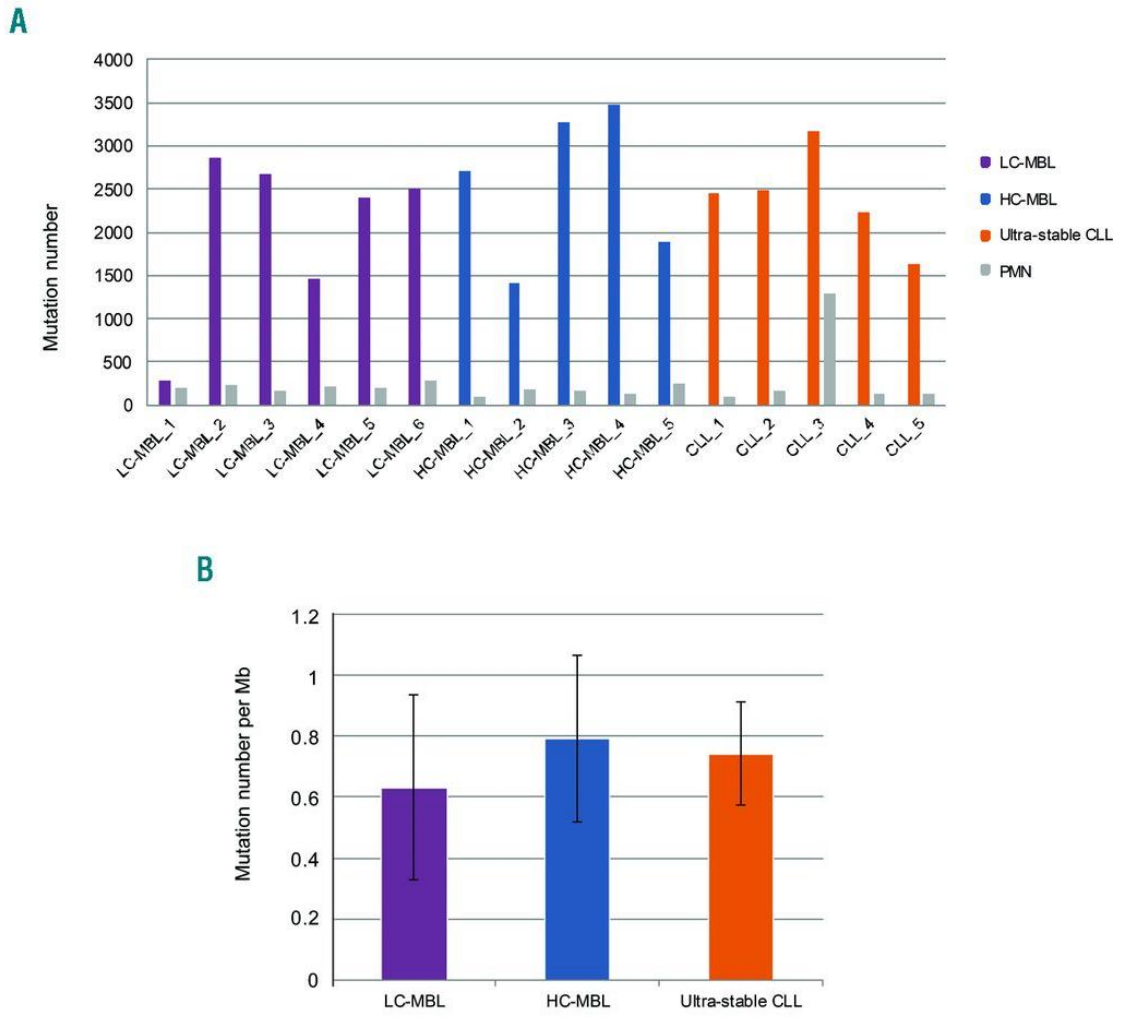

Exonic mutations

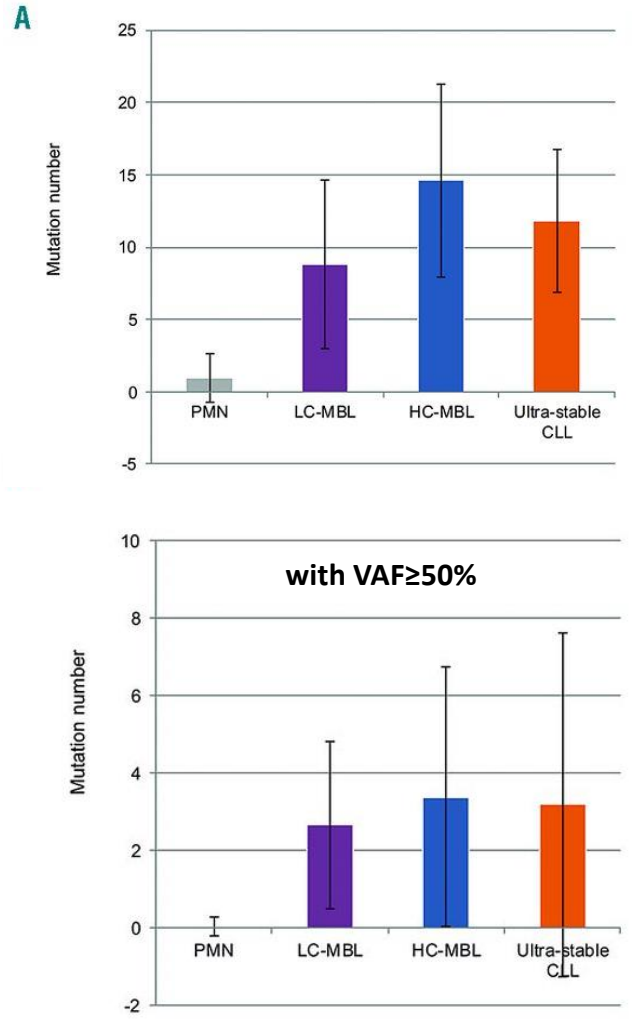

Agathangelidis A et al, *Agathangelidis A et al, Haematologica 2018*

Recurrent chromosomal aberrations by FISH

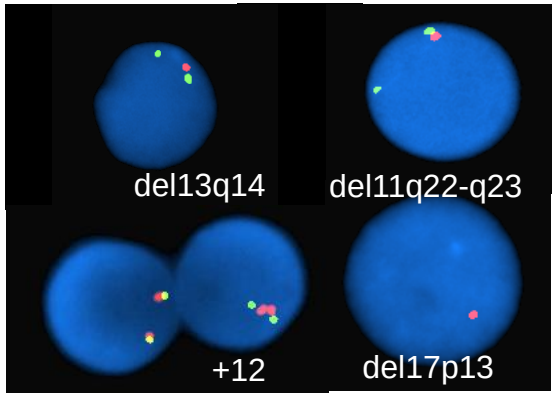

Aberration	Incidence (%)	Median OS (mo)
17p del	3-7	32
11q del	11-25	79
+12	10-16	114
Normal	18-22	111
13q del	33-44	133

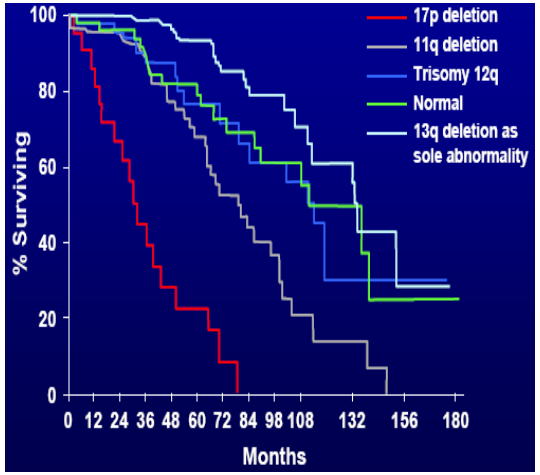

Döhner, New Engl J Med 2000

Chromosome 13

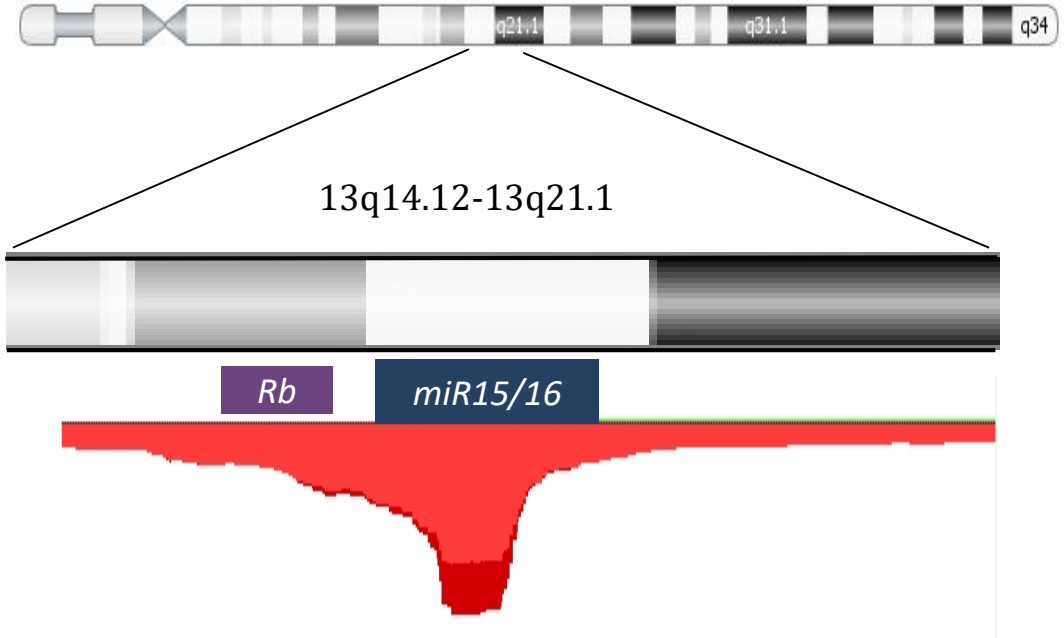

Kind courtesy of R. Rosenquist

del(13q) in CLL natural history

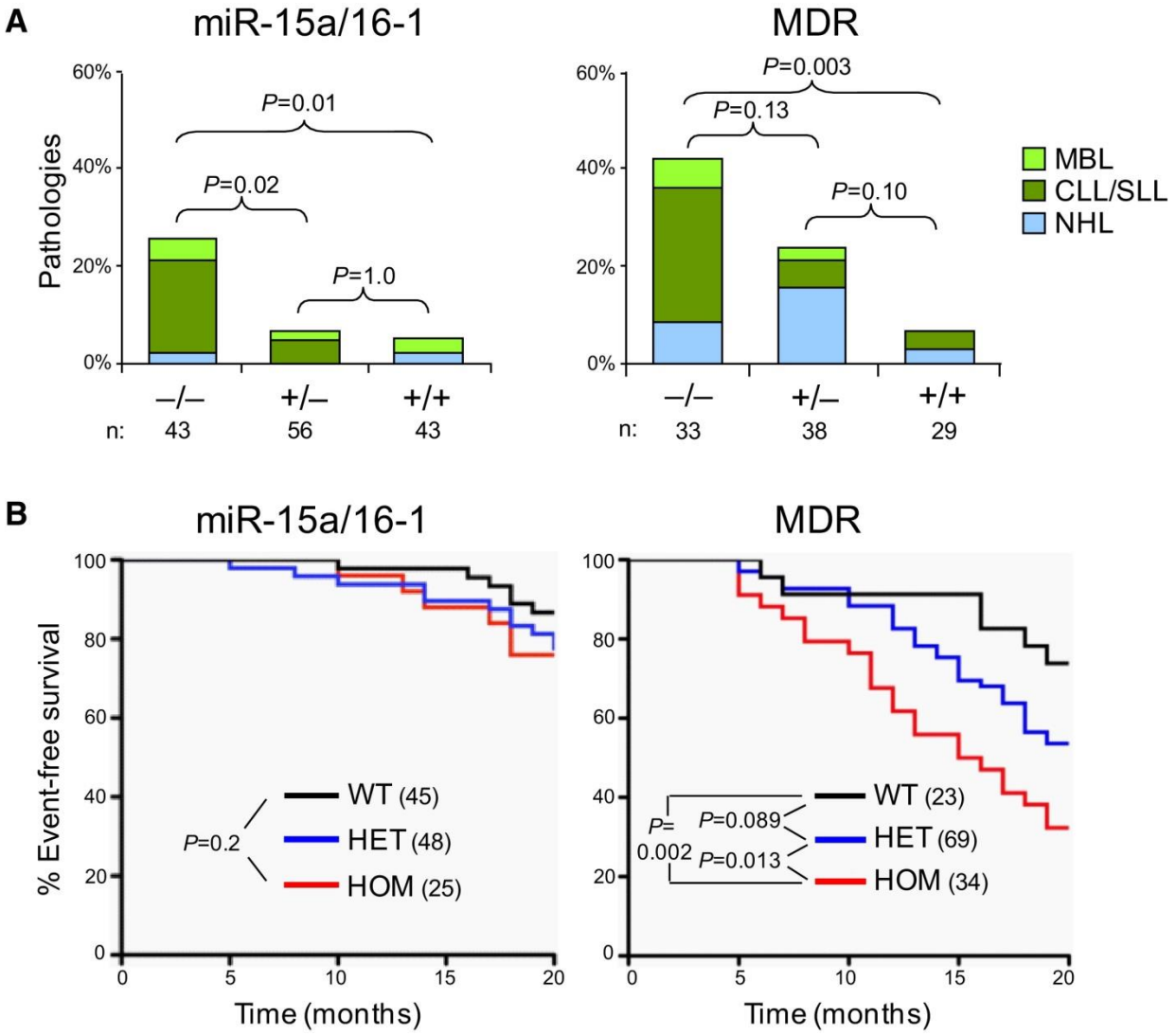

Klein et al, Cancer cell, 2010

CLL: a disease of B cells dependent on the microenvironment

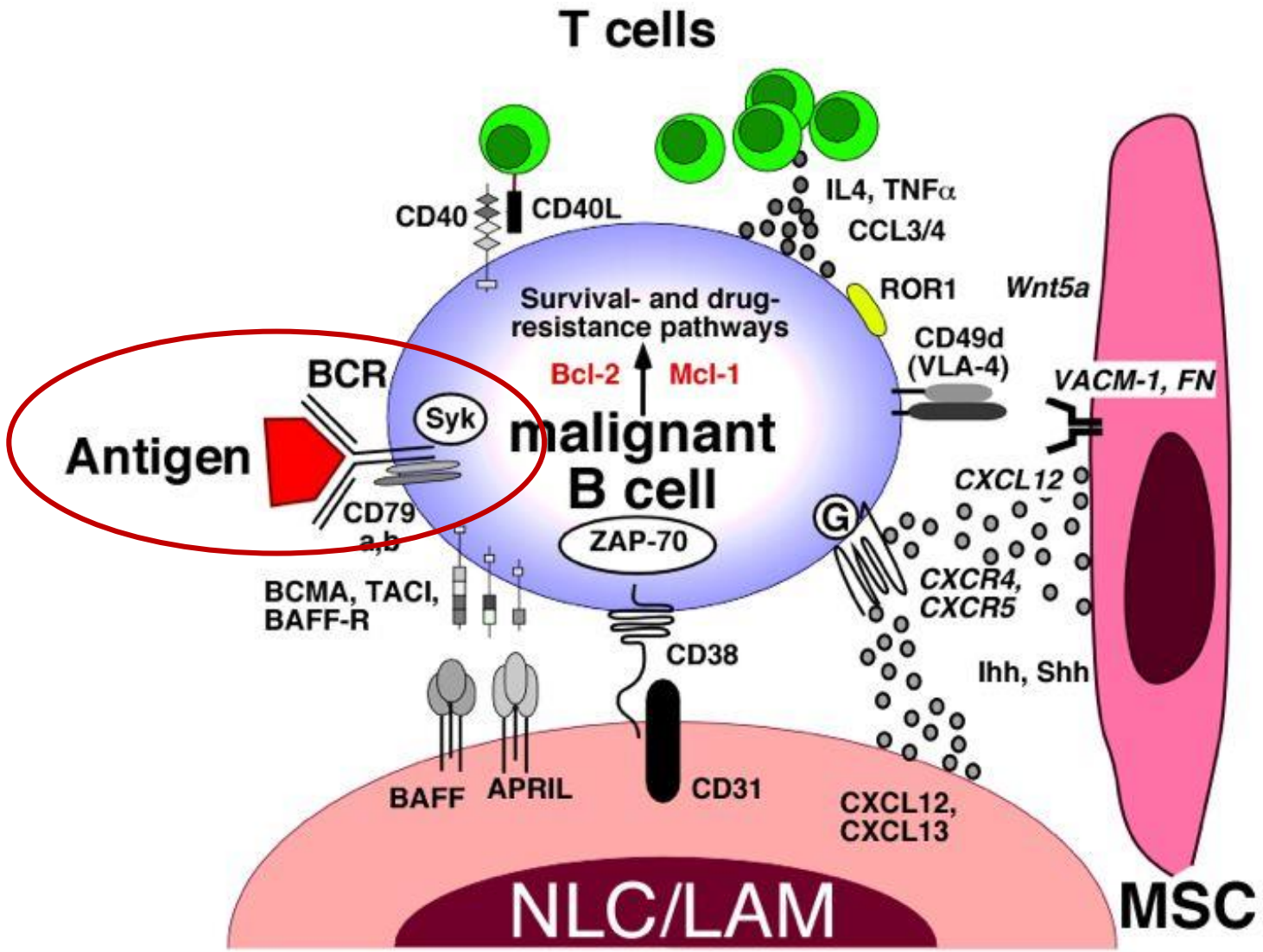

Burger, Ghia et al, Blood, 2009

Several signals for one B cell

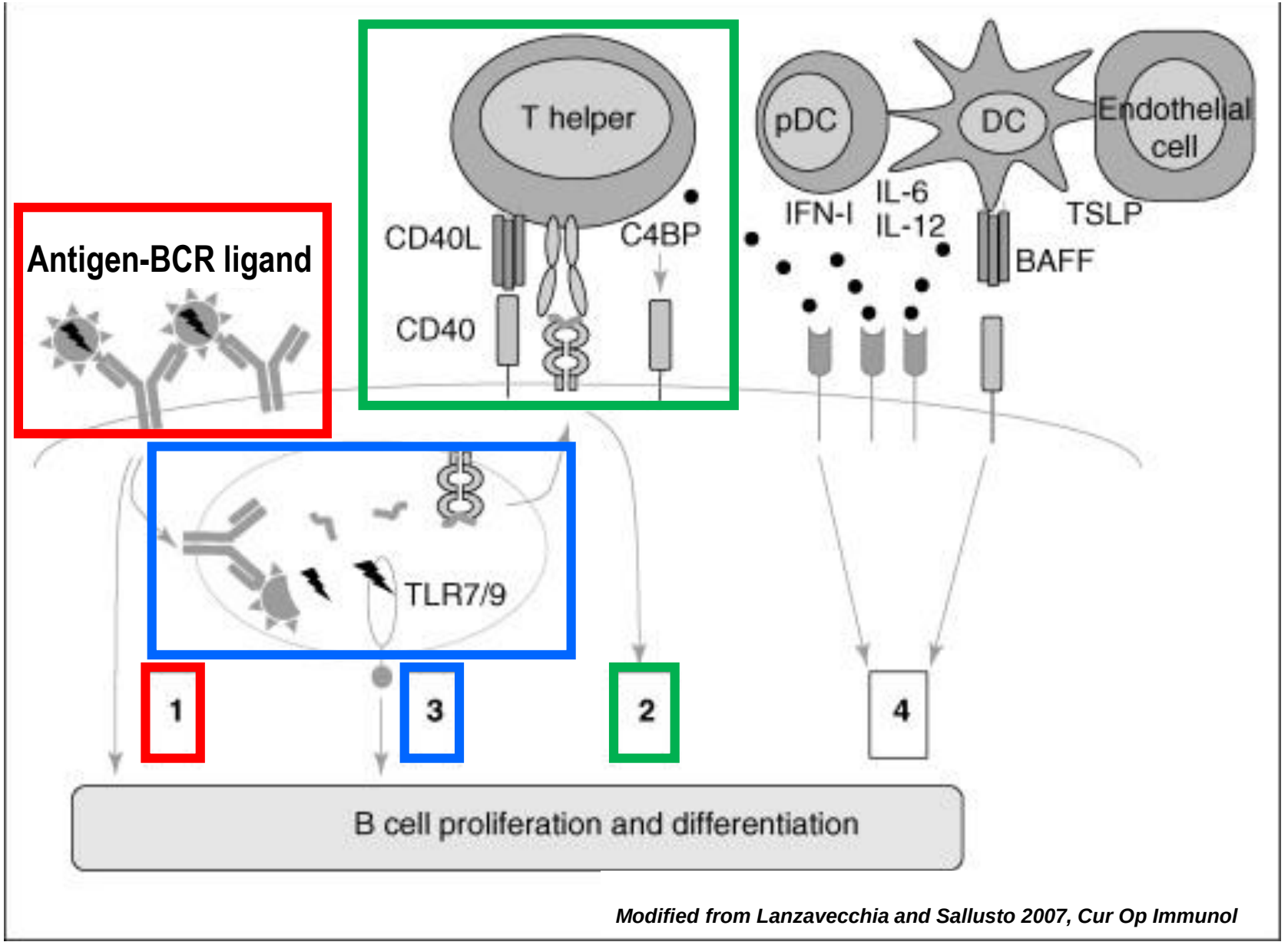

Modified from Lanzavecchia and Sallusto 2007, Cur Op Immunol

T cells in CLL tissues

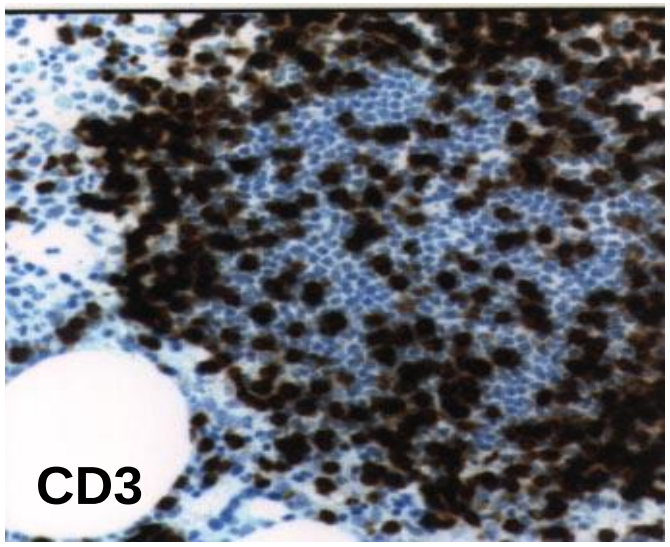

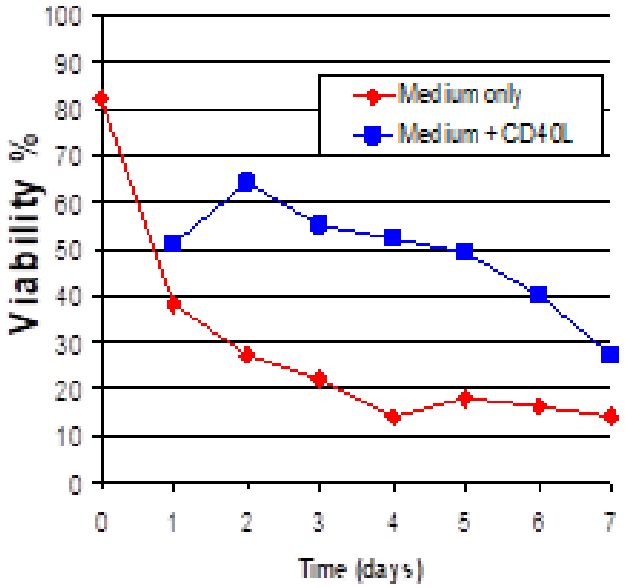

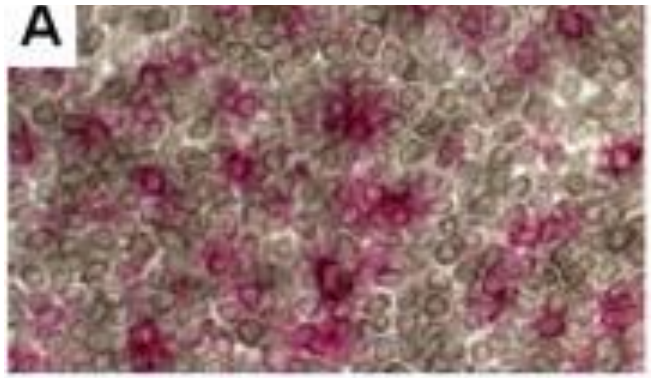

CD4 (red)

CD23 (brown)

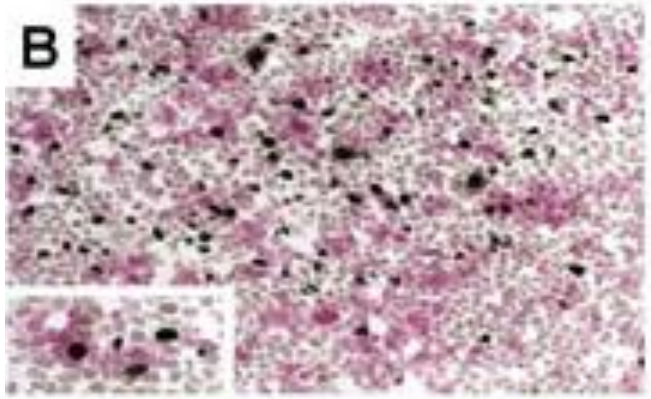

CD4 (red)

Ki67 (brown)

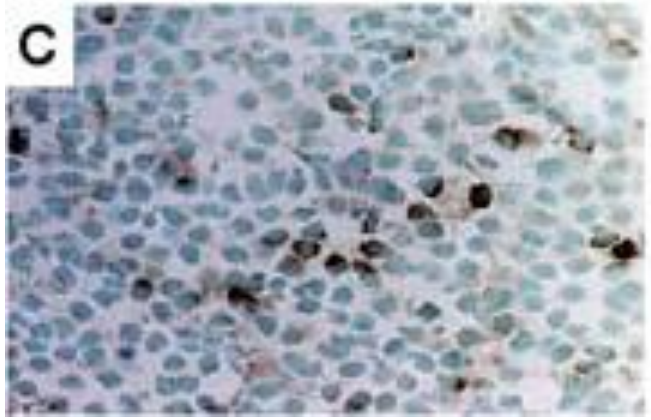

CD40L

Granziero et al, 2001; Ghia et al, 2002; Granziero et al, 2003

Is CD40:CD40L interaction inducing CLL survival?

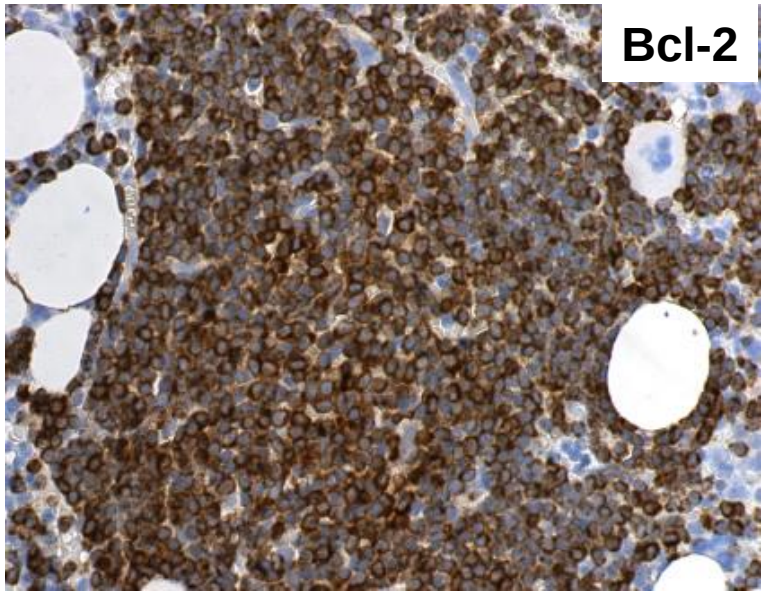

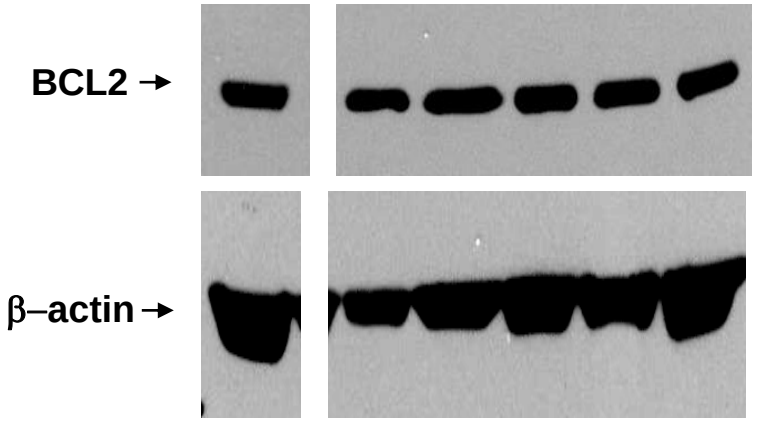

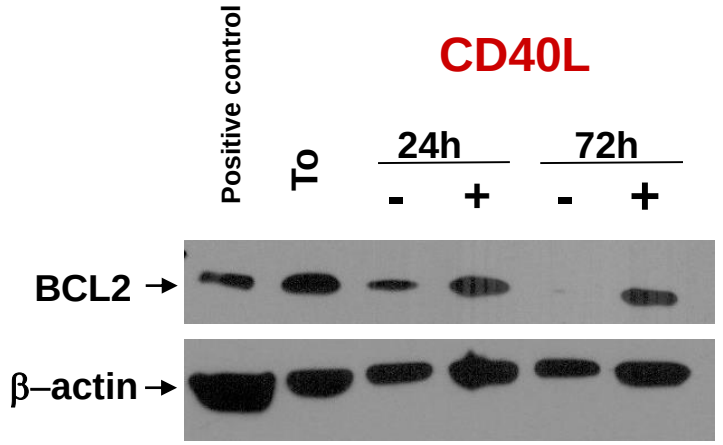

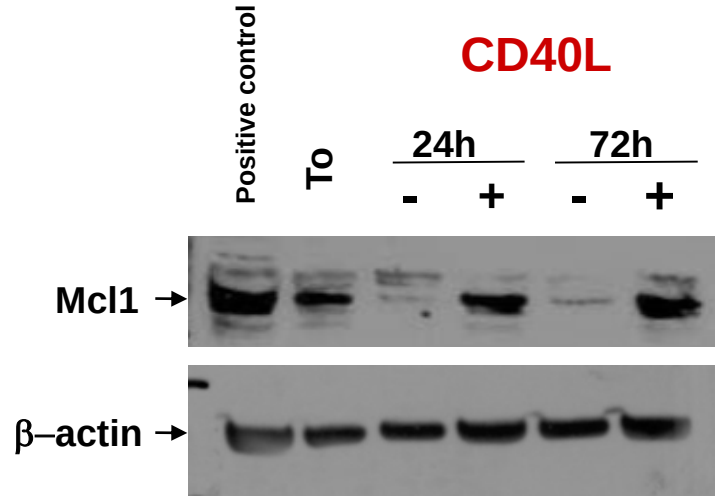

Hanada M et al, Blood 1993, Kitada S et al, Blood 1998

Scielzo et al, Leukemia 2011, Fonte t al, Clin Can Res, 2013

Role of CD4⁺ T cells in CLL development *in vivo*

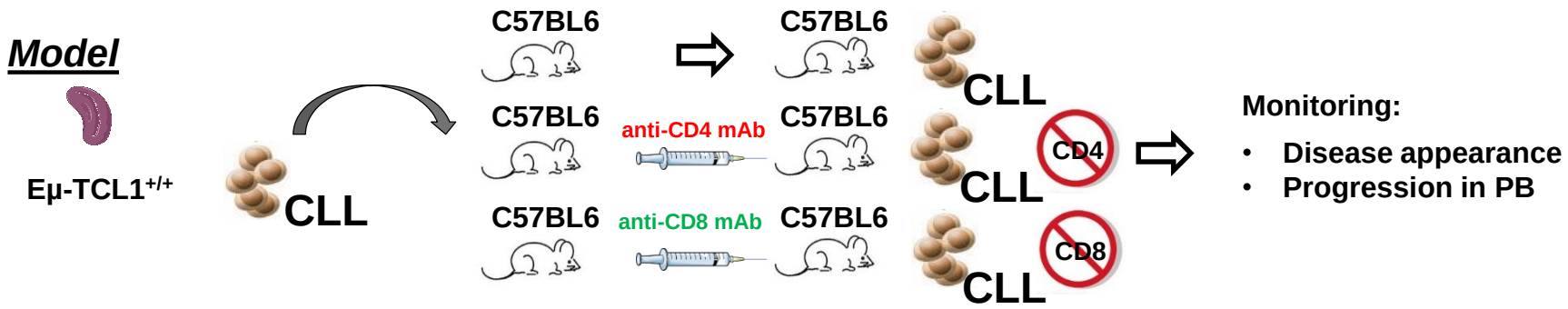

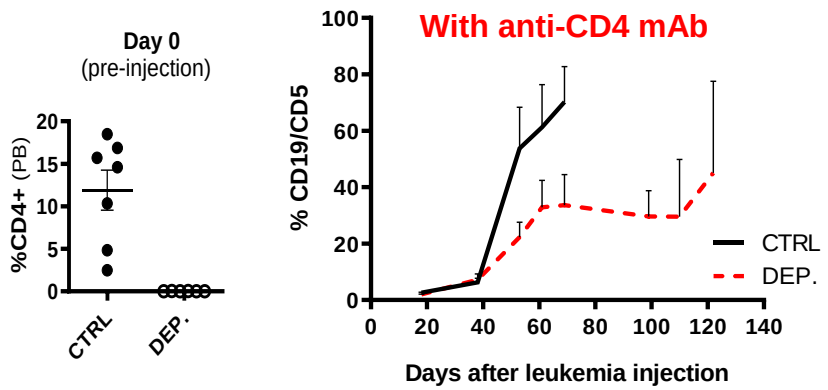

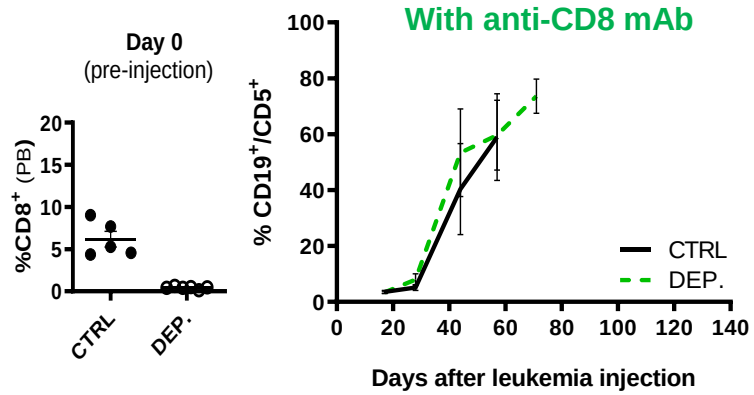

✓ CLL clones do not expand in mice depleted of CD4⁺ T cells but develop normally in mice depleted of CD8⁺ T cells

Grioni M et al, Blood Adv. 2021

Role of CD40/CD40L interactions in CLL *in vivo*

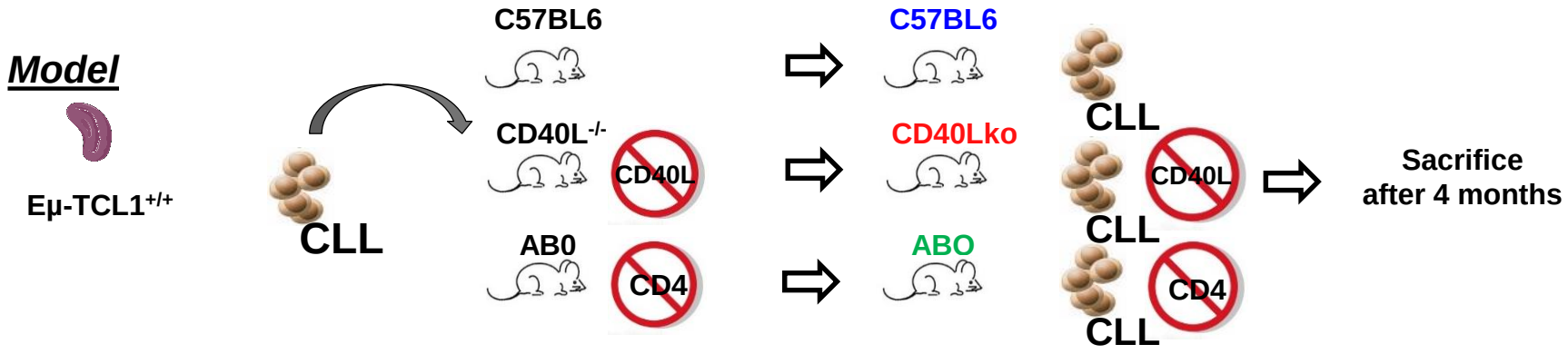

CLL engraftment at Sacrifice (4 months)

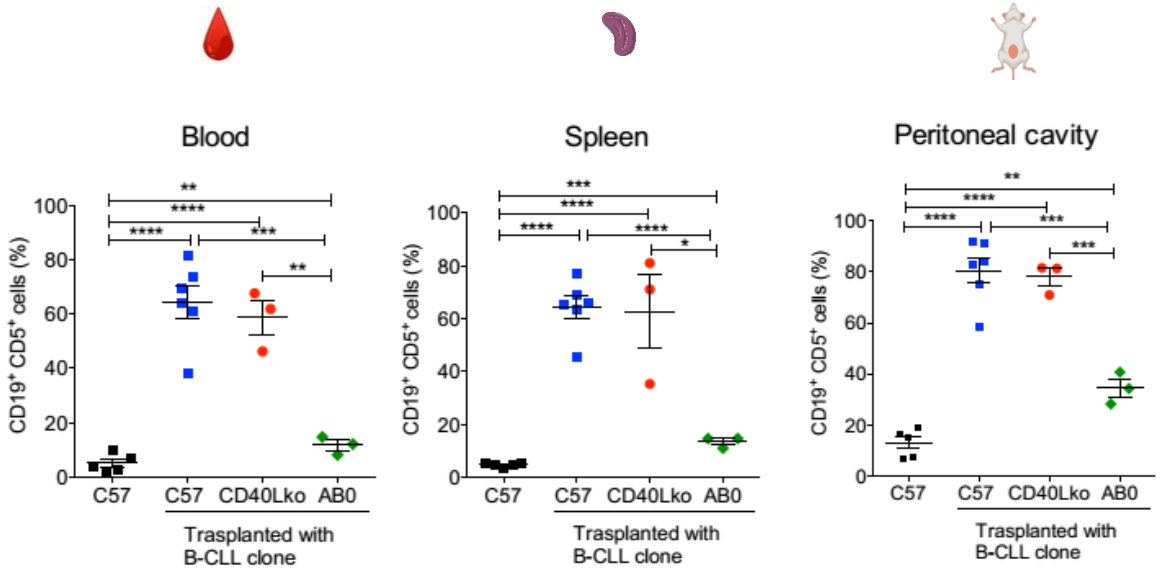

✓ **CD40/CD40L stimulation is dispensable for *in vivo* CLL expansion**

Grioni M et al, Blood Adv. 2021

Role of CD40/CD40L interactions in CLL *in vivo*

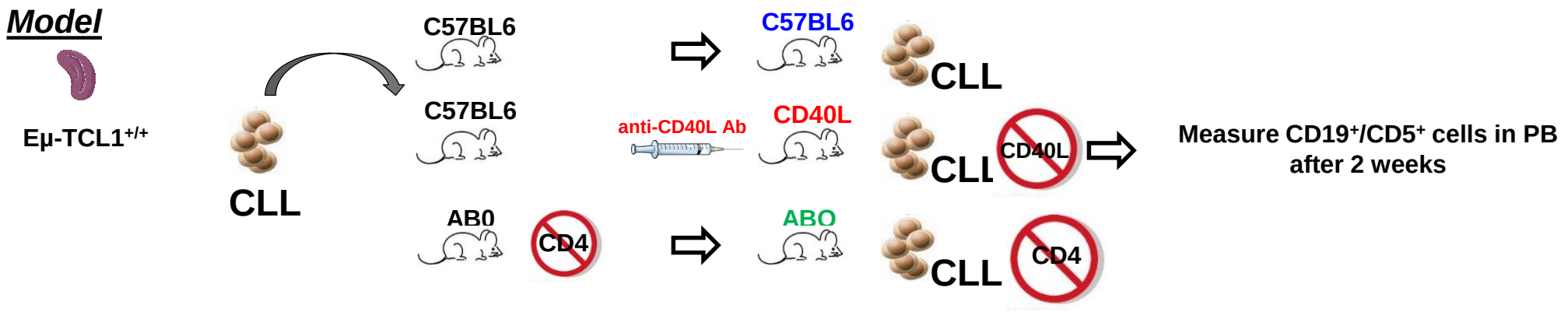

Engraftment in the after 2 weeks

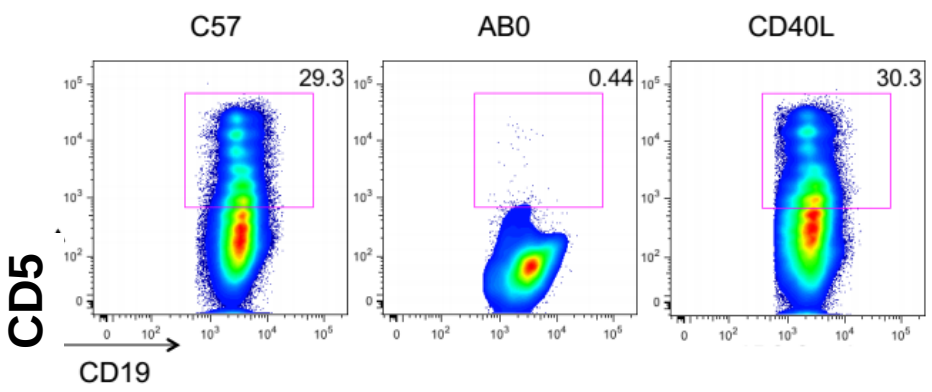

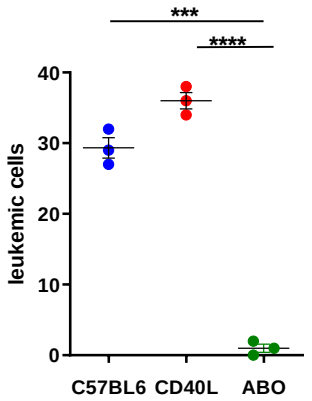

✓ CD40/CD40L stimulation is dispensable for *in vivo* CLL expansion

Grioni M et al, Blood Adv. 2021

B-T cooperation in proliferation centers

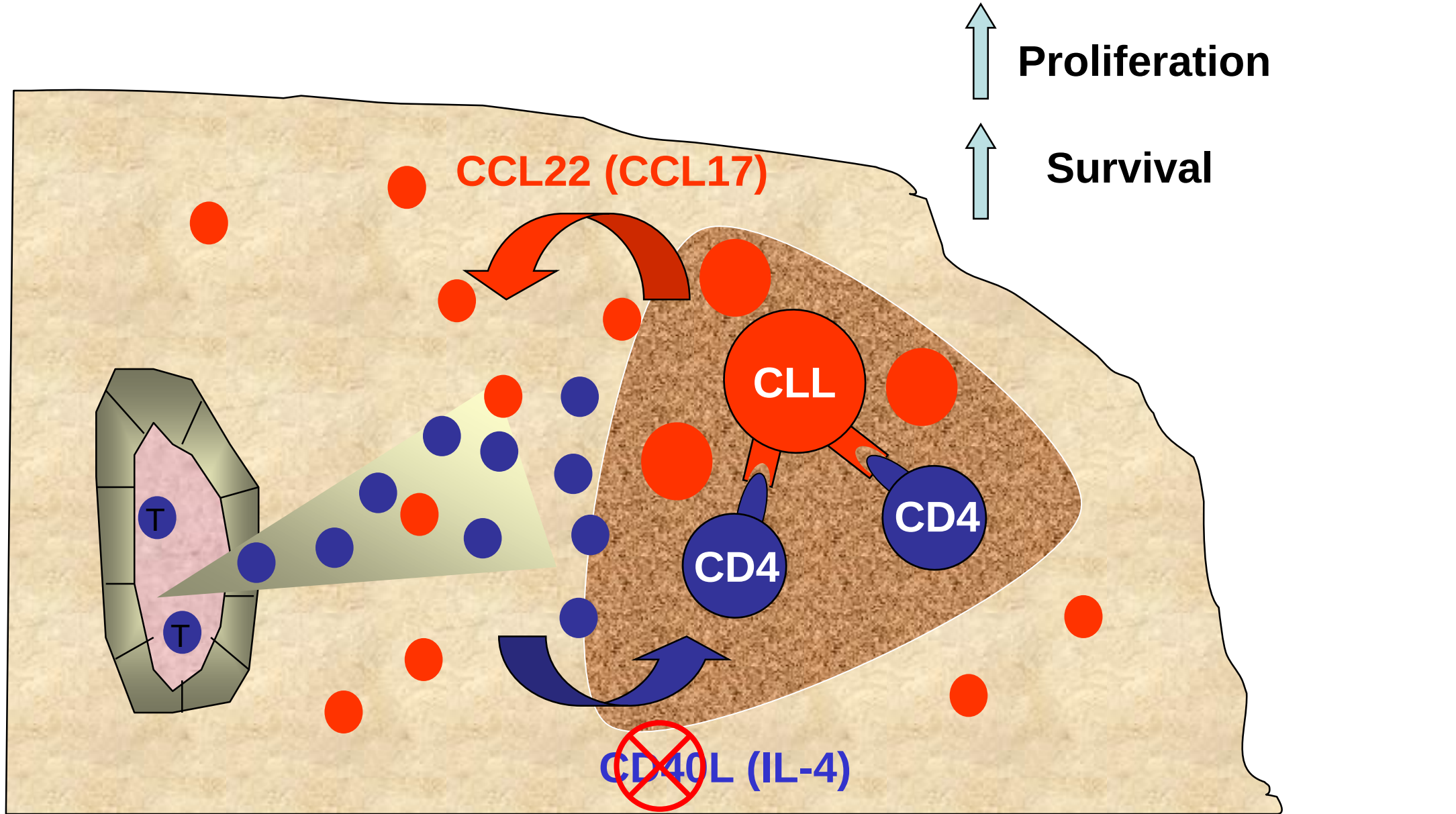

Proliferating CLL cells *in vivo*

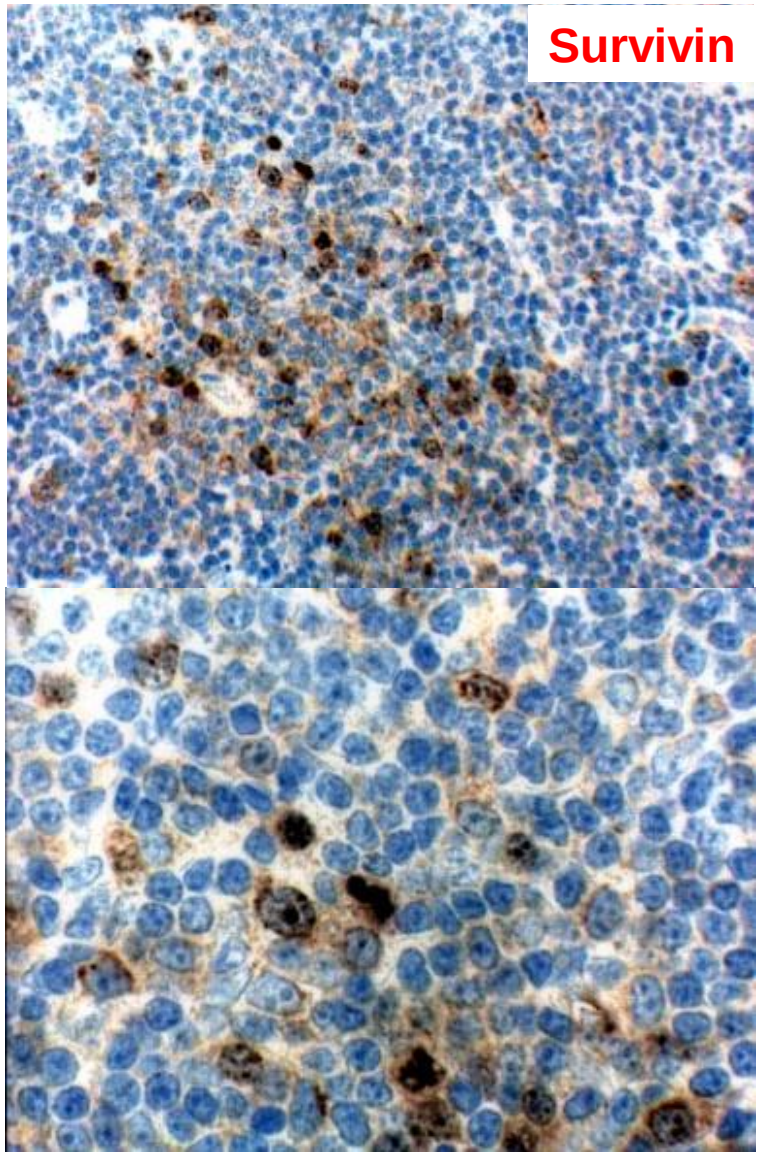

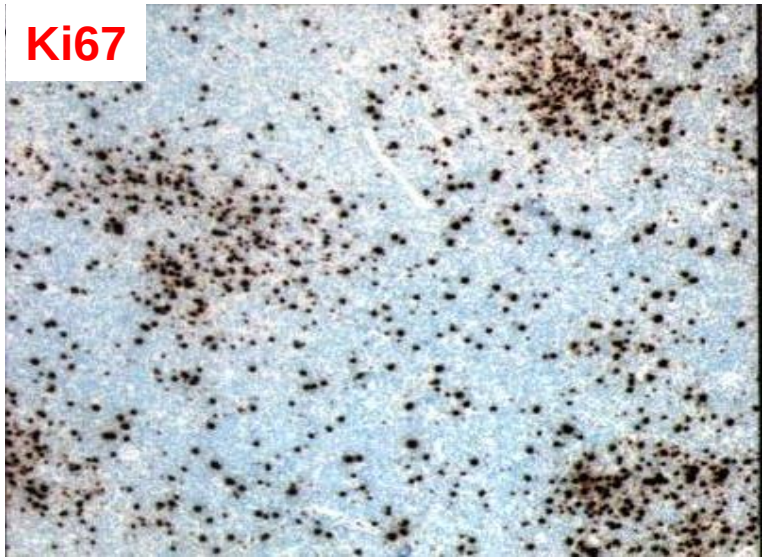

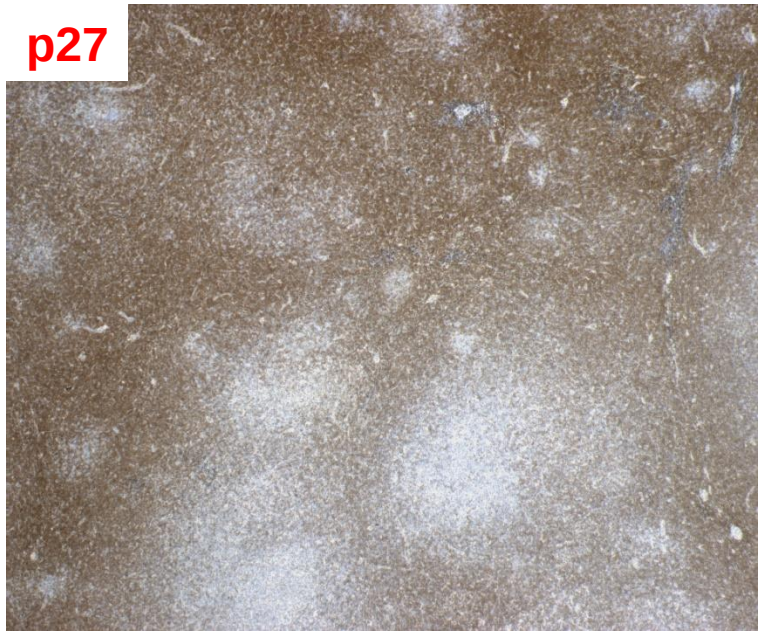

Granziero et al, Blood, 2001

p27 is modulated by CpG

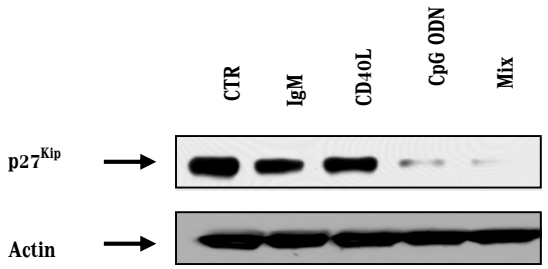

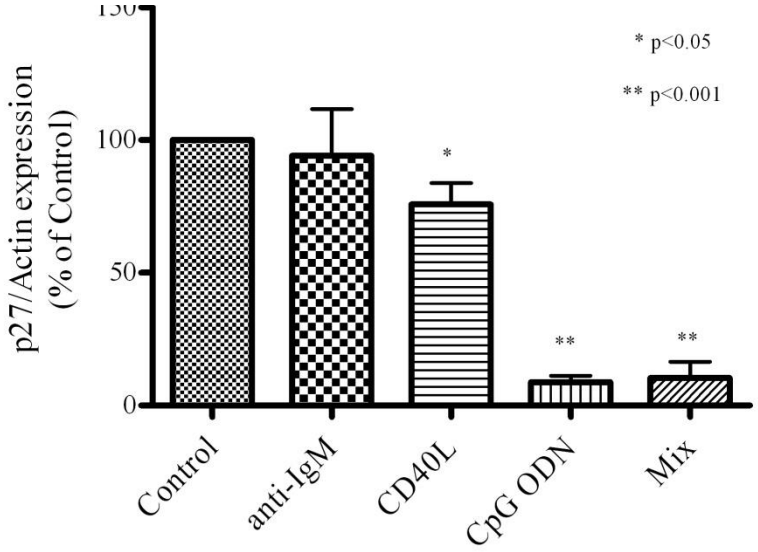

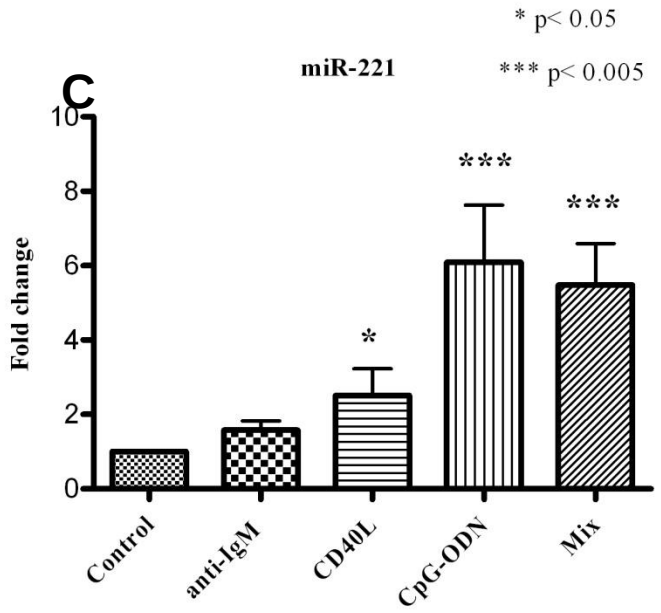

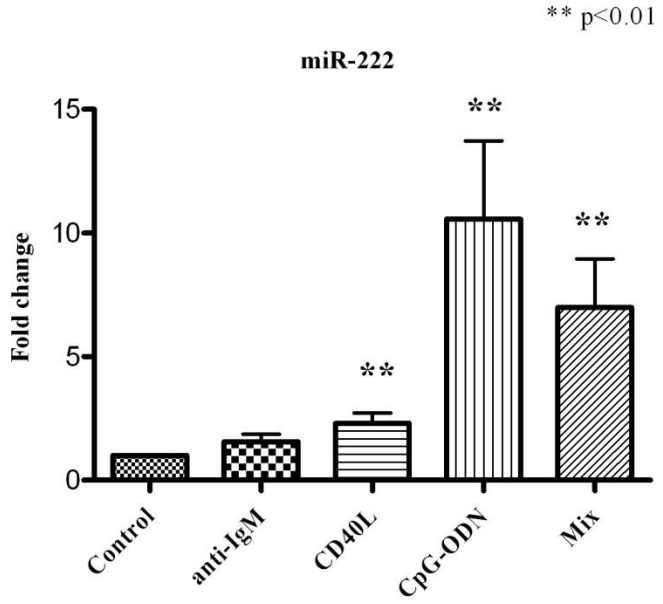

Frenquelli et al, Blood 2010

Several signals for one B cell

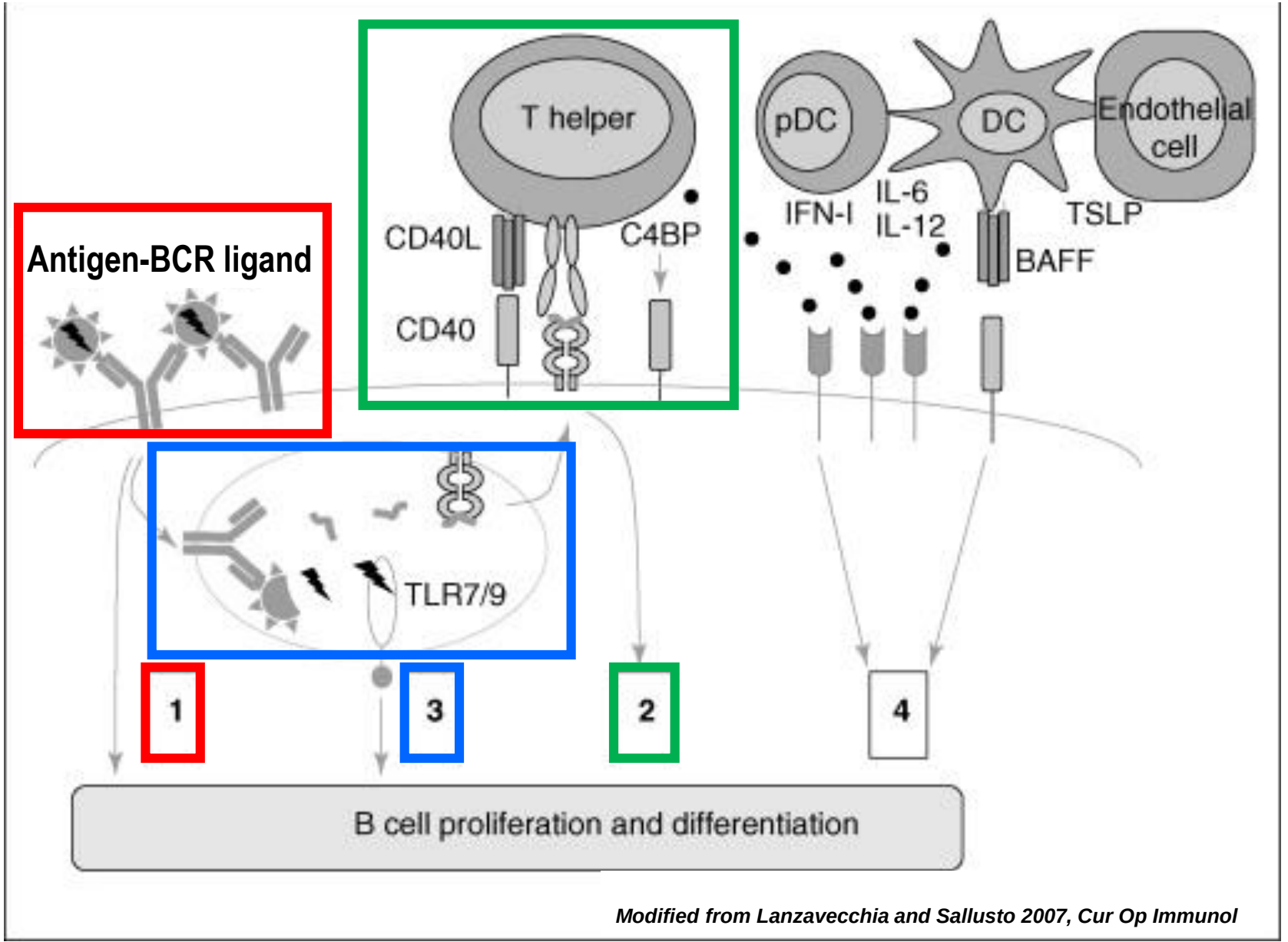

Modified from Lanzavecchia and Sallusto 2007, Cur Op Immunol

TLRs stimulation protects from apoptosis and triggers cell cycle entry

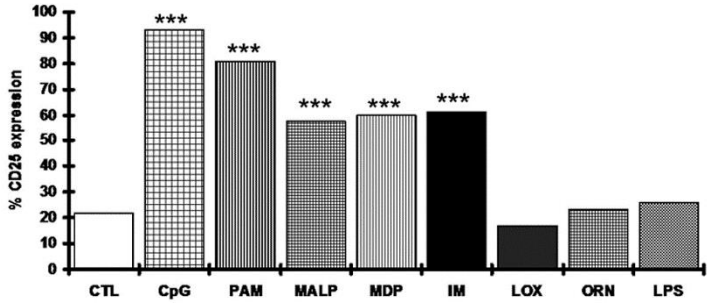

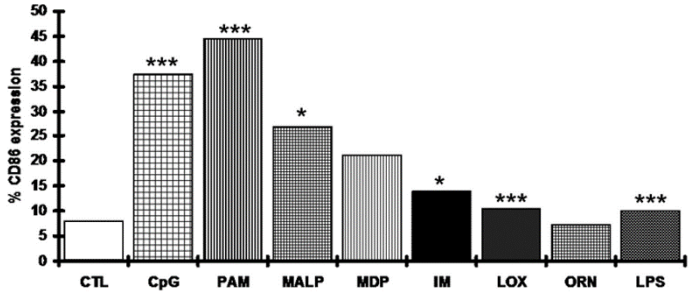

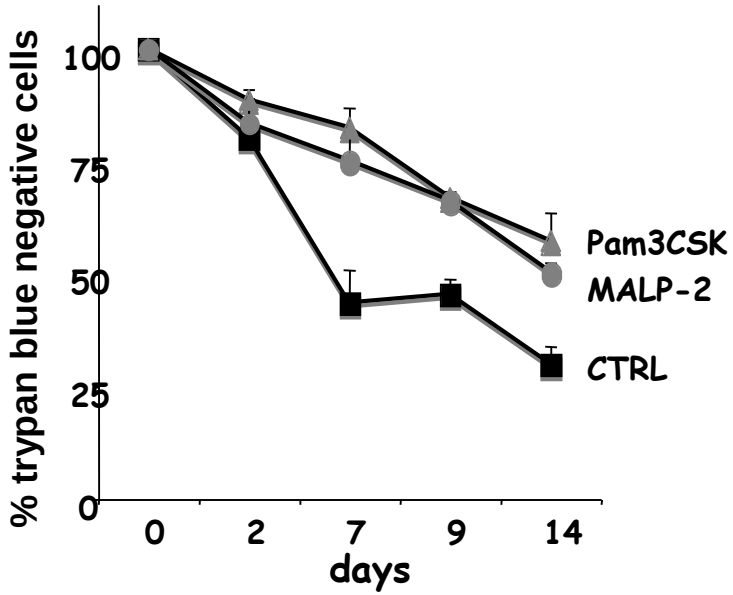

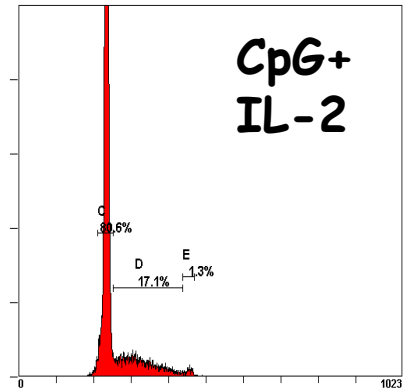

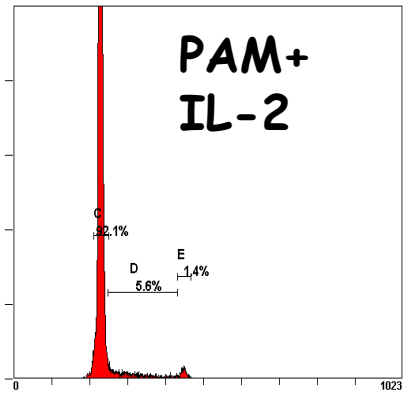

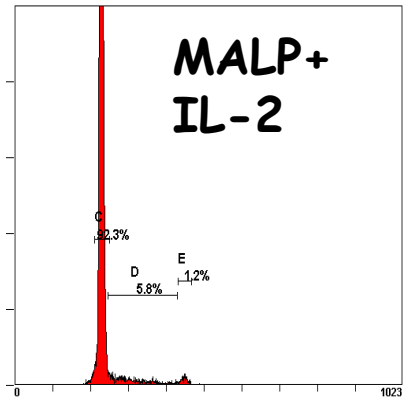

Ntoufa et al, Mol Med 2012

Stroma interactions protect from apoptosis

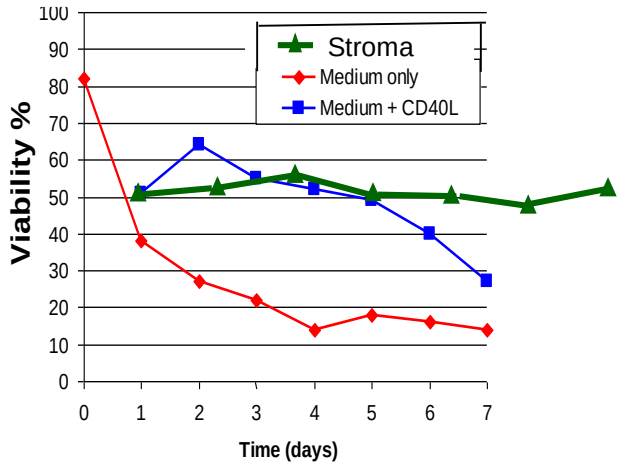

Granziero et al, Blood 2003

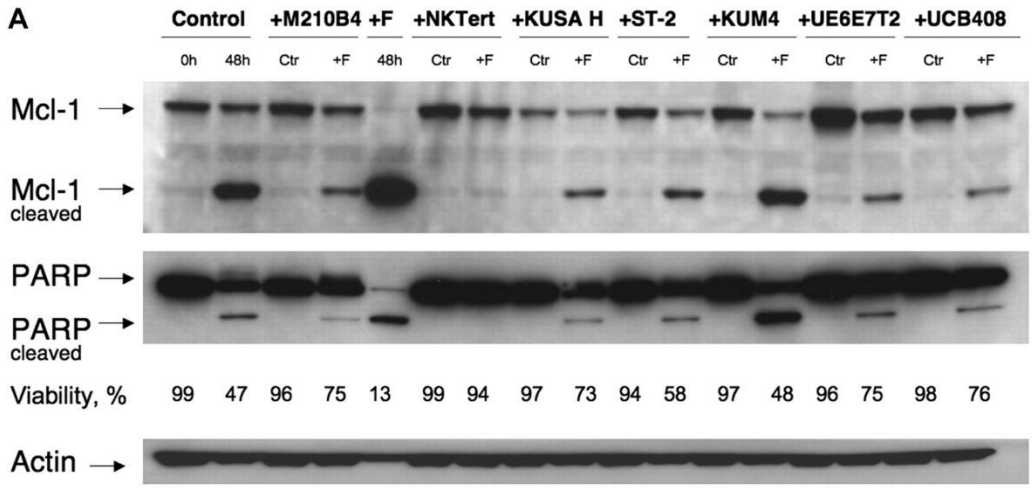

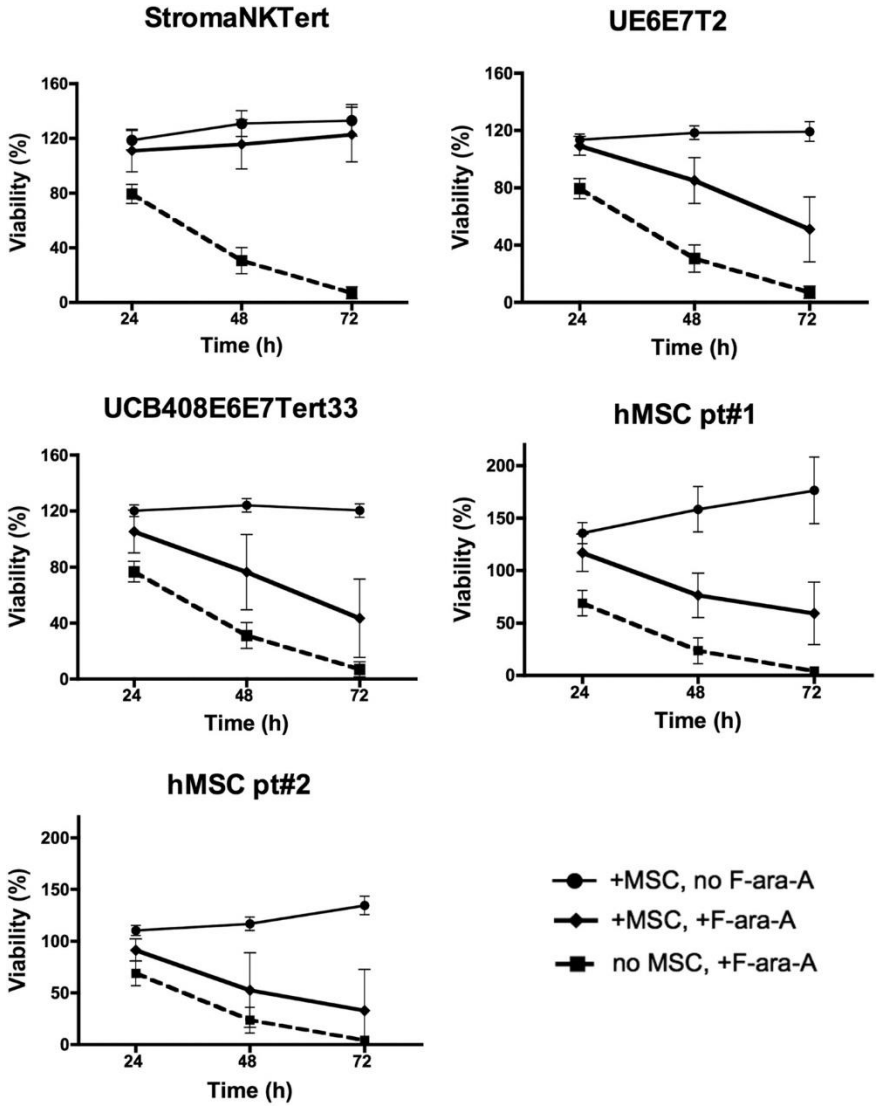

Kurtova A V et al. Blood 2009

Need of 3D structure to reproduce *in vivo* conditions

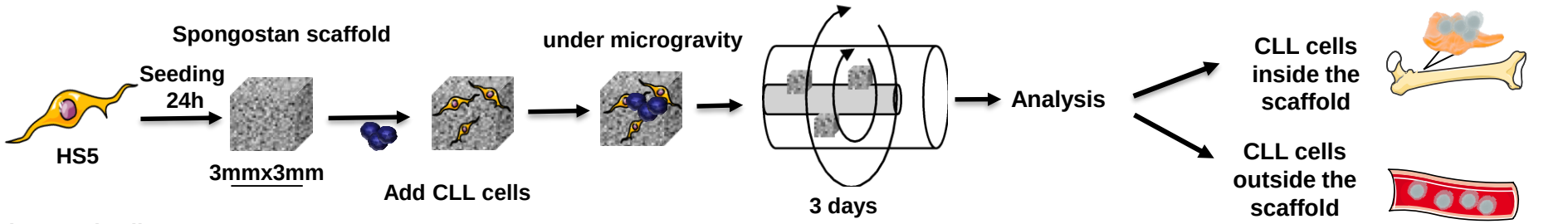

HS5: BONE marrow derived stromal cells

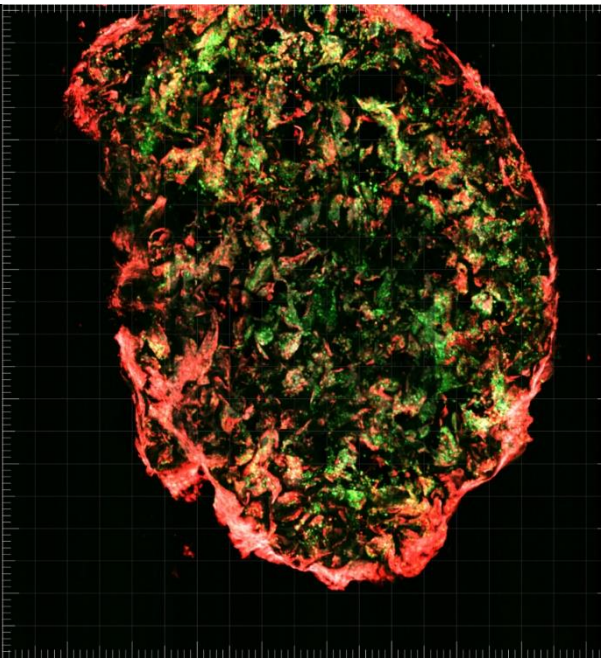

CLL cells inside the scaffold

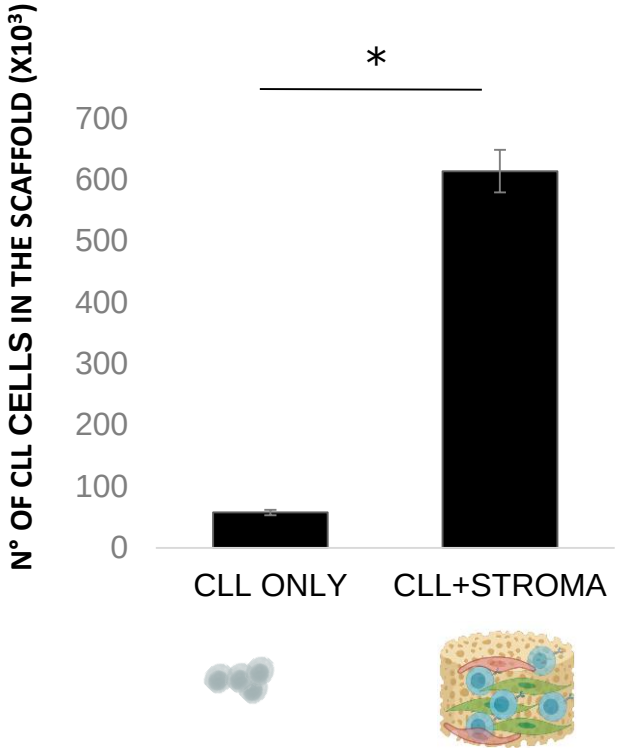

CLL cells inside the scaffold

Confocal analysis

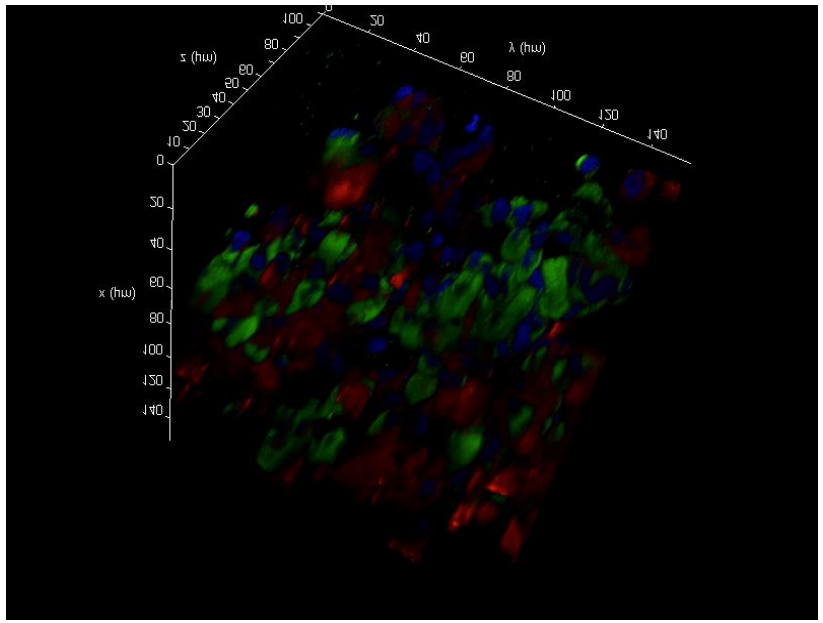

CLL +HS5+Dapi

Barbaglio F, et al. Haematologica 2020

3D multi-organ model to follow the dissemination of CLL cells

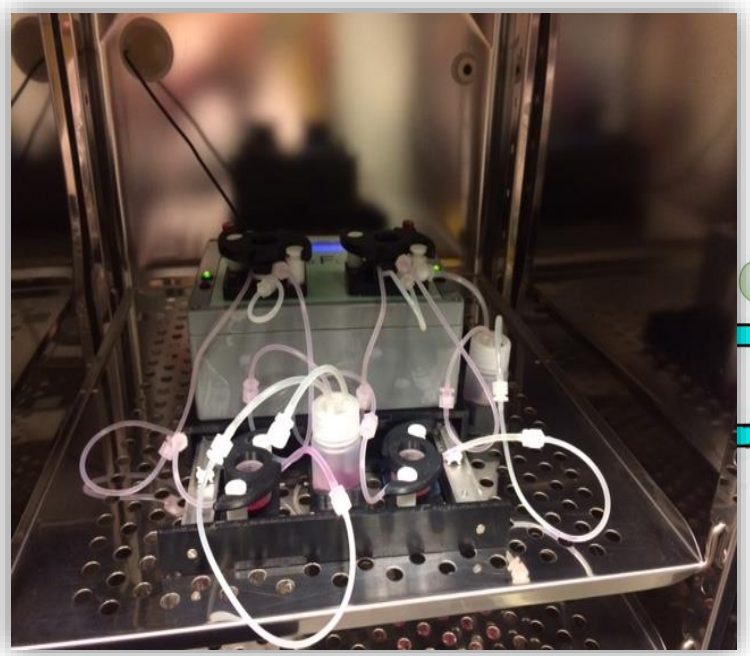

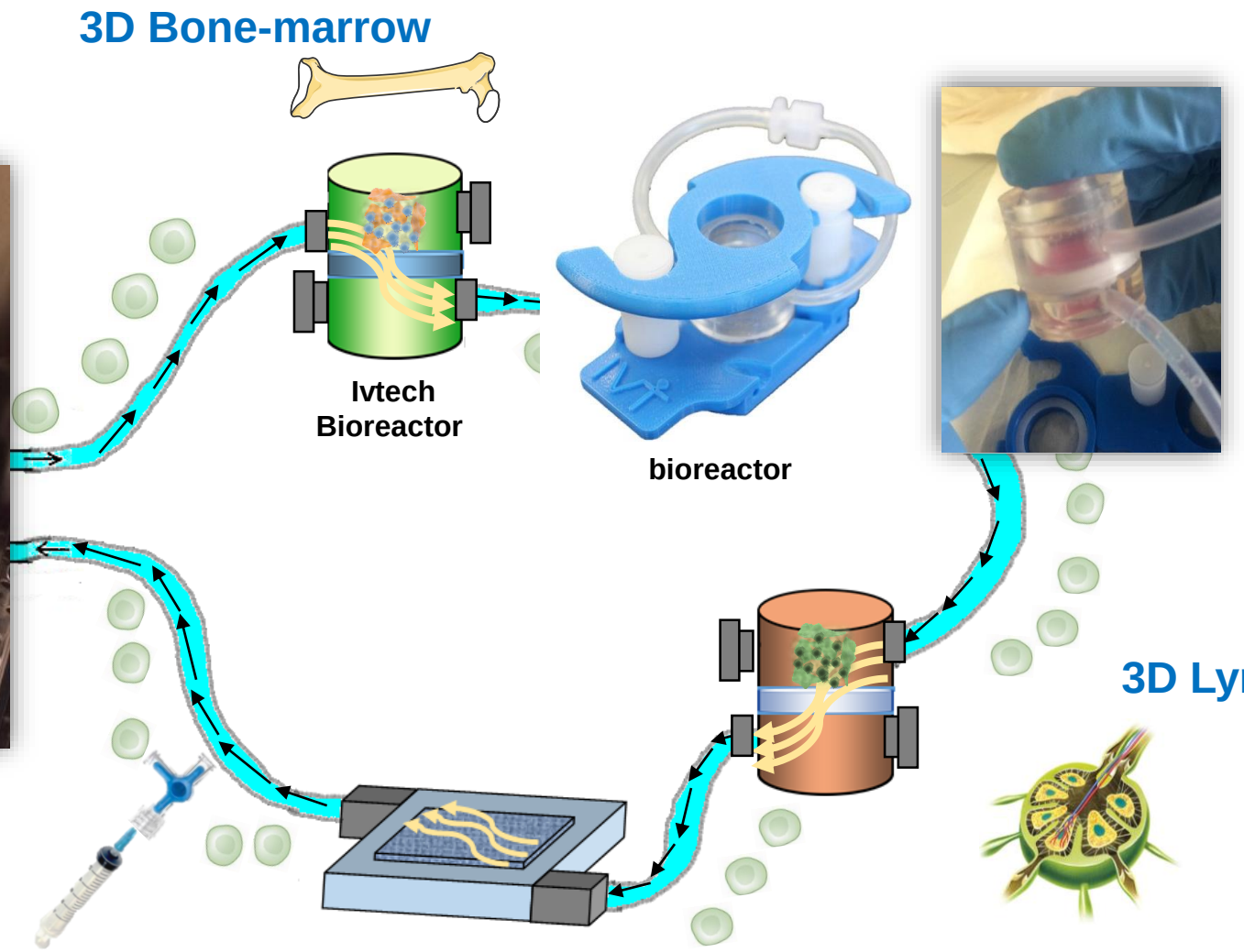

Scielzo C. under development, 2023

Several signals for one B cell

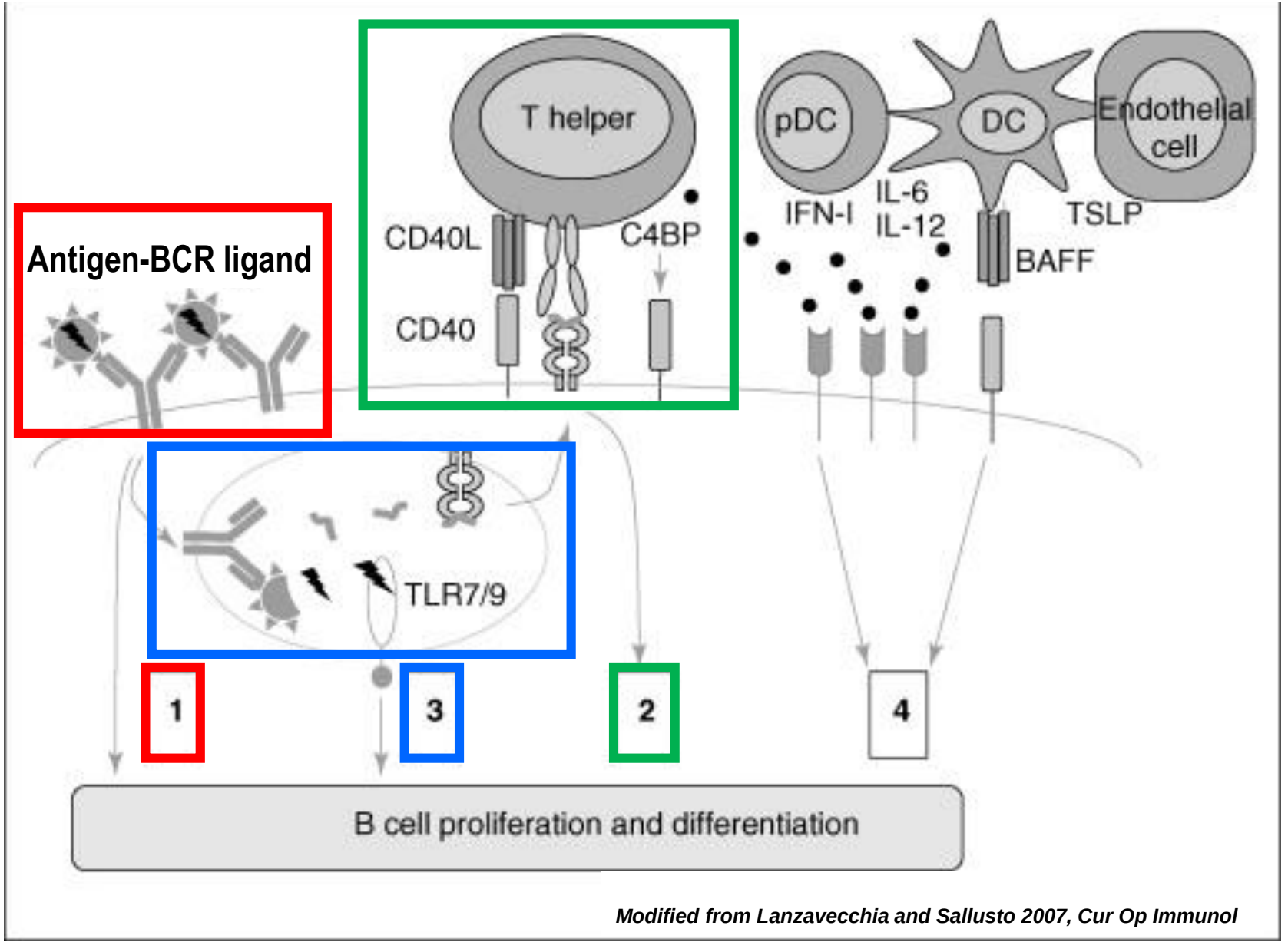

Modified from Lanzavecchia and Sallusto 2007, Cur Op Immunol

The B cell receptor is Key

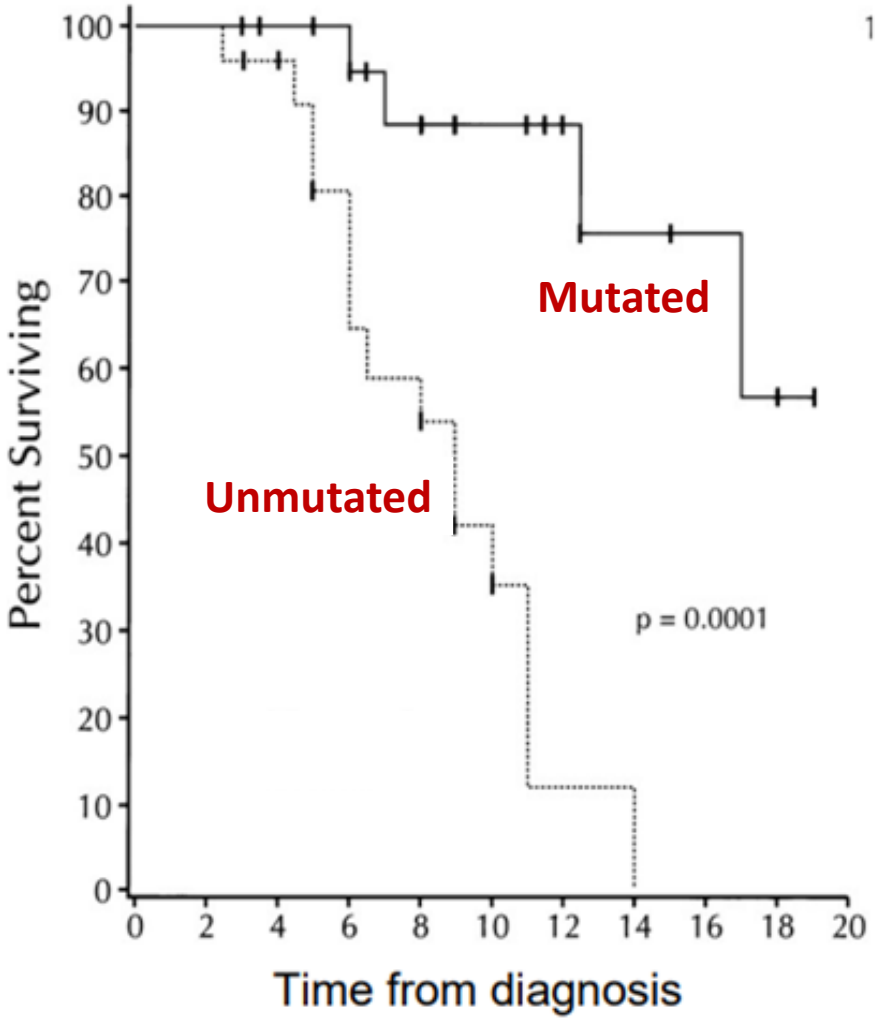

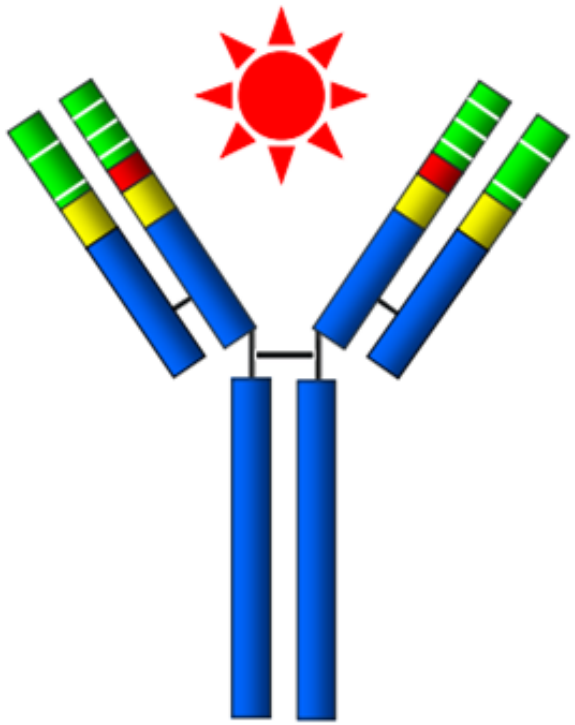

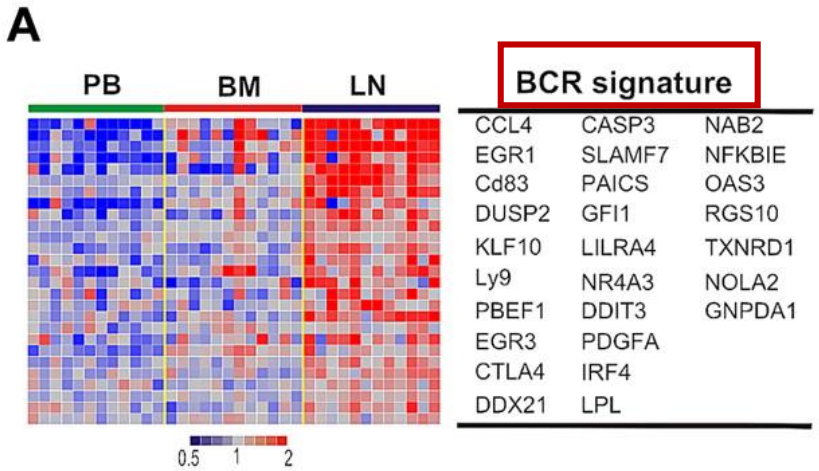

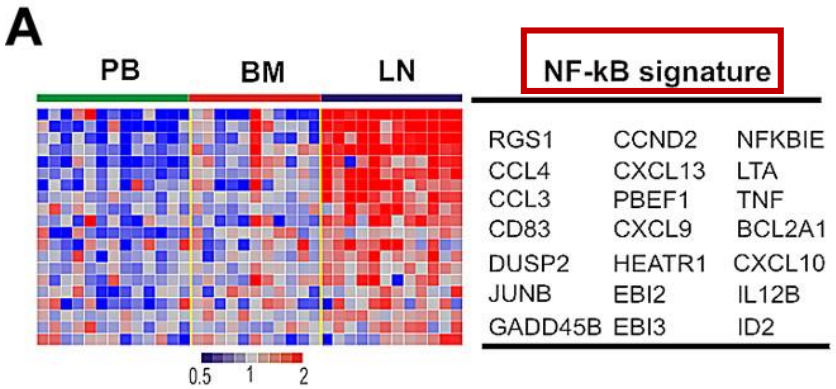

Damle et al, 1999
Hamblin et al, 1999

Herishanu Y et al. Blood 2011

BCR signalling in CLL is heterogeneous

Bad prognosis **Good prognosis**

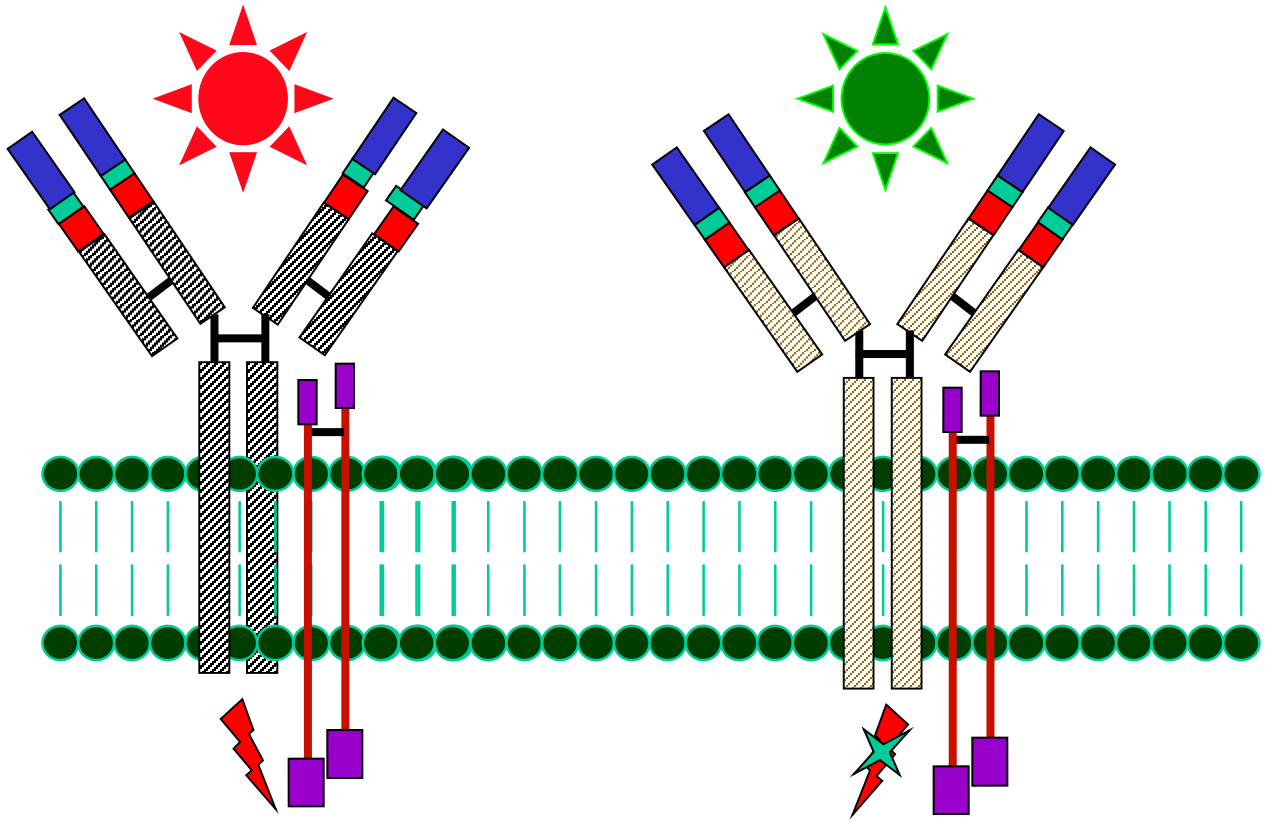

Survival
Proliferation

Anergy

Zupo et al, 1996; Chen et al, 2002; Lanham et al, 2003

Muzio M. et al, Blood 2008; Apollonio B. et al, Blood 2013Ntoufa S et al, J. Immunol 2016

ERK constitutive phosphorylation as a sign of anrgy

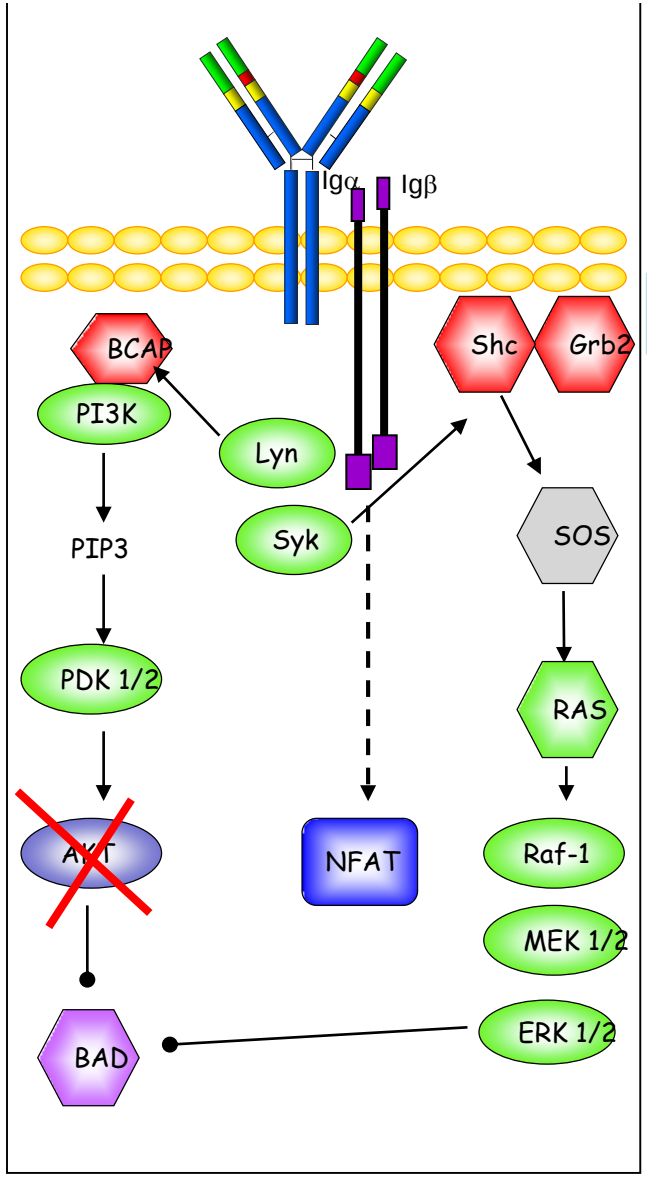

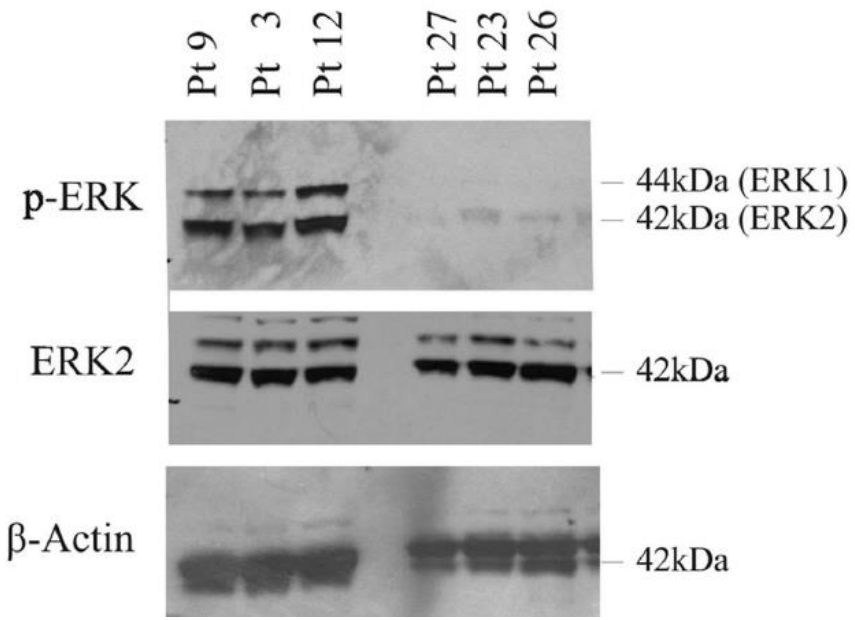

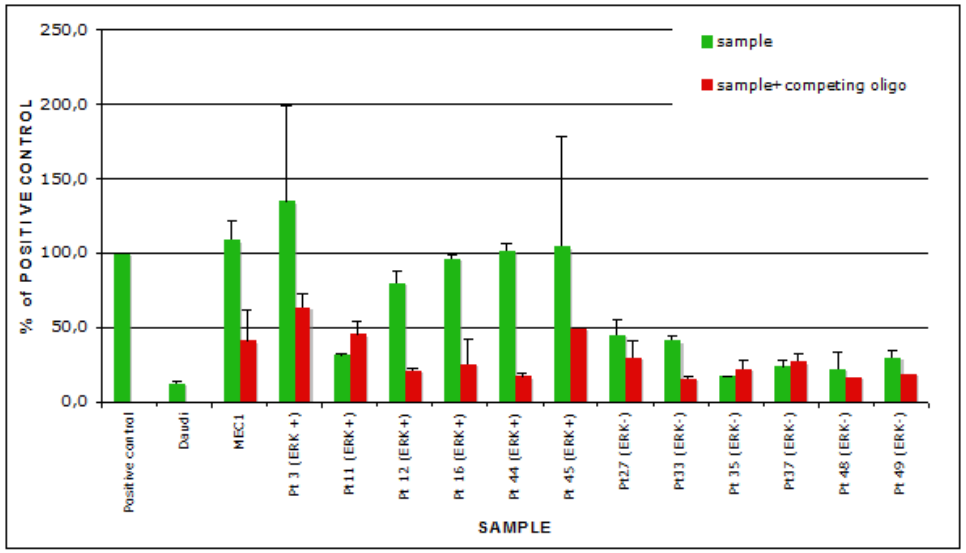

Muzio et al, Blood 2008

BCR reactivity in CLL: self and foreign antigens

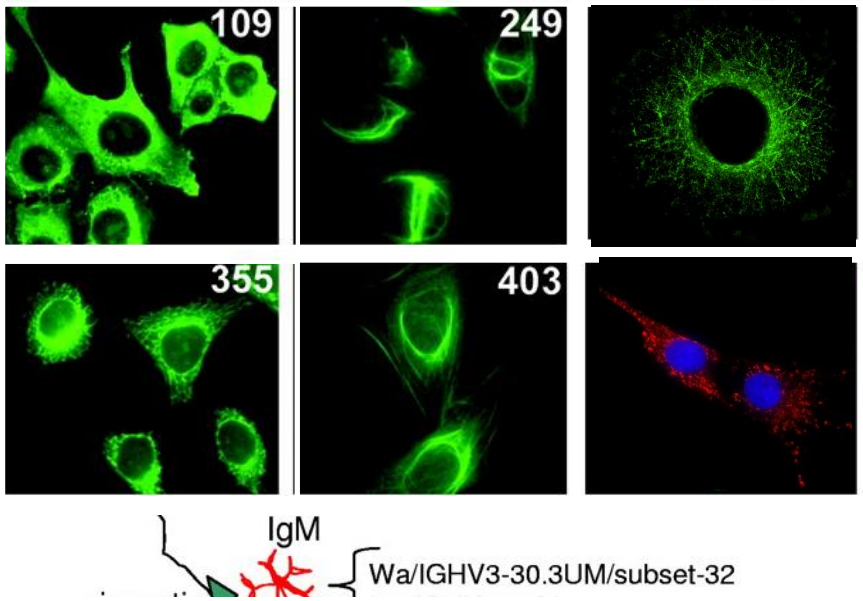

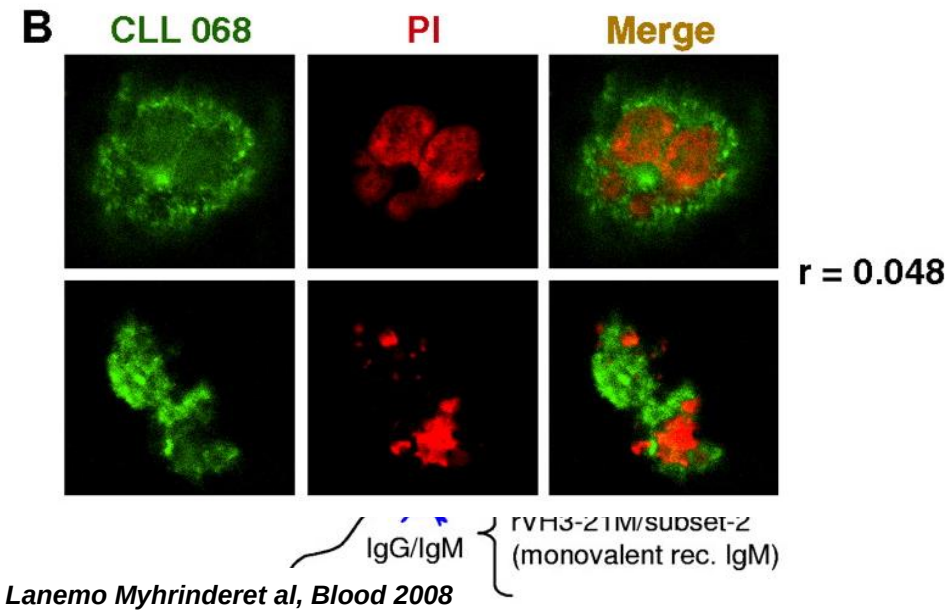

Hervé et al, JCI 2005, *Lanemo Myhrinderet al, Blood 2008*

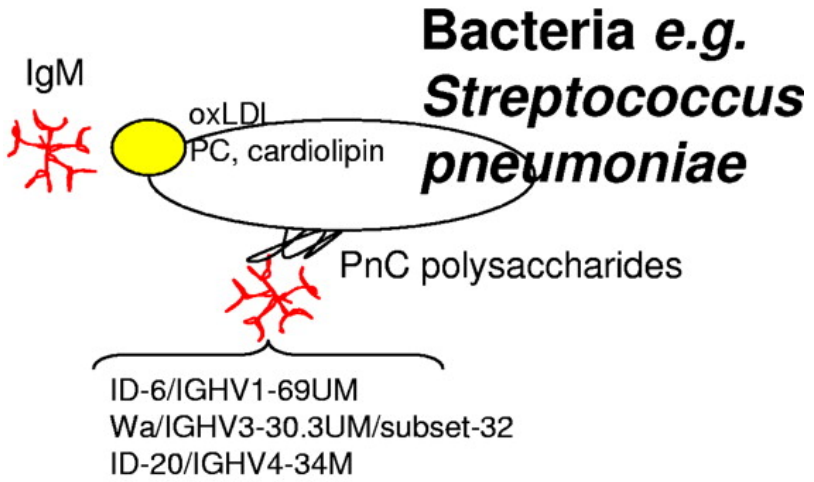

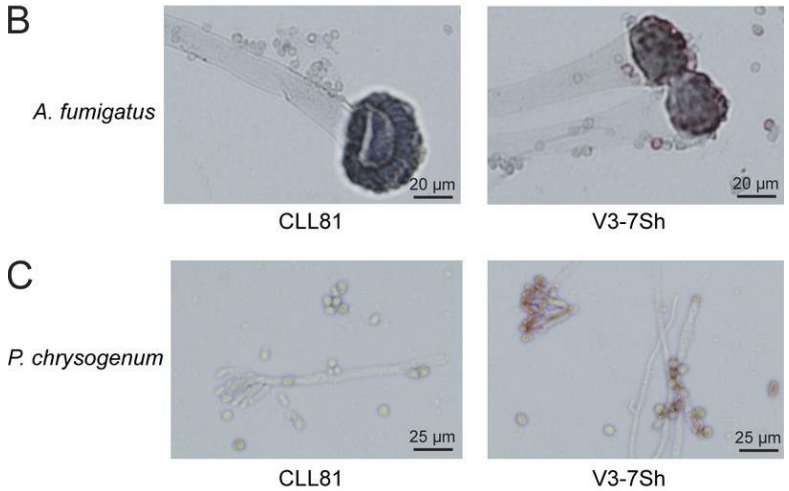

Lanemo Myhrinder et al, Blood 2008, Hoogeboom et al, JEM 2013, Kostareli et al, Leukemia 2011; Hwang et al, PlosOne 2014; Liu et al, ASH 2014

Autonomous signalling in CLL

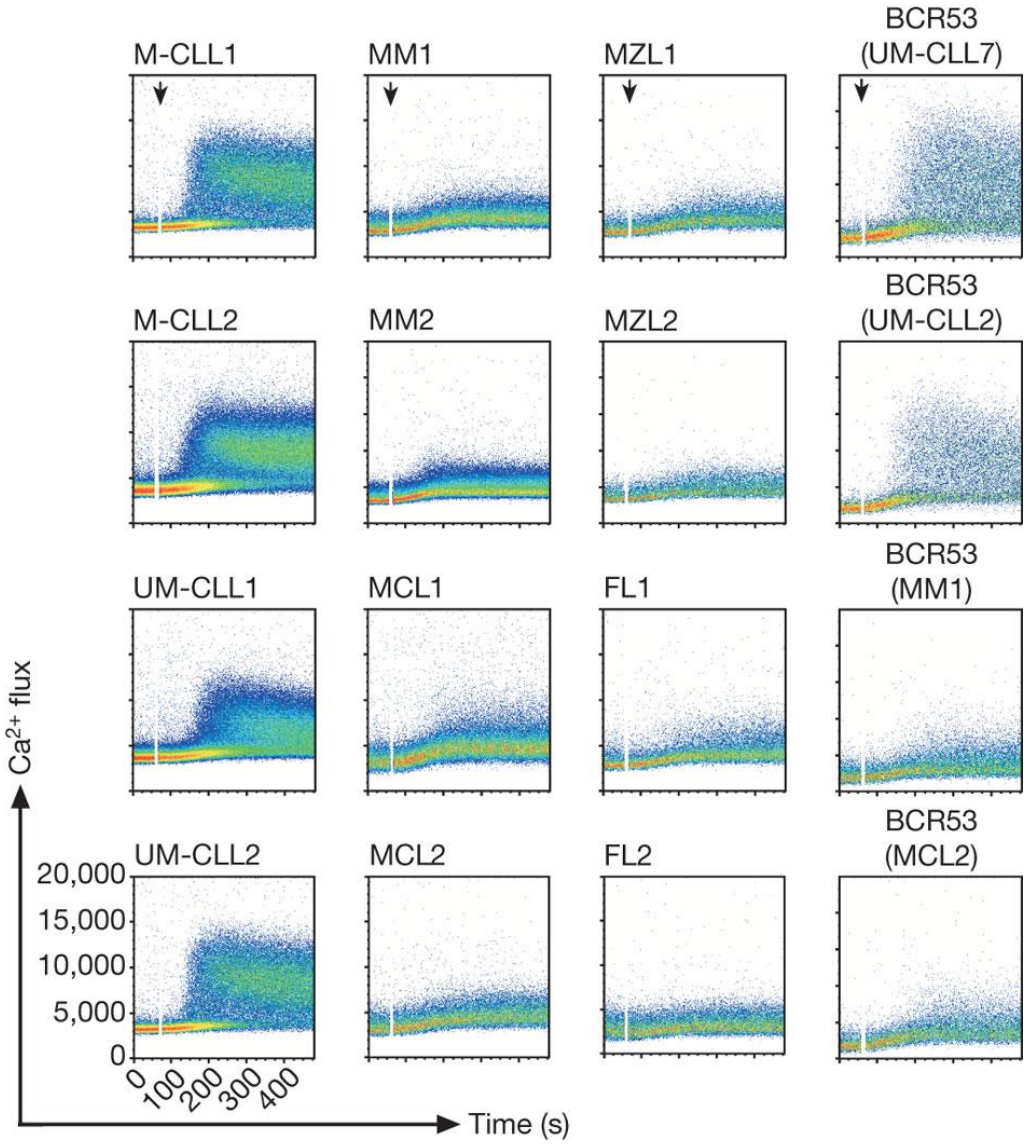

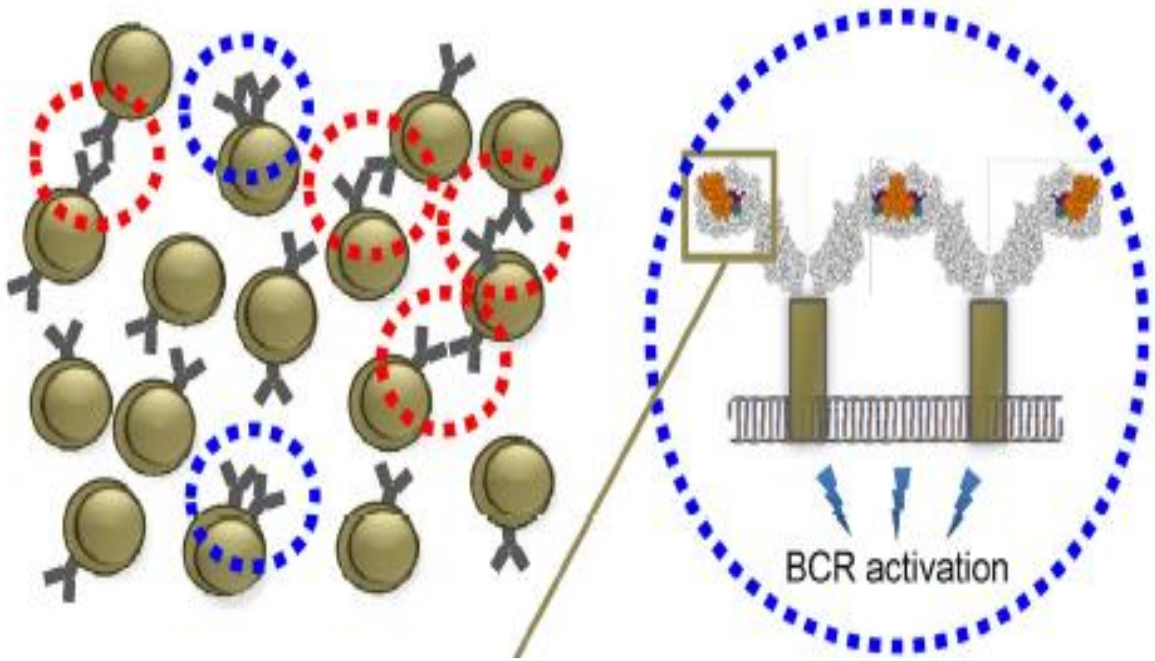

Dühren-von Minden et al, Nature 2012; Binder et al, Blood 2013

Back to basic immunology

probability that ***two different B cell*** clones carry identical B cell receptors

$1:10^{-12}$

0.000000000001%

BcR stereotypy 41%

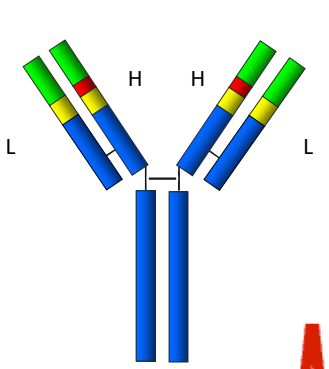

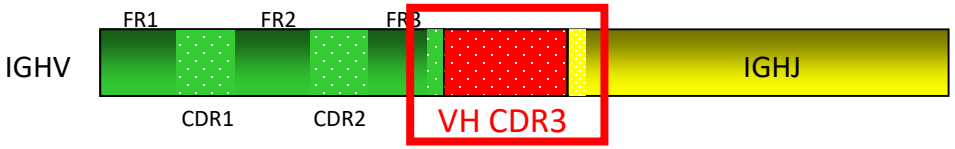

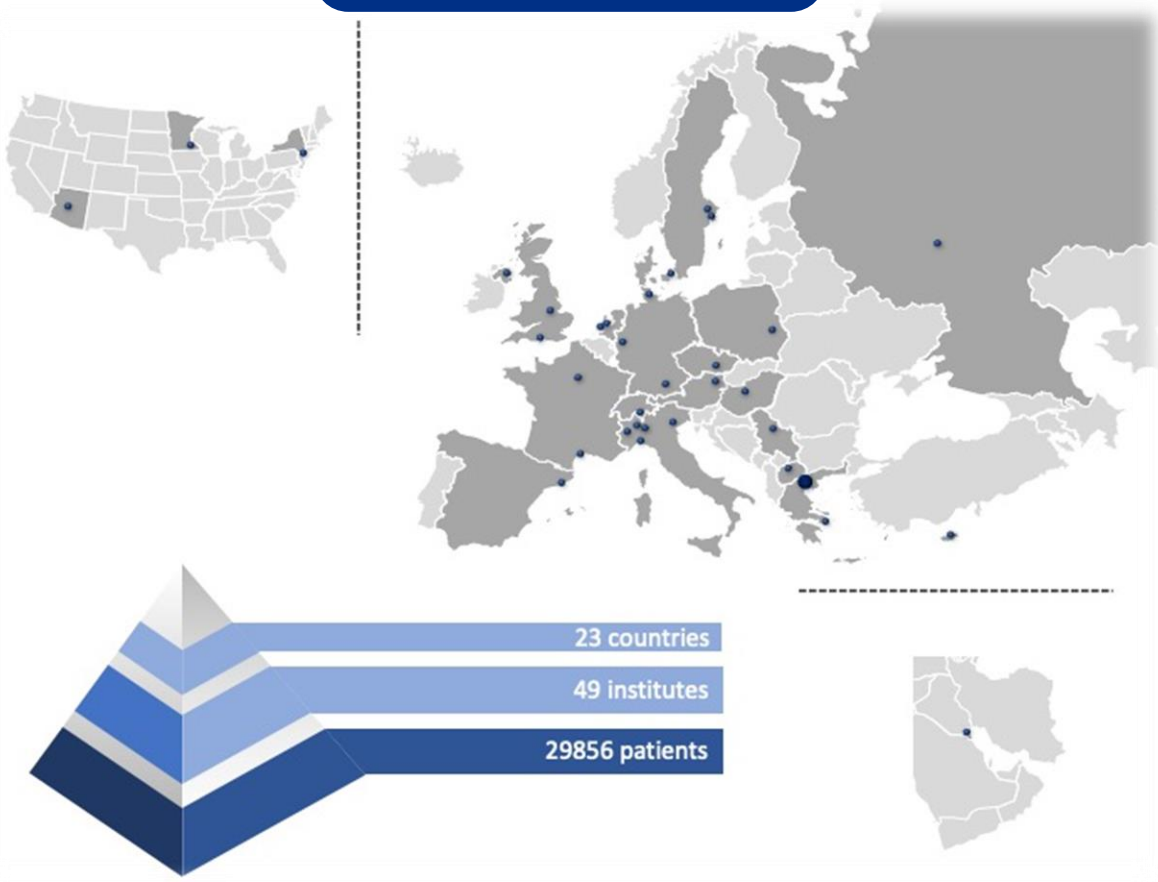

ERIC european research initiative on CLL

Agathangelidis et al, 2021 Blood

Clinical relevance of major stereotyped receptors

4 major stereotyped subsets; ~7% of all CLL

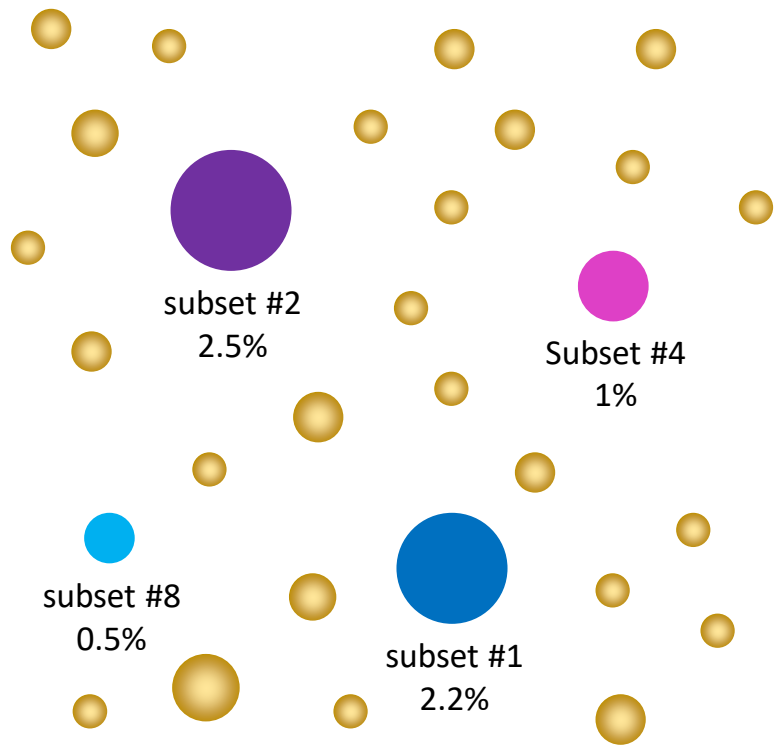

distinct clinical outcomes for subsets #2 and #4, independently of genomic aberrations or SHM status

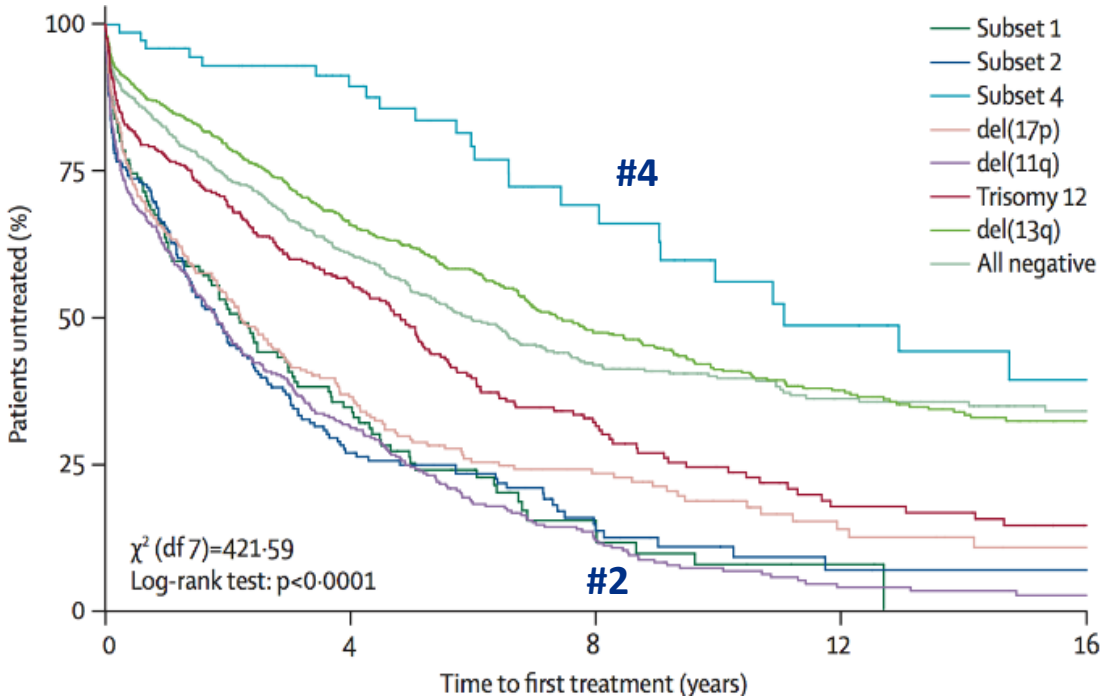

Baliakas et al. Lancet Haematol 2014

Subset 4

V gene	N1	D gene	N2	J gene

Subset 4:

- expresses IGHV4-34/IGKV2-30 BcR IG
- is G-switched
- carry long and positively charged VH CDR3s
- INDOLENT/ANERGIC

Subset 4 CLL is anergic to BCR stimulation

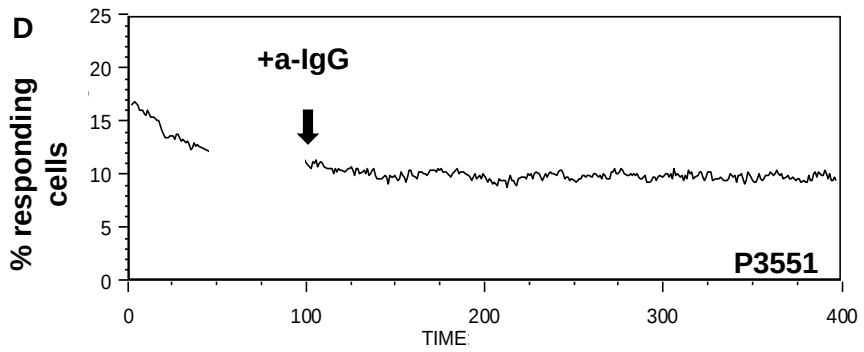

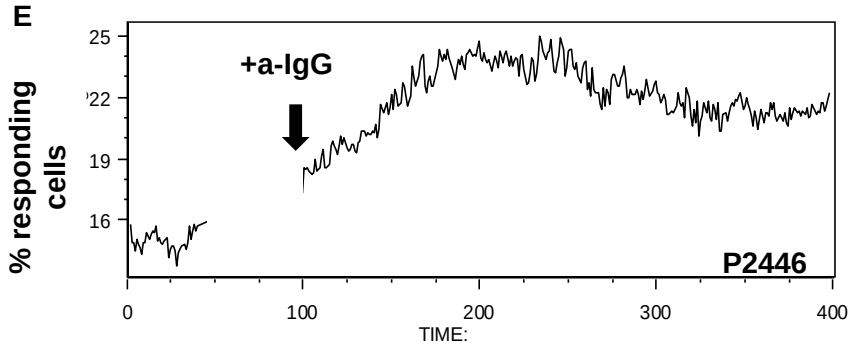

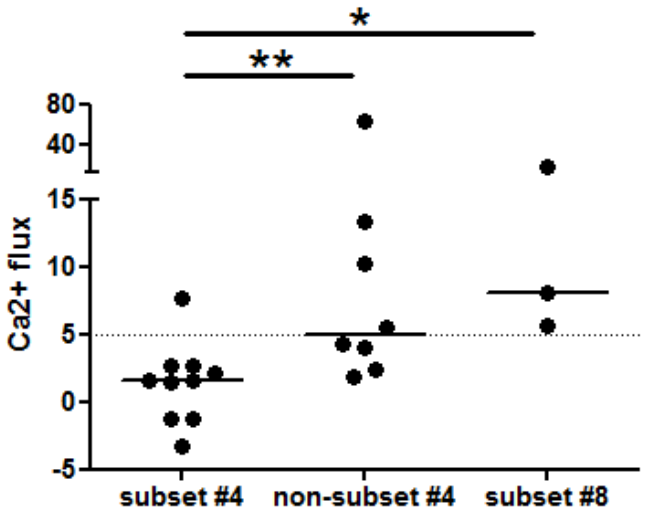

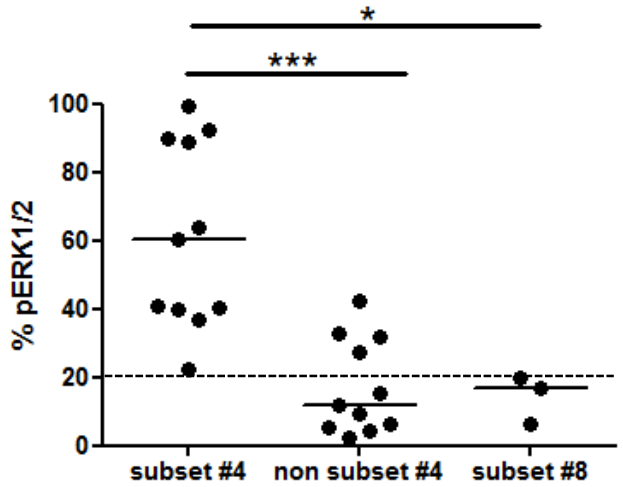

Ntoufa et al, J. Immunol 2016

Subset 4: self recognition of CLL Fab

CLL240

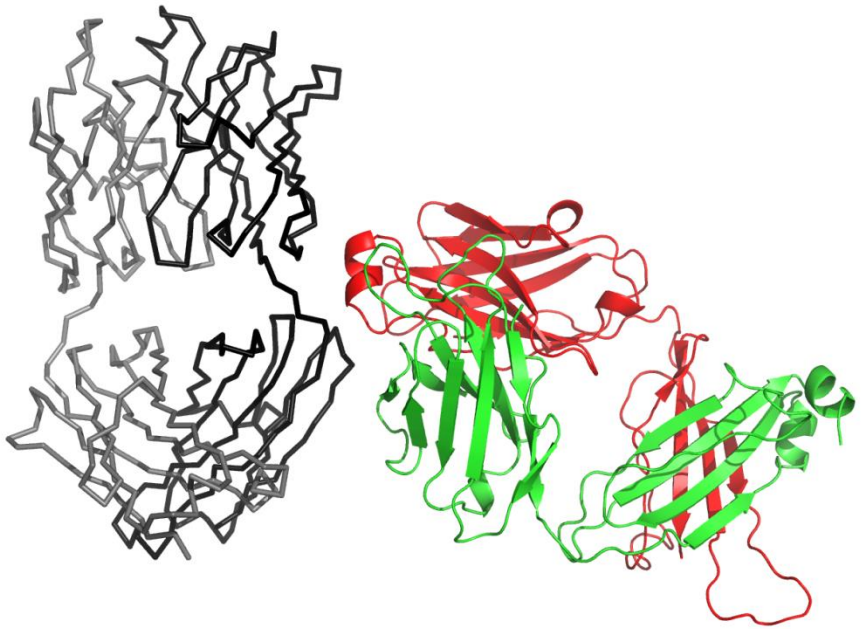

CLL183

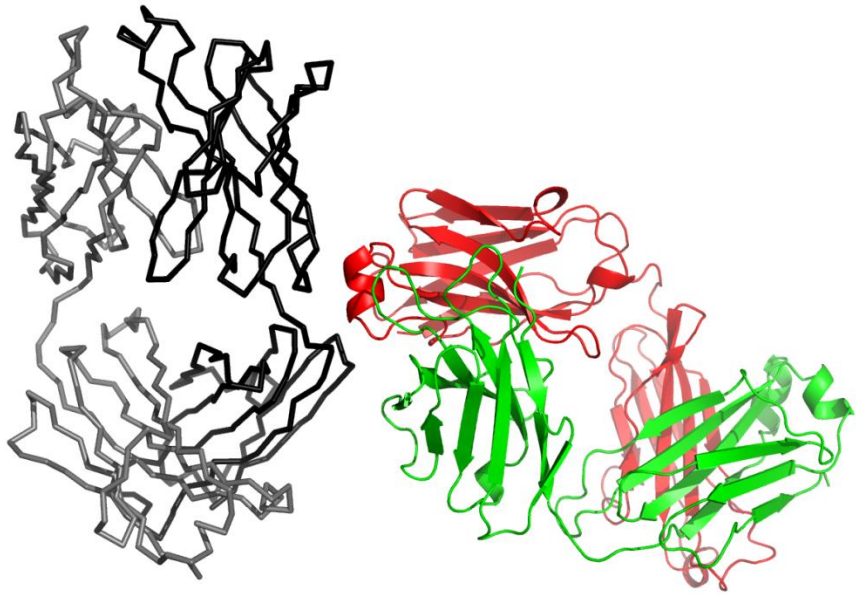

Interaction with the V-C hinge (VH FR1 and CH1 domains)

Minici C, Gounari M et al, Natture Comm 2017

Subset 4: self recognition of CLL Fab

CLL183

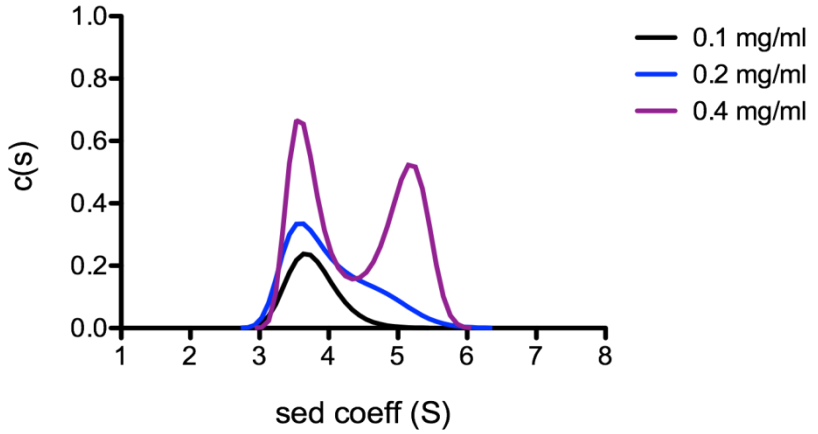

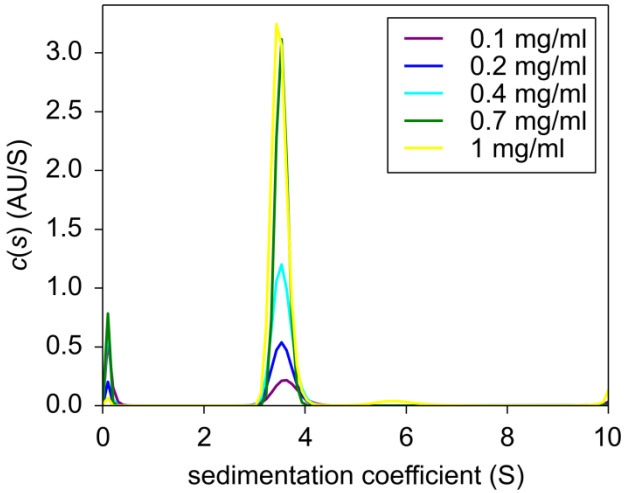

Mutated Ab

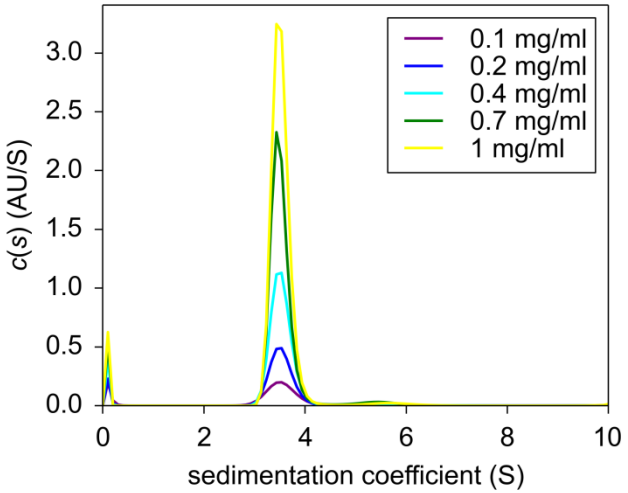

Mutated Ag

Minici C, Gounari M et al, Natture Comm 2017

Stereotyped subsets have a distinct clinical course

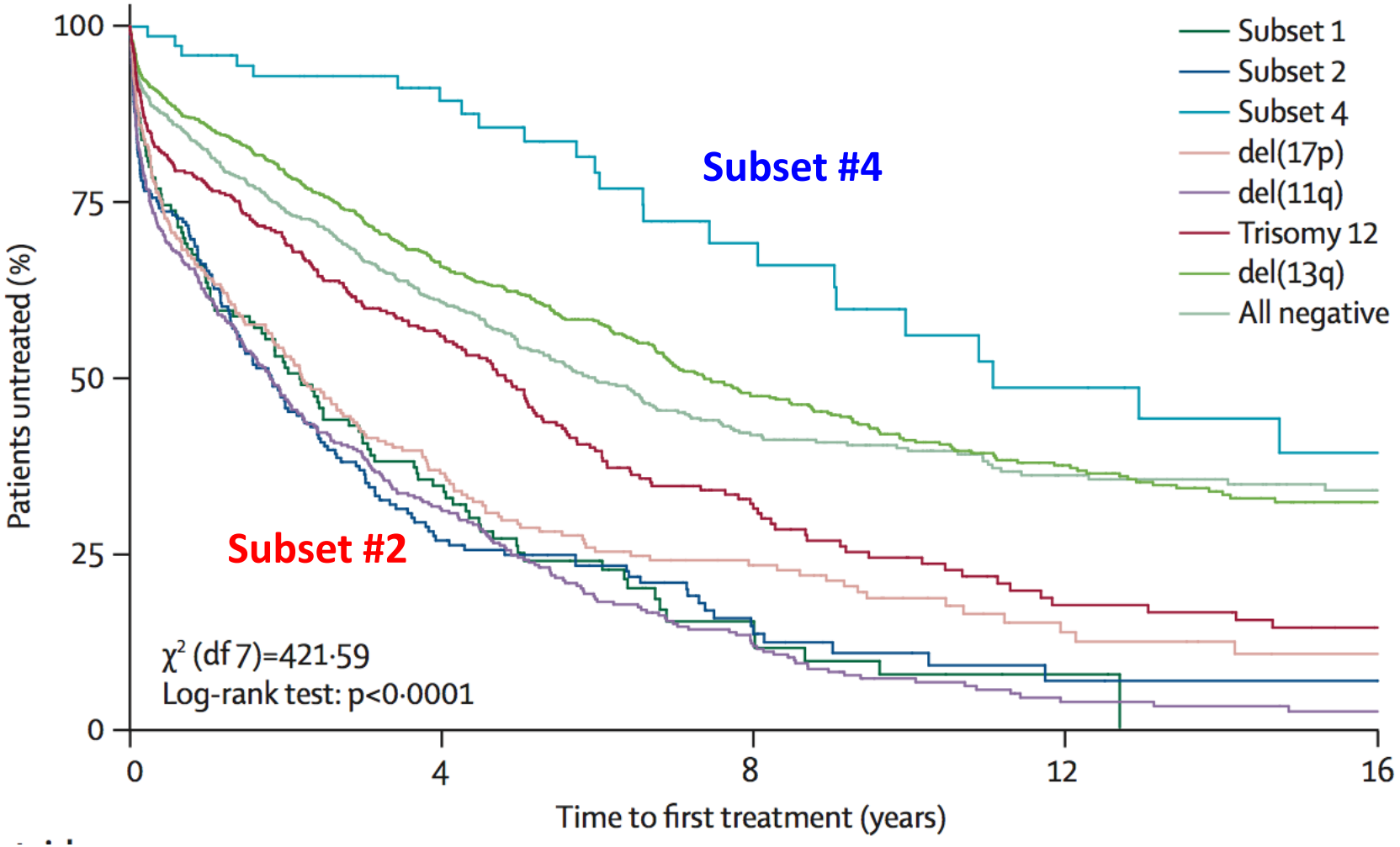

Baliakas et al. Lancet Haematol 2014

Subset 2

V gene	N	J gene

Subset 2 express BcR IGM with:

- **heavy chains with IGHV3-21/IGHJ6 genes**
- **light chains with IGLV3-21 gene**
- **9 amino-acid-long VH CDR3**
- **AGGRESSIVE/BCR RESPONSIVE**

Poor clinical course is independent of genomics

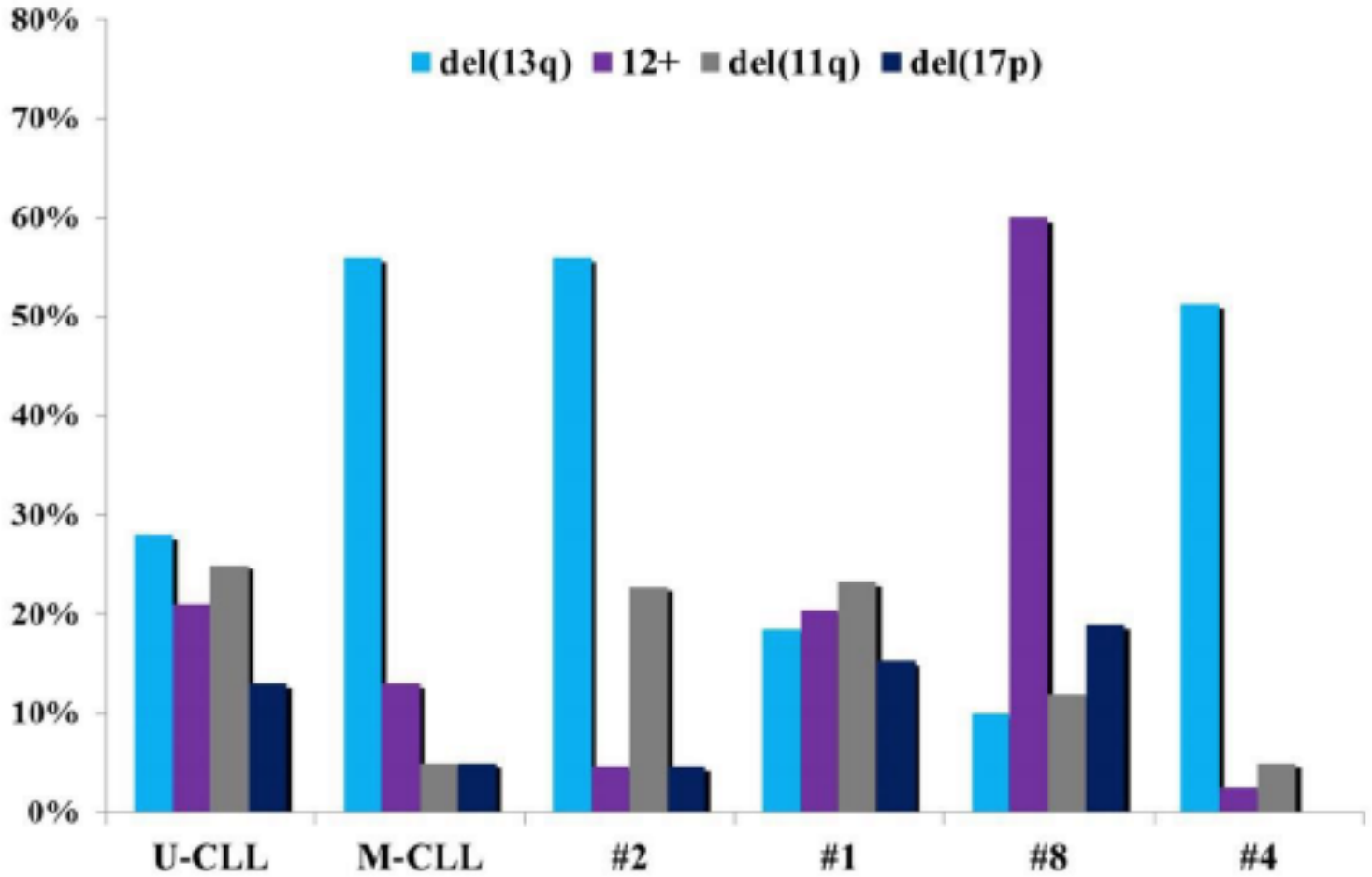

Baliakas et al. Lancet Haematology 2014

Gene mutations and IG stereotypy

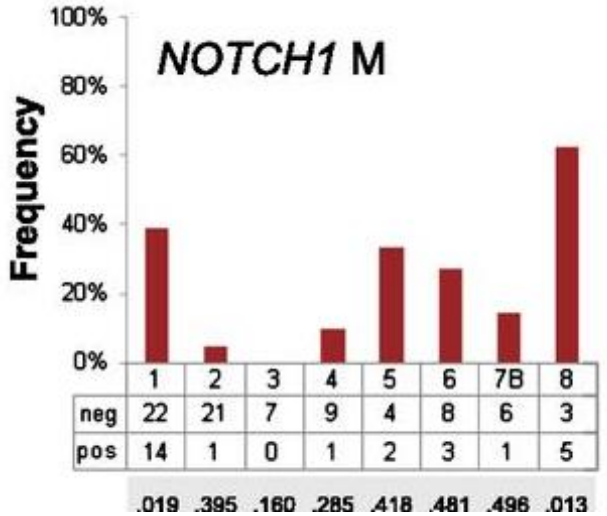

	1	2	3	4	5	6	7B	8
neg	22	21	7	9	4	8	6	3
pos	14	1	0	1	2	3	1	5
	.019	.395	.160	.285	.418	.481	.496	.013

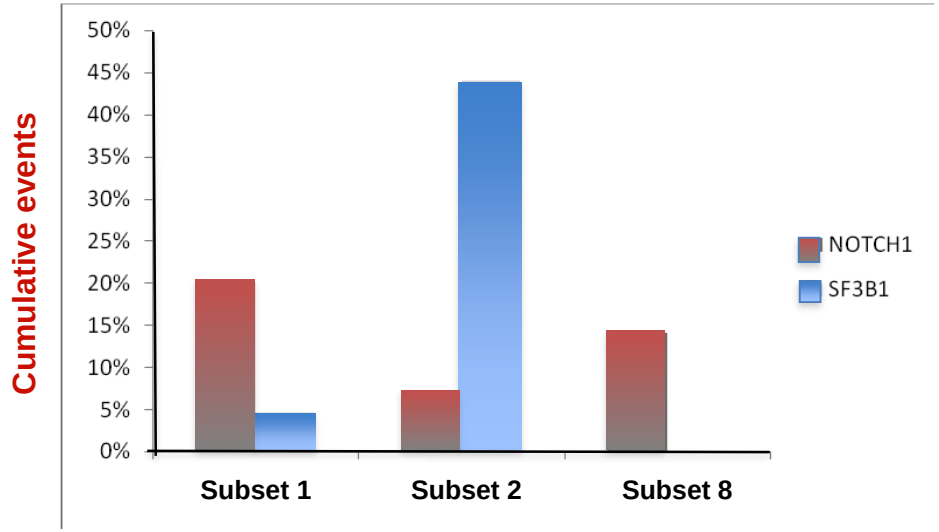

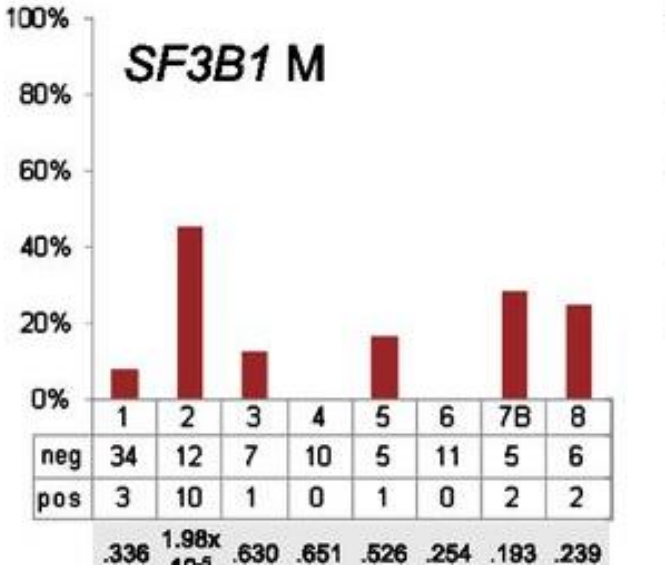

	1	2	3	4	5	6	7B	8
neg	34	12	7	10	5	11	5	6
pos	3	10	1	0	1	0	2	2
	.336	1.98x	.630	.651	.526	.254	.193	.239

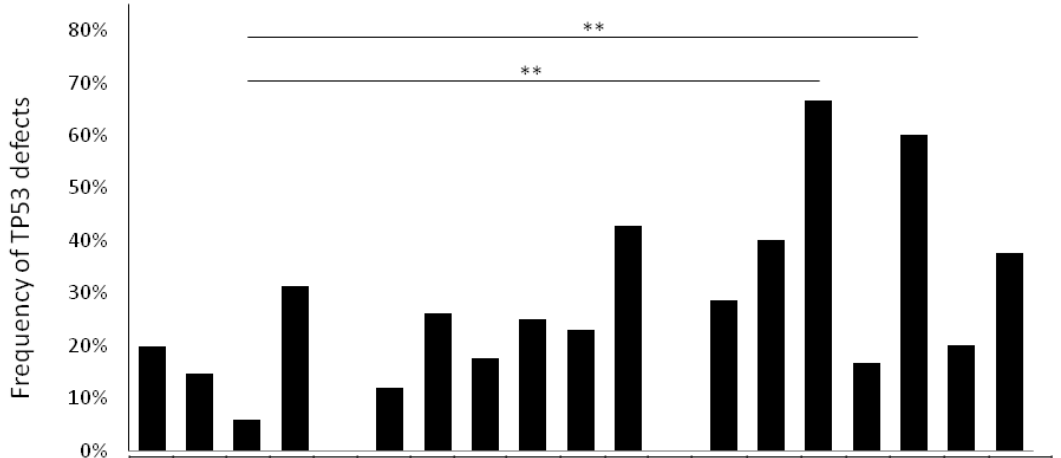

	all	#1	#2	#3	#5	#6	#7all	#8	#10	#28A	#31	#50	#59	#95	#99	#117	#202	#205	#N7/4-34
no TP53 defect	955	52	63	11	14	22	34	14	9	10	4	7	5	3	2	5	2	4	5
TP53 defect	235	9	4	5	0	3	12	3	3	3	3	0	2	2	4	1	3	1	3

Rossi et al, Blood, 2013

Strefford et al, Leukemia, 2013; Malcikova et al, BJH 2014

Aggressive subsets respond avidly via the BcR

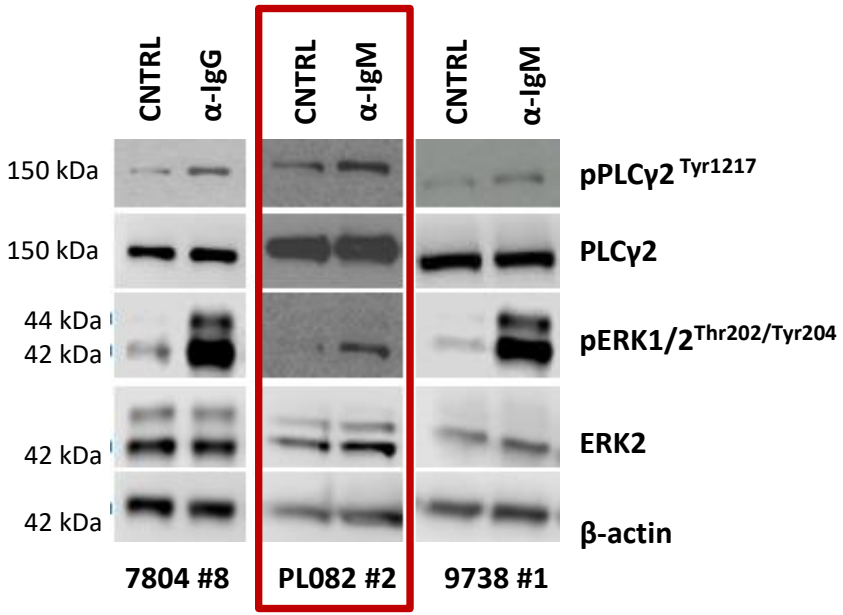

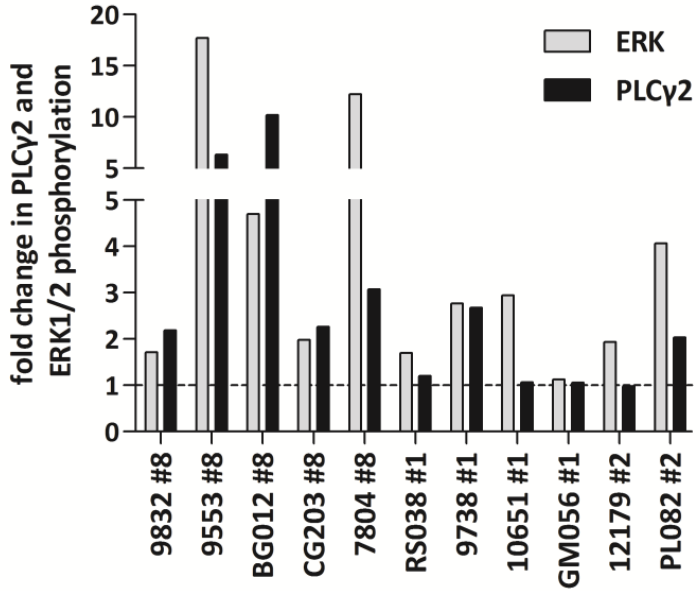

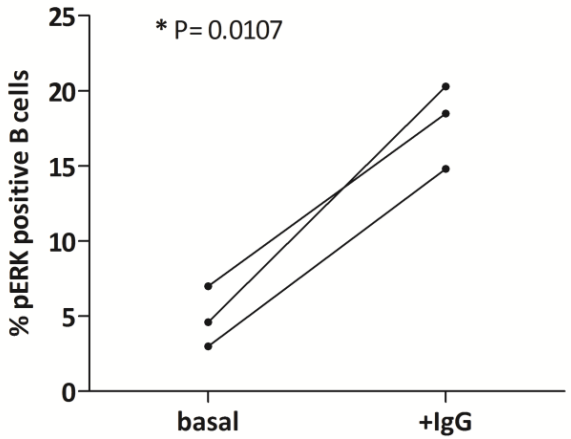

Ntoufa et al, J. Immunol 2016

Self-association of subset 2 BCR in the crystals

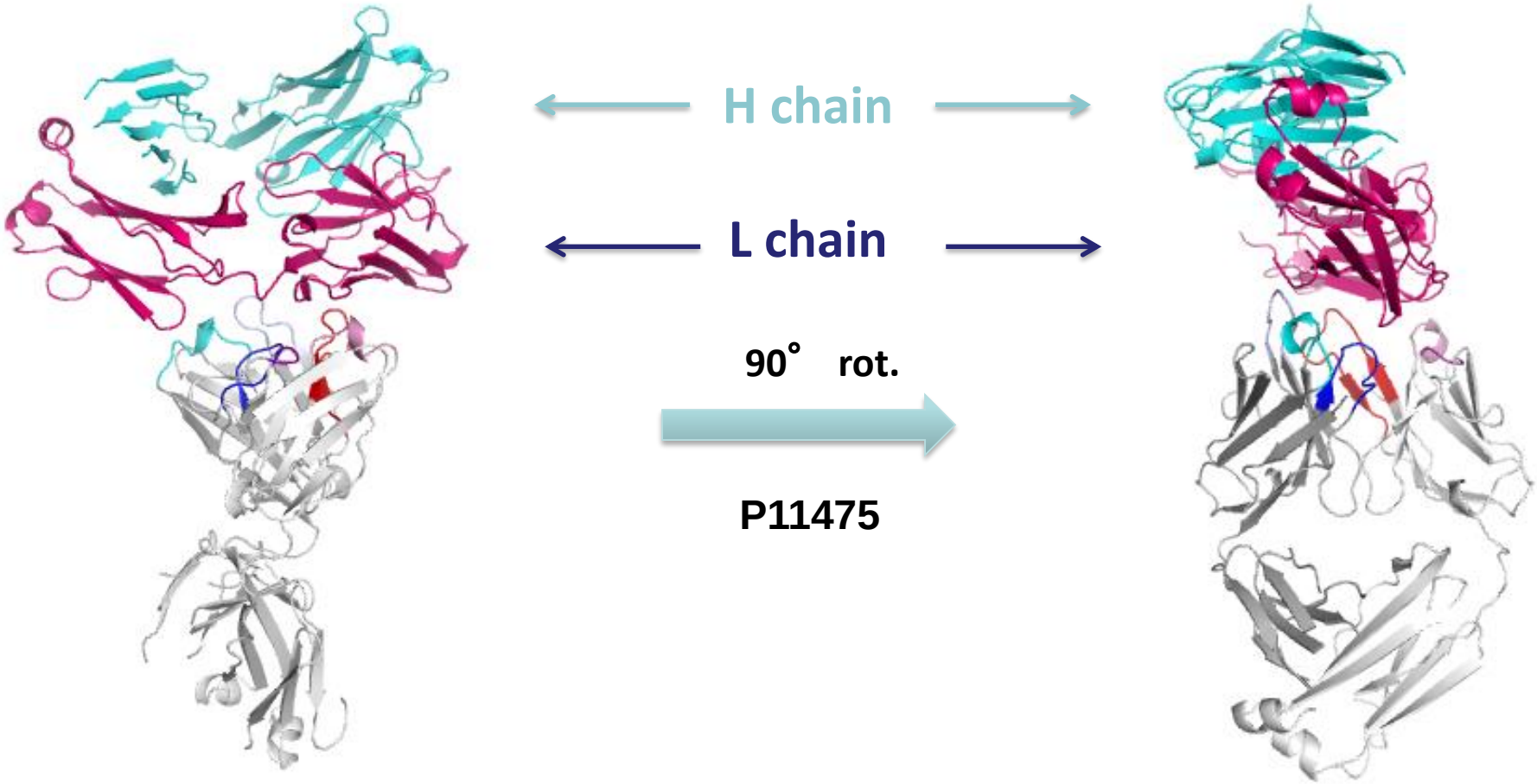

The epitope is composed of:

- **residues in the FR1 region of the VL domain,**
- **residues in the VL-CL linker region**

Minici C, Gounari M et al, Natture Comm 2017

Interactions is light chain mediated, mainly by LCDR2

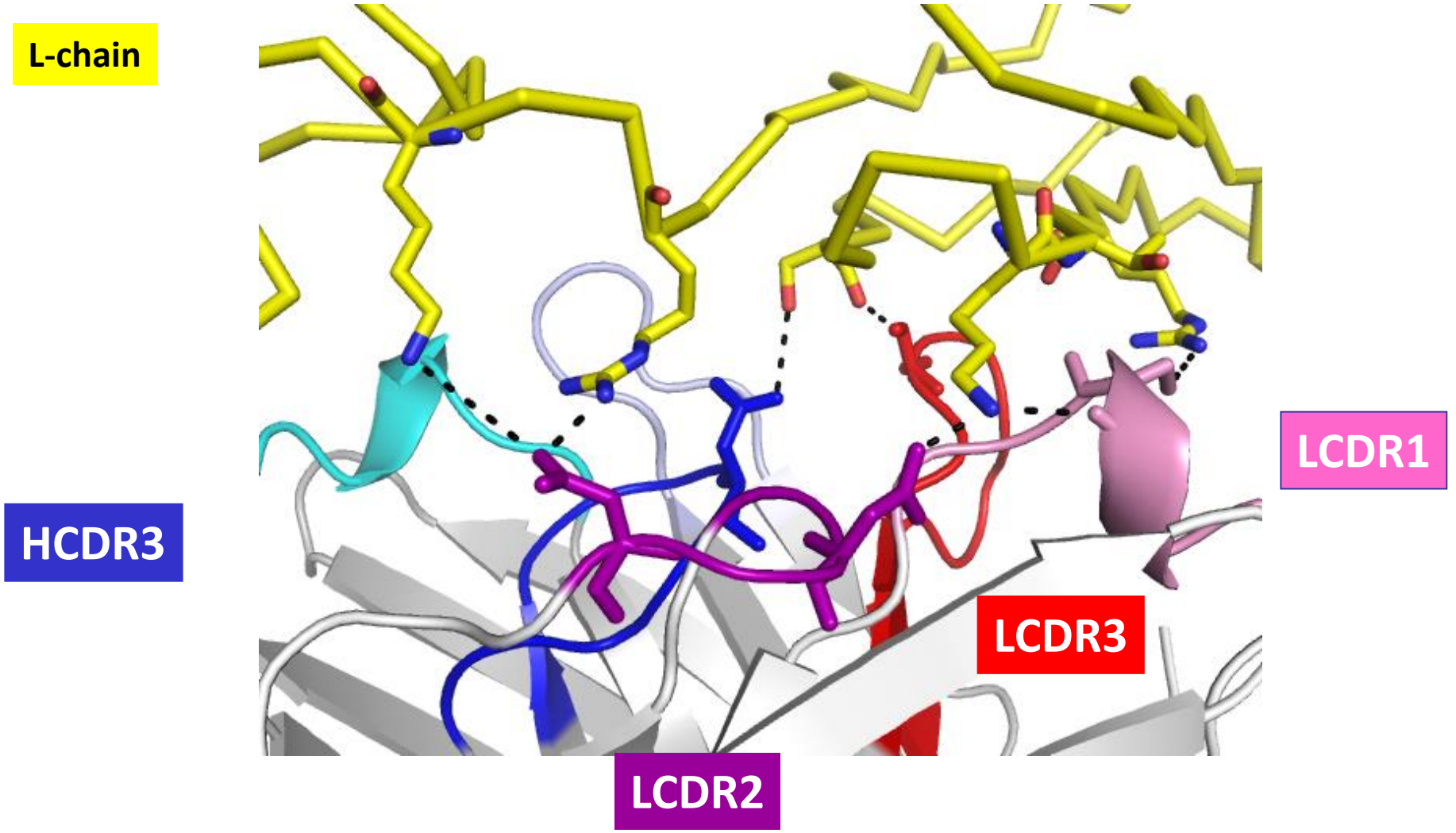

Only IGLV3-21 has a CDR2 sequence that contains the crucial residues

Minici C, Gounari M et al, Nature Commn 2017

Subset #2: weak interaction in solution

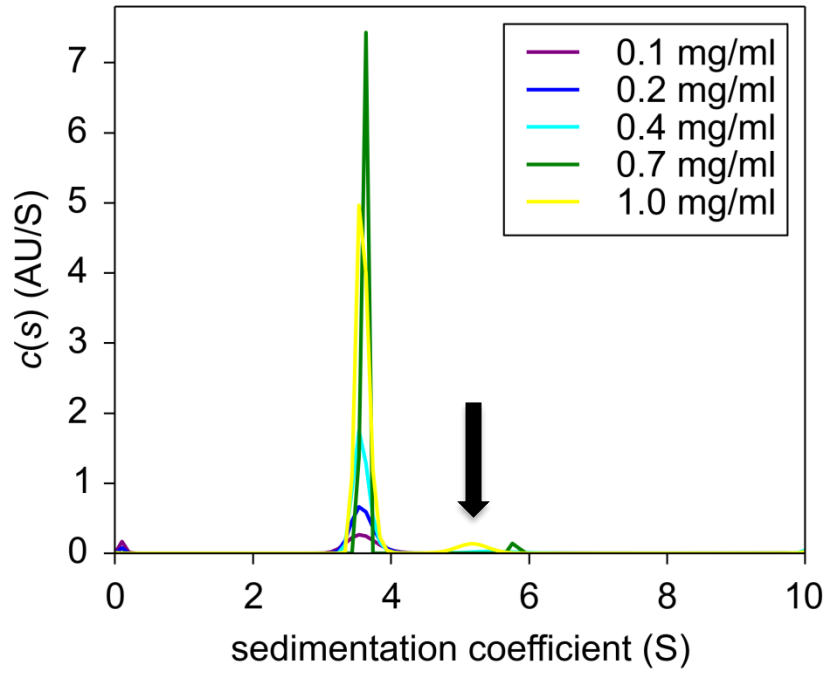

P11475
(Subset 2, IgM)

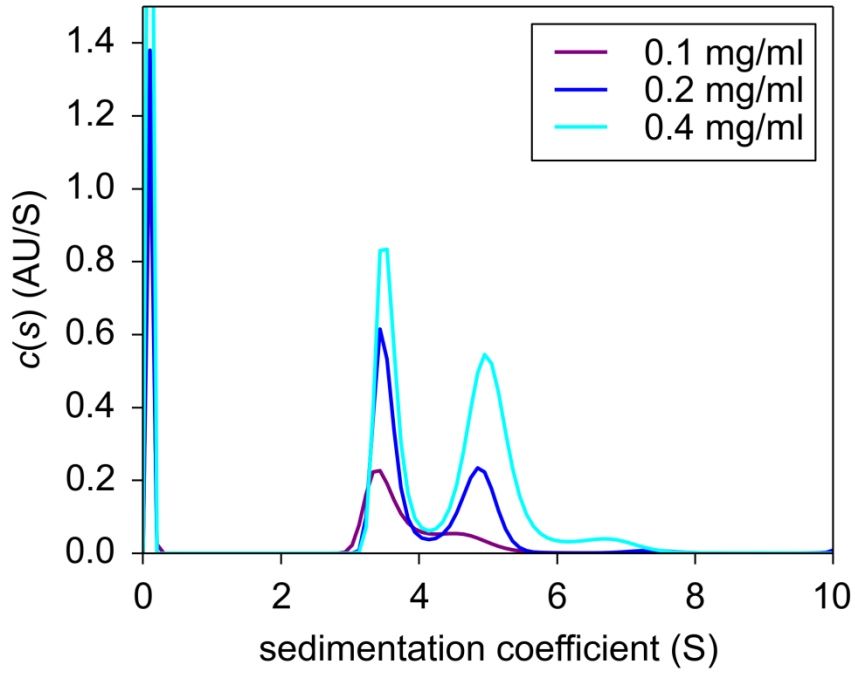

CLL183
(Subset 4, IgG)

Weak interaction, and fast dissociation of the complex.
Buried surface (420 Å^2) supports weak interaction.

Minici C, Gounari M et al, Nature Commn 2017

BCR signalling in CLL is heterogeneous

Aggressive

Indolent (anergic)

weak, transient binding

tight, stable binding

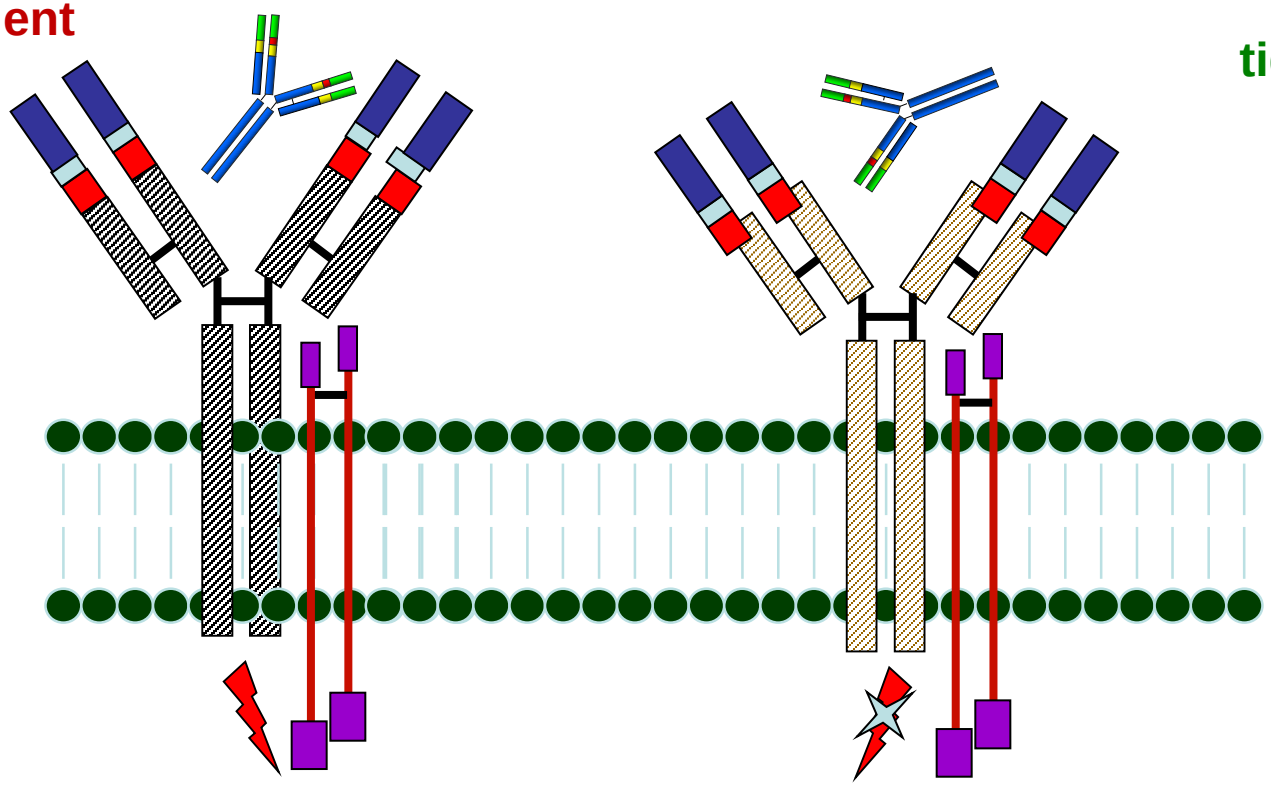

Survival
Proliferation

Anergy

Minici C, Gounari M et al, Nature Commn 2017

CLL: From biology to therapies

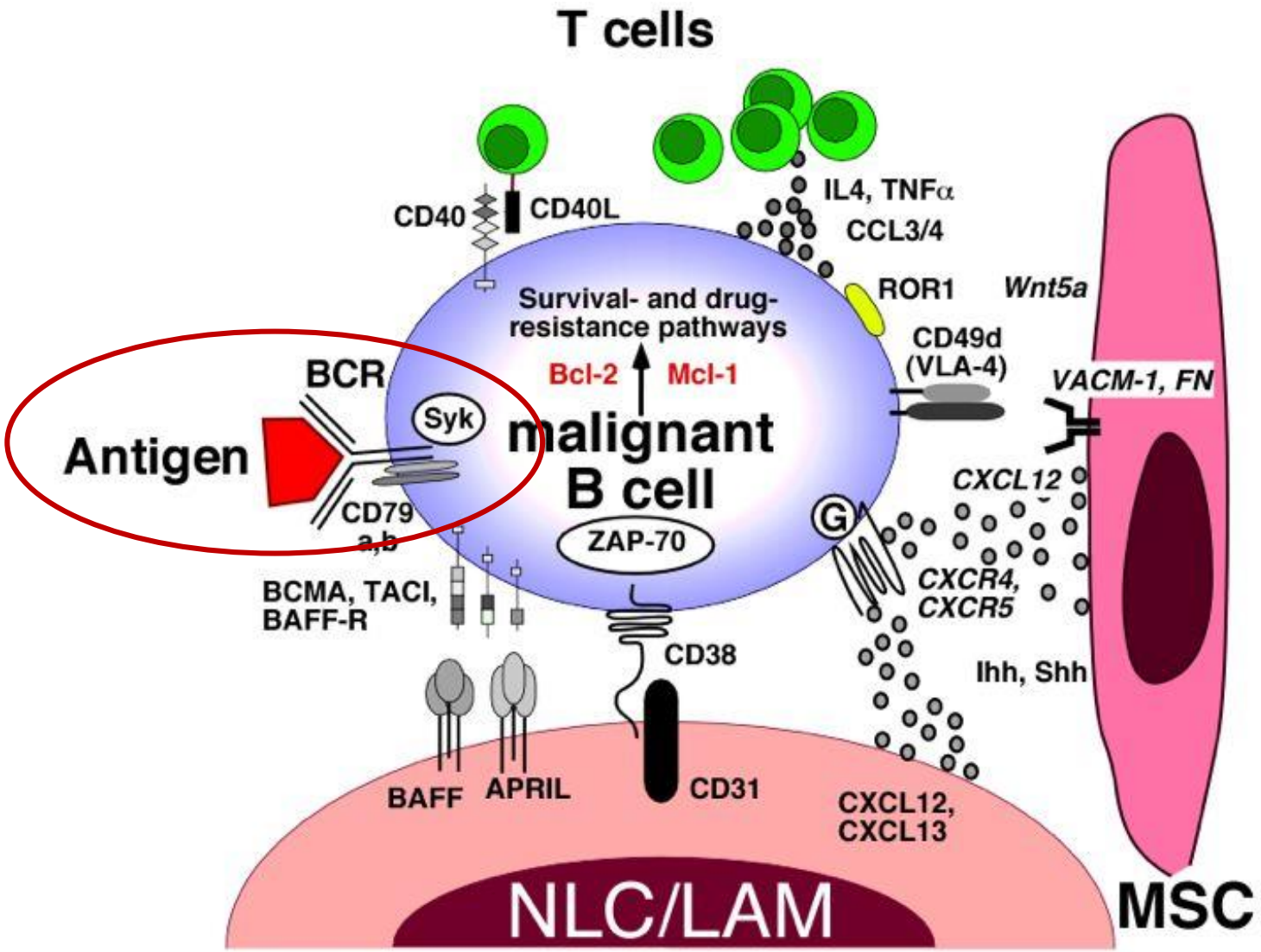

Burger, Ghia et al, Blood, 2009

Target therapies in CLL

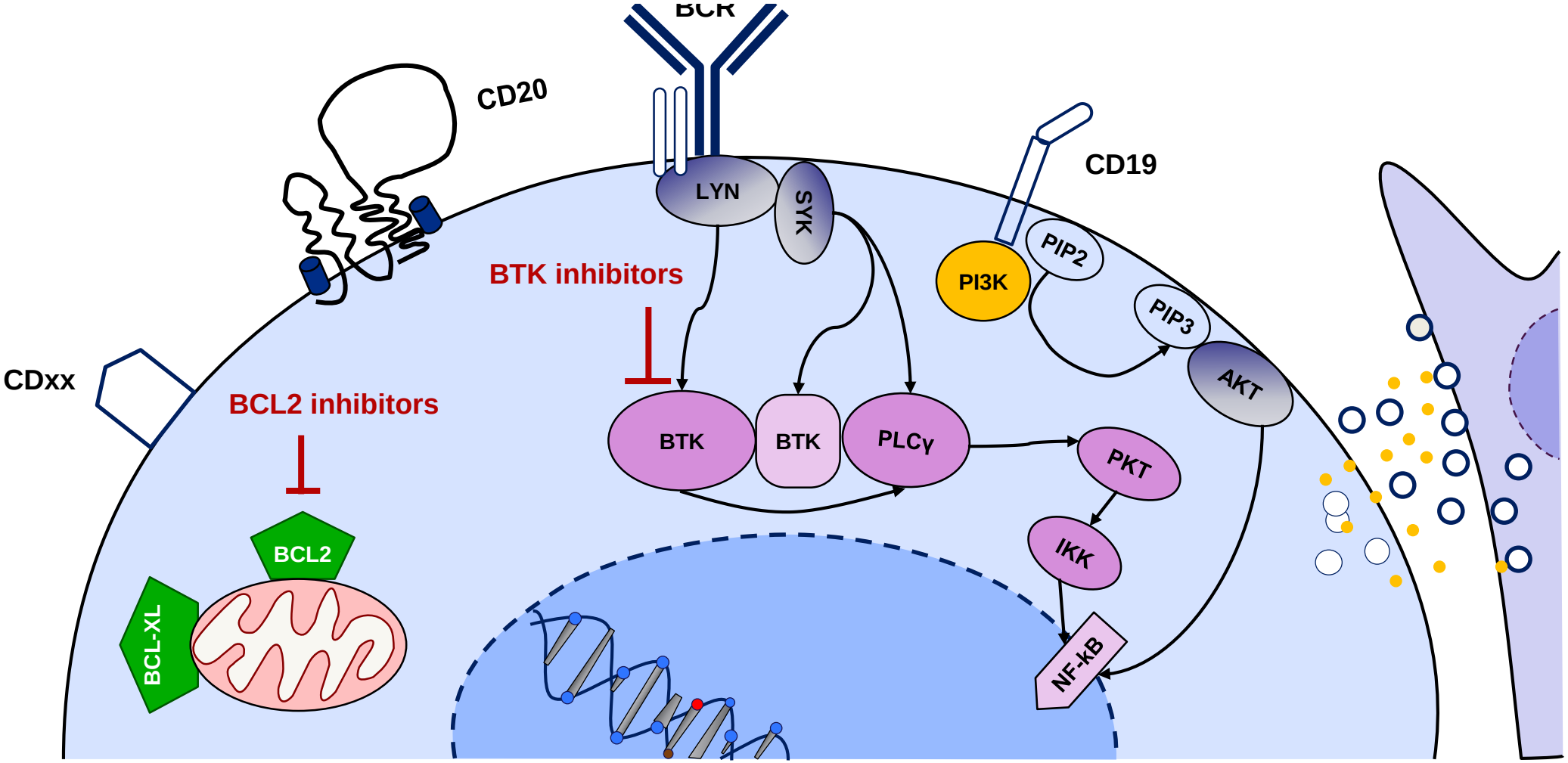

BTK inhibitors

1st generation: Ibrutinib (NEJM 2015)

2nd generation: Acalabrutinib (NEJM 2016; Lancet 2020), Zanubrutinib (Lancet Oncol 2022)

3rd generation: Pirtobrutinib (Lancet 2021, NEJM 2023), Nemtabrutinib

BCL2 inhibitors

1st generation: Venetoclax (NEJM 2016, 2018, 2019)

Cartoon adapted from Byrd J, et al. J Clin Oncol 2014

Overall Survival similar to an Age-Matched Population ≥ 65yy

– OS estimate (8-year) was comparable for the Ibr-treated pts ≥65 years (201 cases) vs age-matched general population (**Figure A**)

– OS estimate (12-year) was also comparable for the overall Ibr-treated 603 cases) vs age-matched general population (**Figure B**).

A

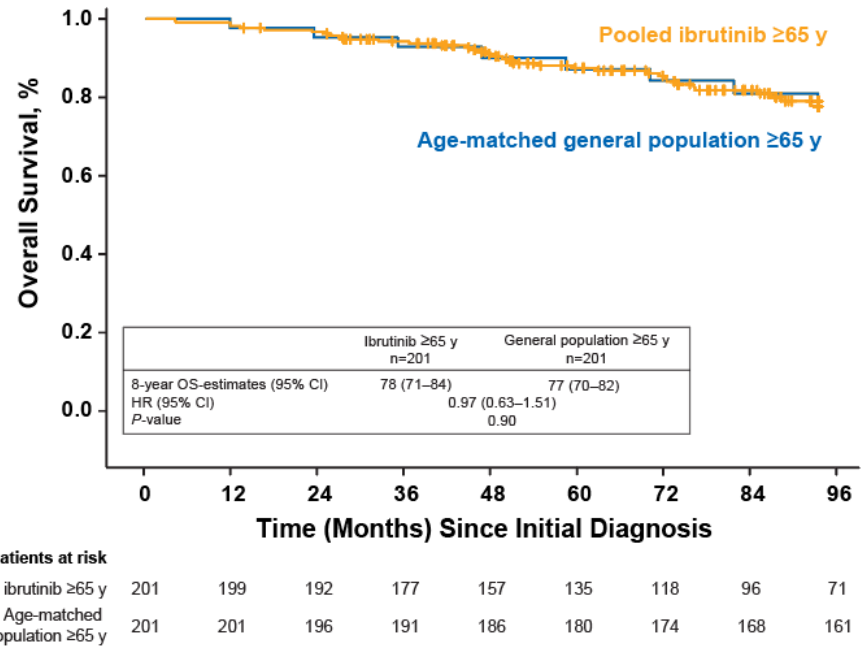

median follow-up of 6.8 years

B

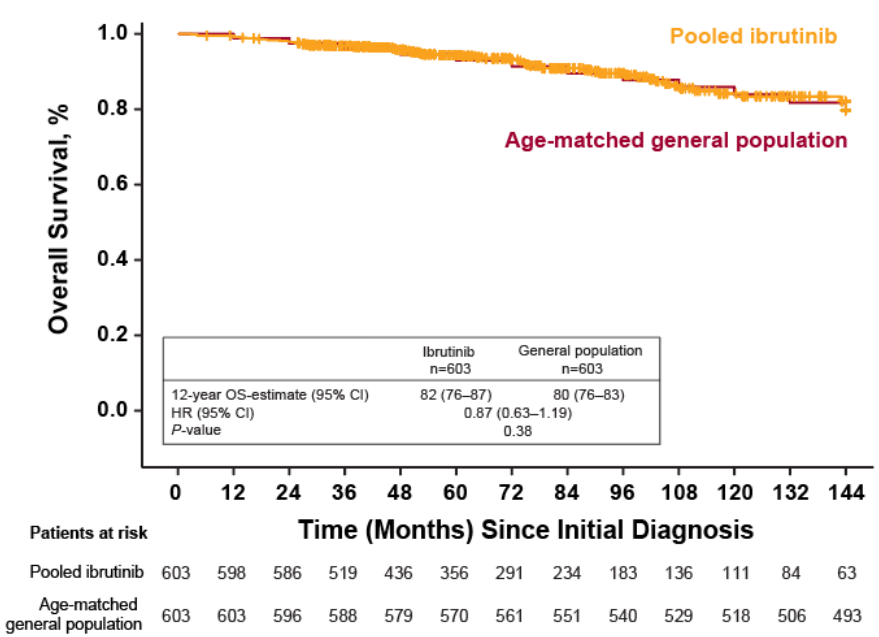

median follow-up of 5.9 years.

[a]*Data after 96 months is not represented in the KM curve;* [b]*Data after 144 months is not represented in the KM curve*

Ghia et al., ASH 2022; P1809 (poster presentation)

CLL 14: Venetoclax + obinutuzumab - *MRD rates and PFS*

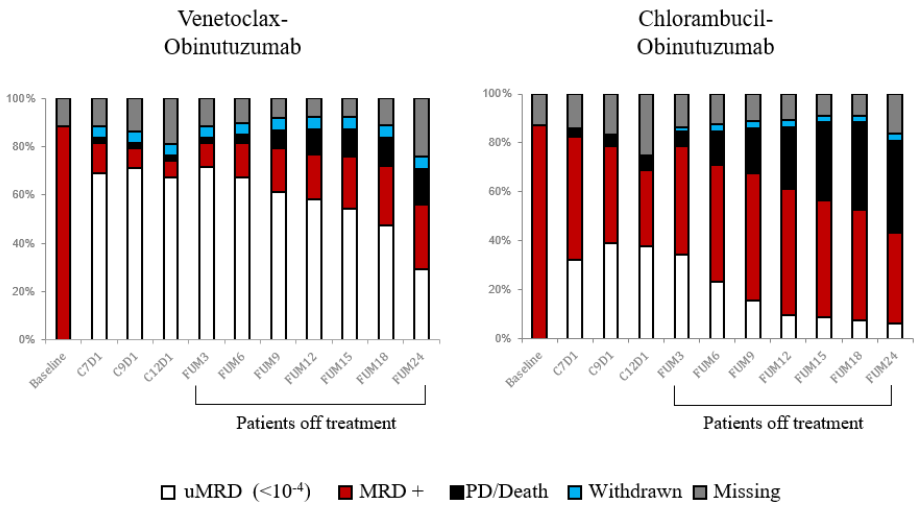

Undetectable MRD by NGS	**Venetoclax-Obinutuzumab**	**Chlorambucil-Obinutuzumab**
Number of patients, N	**216**	**216**
Minimal residual disease level		
$< 10^{-6}$	42 %	7 %
$\geq 10^{-6}$ and $<10^{-5}$	26 %	13 %
$\geq 10^{-5}$ and $<10^{-4}$	11 %	14 %
$\geq 10^{-4}$ and $<10^{-2}$	6 %	23 %
$\geq 10^{-2}$	5 %	29 %
No sample/not evaluable	12 %	14 %

By NGS in peripheral blood 3 months after completion of treatment

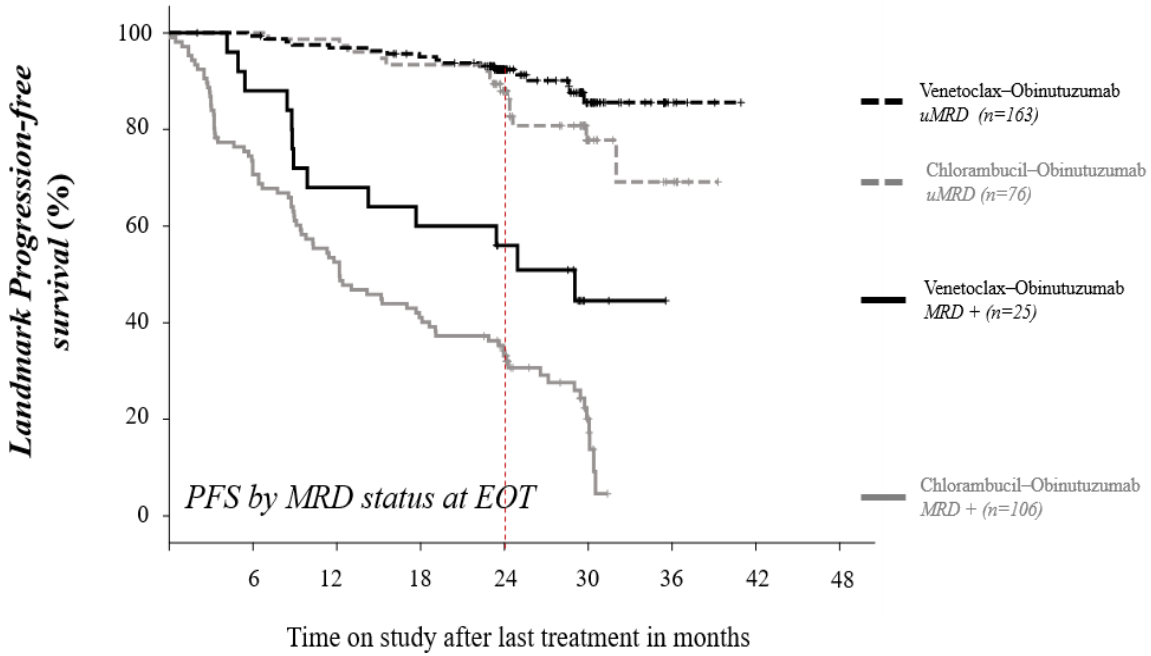

Adaptive Clonoseq assay, cut-off: 10^{-4}, 10^{-5} and 10^{-6}

Fischer et al. N Engl J Med 2019;380:2225-36

Phase 2 CAPTIVATE: study design

CAPTIVATE (PCYC-1142) is an international, multicenter phase 2 study evaluating first-line treatment with 3 cycles of ibrutinib followed by 12 cycles of combined ibrutinib + venetoclax that comprises 2 cohorts: MRD and FD

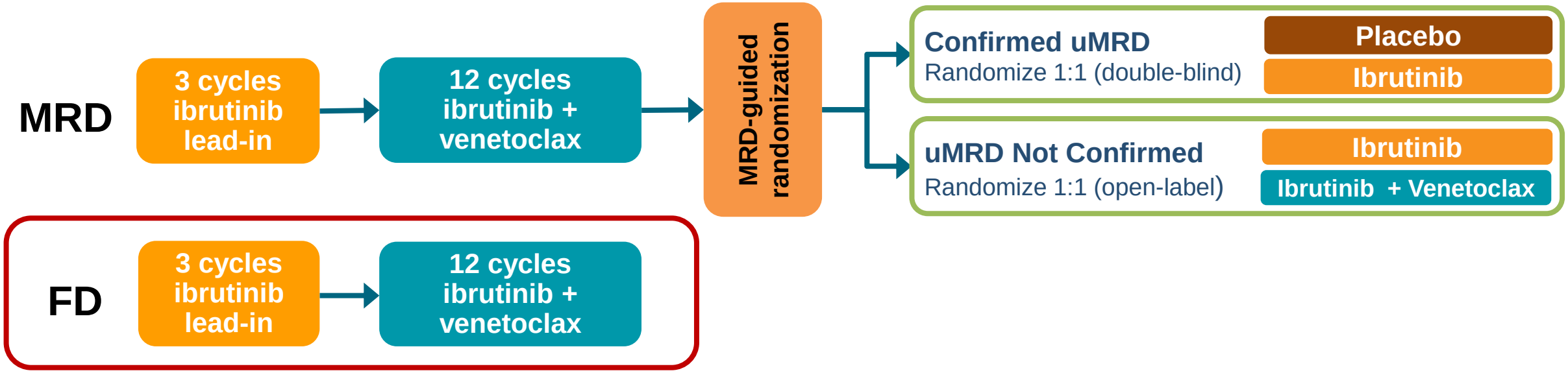

FD: fixed duration

Moreno et al, EHA 2022, P669 (poster presentation); Ghia et al. ASCO 2021, CAPTIVATE-FD; Wierda et al., ASH 2020; 123

Phase 2 CAPTIVATE: 3-years PFS in the FD cohort

Best overall response

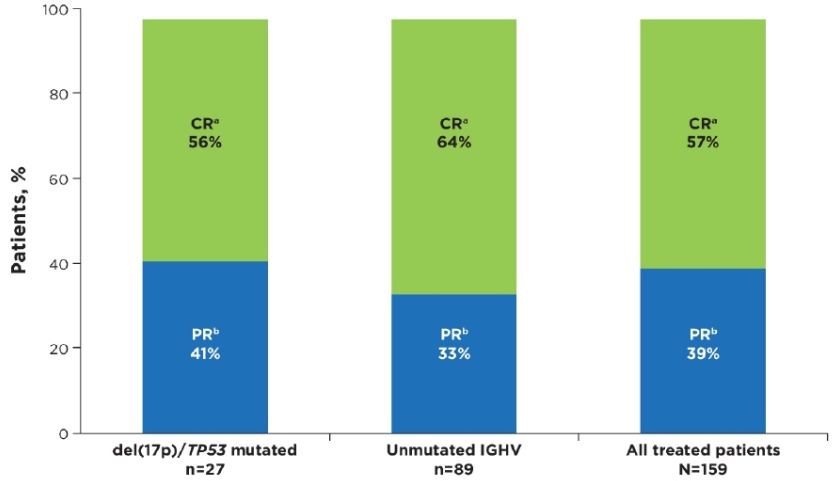

Best uMRD Rates With del(17p)/*TP53*Mut or Unmutated IGHV[a]

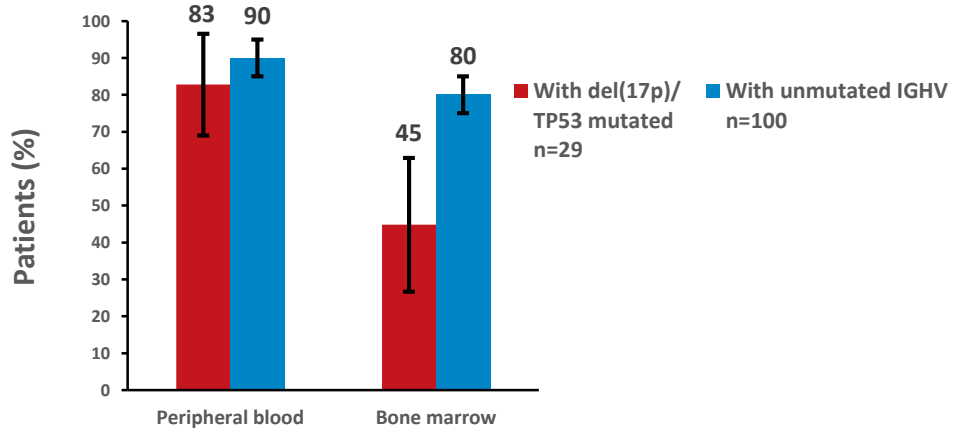

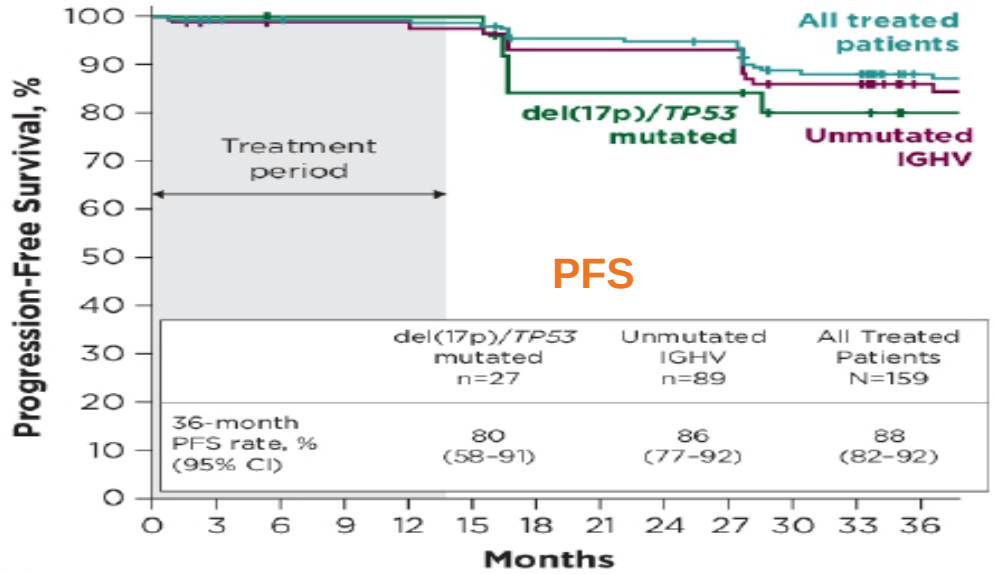

Patients at Risk													
All treated patients	159	155	153	152	152	151	144	144	143	142	131	130	117
Unmutated IGHV	89	86	85	85	85	84	79	79	79	79	72	72	63
del(17p)/ *TP53* mutated	27	27	26	26	26	26	21	21	21	21	18	18	15

Estimated 36-month PFS rates

- Unmutated IGHV: 86% (95% CI 77, 92)
- Del(17p)/TP53mut: 80% (80% CI 58, 91)

CI, confidence interval; CR, complete response; CRi, CR with incomplete bone marrow recovery; DOCR, duration of CR; FD, fixed duration; IGHV, immunoglobulin heavy chain; MRD, minimal residual disease; uMRD, undetectable MRD; PFS, progression-free survival; PR, partial response

Moreno et al, EHA 2022, P669 (poster presentation); Ghia et al. ASCO 2021, CAPTIVATE-FD; Wierda et al., ASH 2020; 123

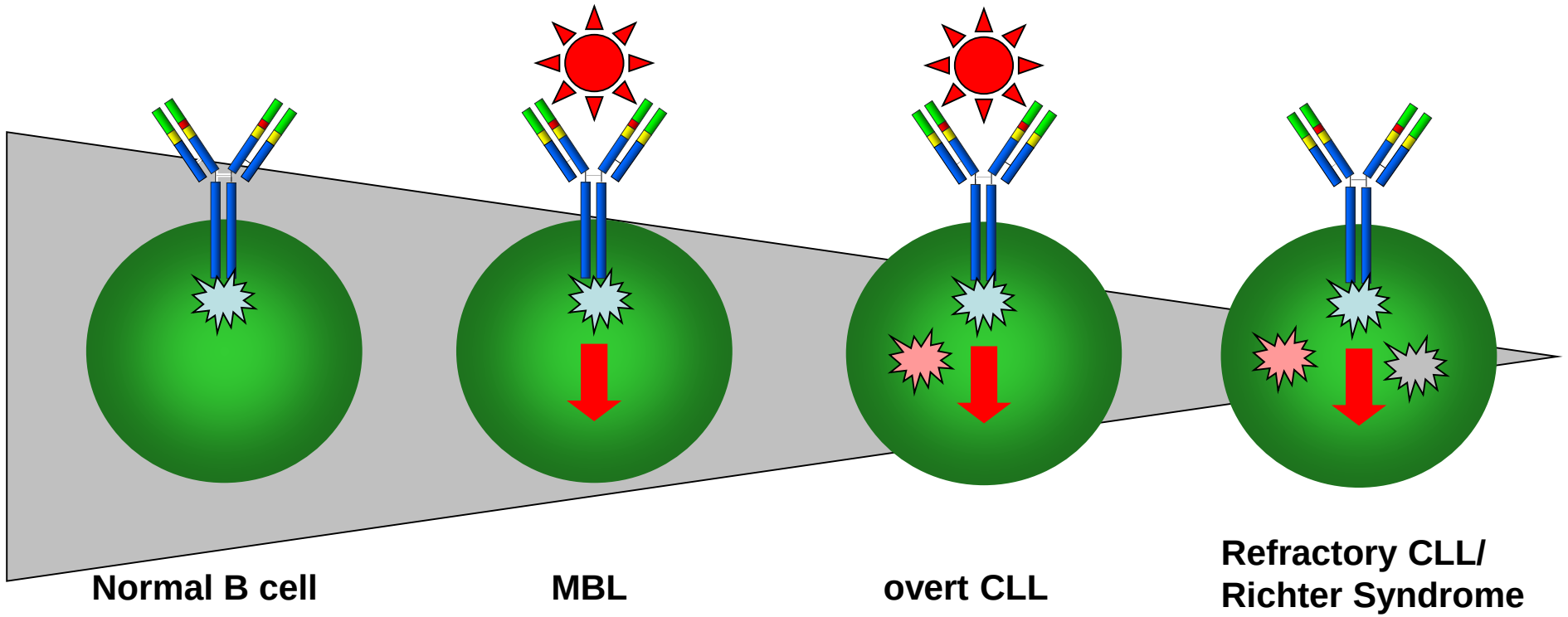
Normal B cell
MBL
overt CLL
Refractory CLL/
Richter Syndrome

Acknowledgments

B Cell Neoplasia Unit

Jessica Bordini
Chiara Lenzi
Alessia Morabito
Michela Frenquelli
Alessandro Campanella
Athanasios Pseftogkas
Francesca Gandini
Silvia Heltai
Daniela Belloni
Caterina Taccetti
Pamela Ranghetti
Eleonora Perotta
Stoli Klaudia
Giulia Milani

Strategic Research Program on CLL

Lydia Scarfò
Elisa Albi
Francesca Martini
Emanuela Sant'Antonio
Antonella Capasso
Maria Colia
Catalina Combi
Eloise Scarano

Center for Omics Sciences -COSR

Francesca Genova
Dejan Lazarevic
Giovanni Tonon

CERTH - Greece

Kostas Stamatopoulos
Fotis Psomopoulos

Karolinska Institute

Richard Rosenquist
Viktor Ljungstrom/Larry Mansouri

Stereotyped HCDR3: a novel therapeutic target?

These **unique and shared** sequences can be exploited as candidate antigens for immunotherapy approaches

CDR3 Subset	Consensus Sequence	MHC class II # binding Peptide *(15-mer)*	DRB1	Binding Score*
1	CARVQWLIHENFDYW	CARVQWLIHENFDYW	*0301 *0701	19 14
	CARAQWLVLLAFDYW	ARAQWLVLL (HLA-A*0201)		20
2	CARDANGMDVW	TAVYYCARDANGMDV	*0701	22
		VYYCARDANGMDVWG	*0301	16
	CAIDRNGMDVW	AVYYCAIDRNGMDVW TAVYYCAIDRNGMDV	*0701 *0701	24 22
6	CARGGQYDYVWGSYRPNDAFDIW	YDYVWGSYRPNDAFD	*0301; *0701	17; 14
	CARGGDYDYVWGSYRPMMLFDIW	YDYVWGSYRPMMLFD	*0301; *0701	16; 22
	CARVLNYDYIWGSYRPINWFDPW	ARVLNYDYIWGSYRP	*0301	20
8	CARQTGYSSSWYGHNWFDPW	CARQTGYSSSWYGHN	*0301; *0701	10; 14
		QTGYSSSWYGHNWFD	*0701	16
	CARHVGYSSSWYGINWFDPW	ARHVGYSSSWYGINW	*0701; *0301	22; 11
	CARIIGYSSSWYGPINWFDPW	IIGYSSSWYGPINWF	*0701	24
		CARIIGYSSSWYGPI	*0301; *0701	20; 22
		ARIIGYSSSWYGPIN	*0301; *0701	11; 22
10	CARHRLGYCSSTSCYYYYYGMDVW	RLGYCSSTSCYYYYY	*0301; *0701	11; 30

: HLA-DRb1;

*: binding score calculated by the SYFPEITHI software (www.syfpeithi.de);

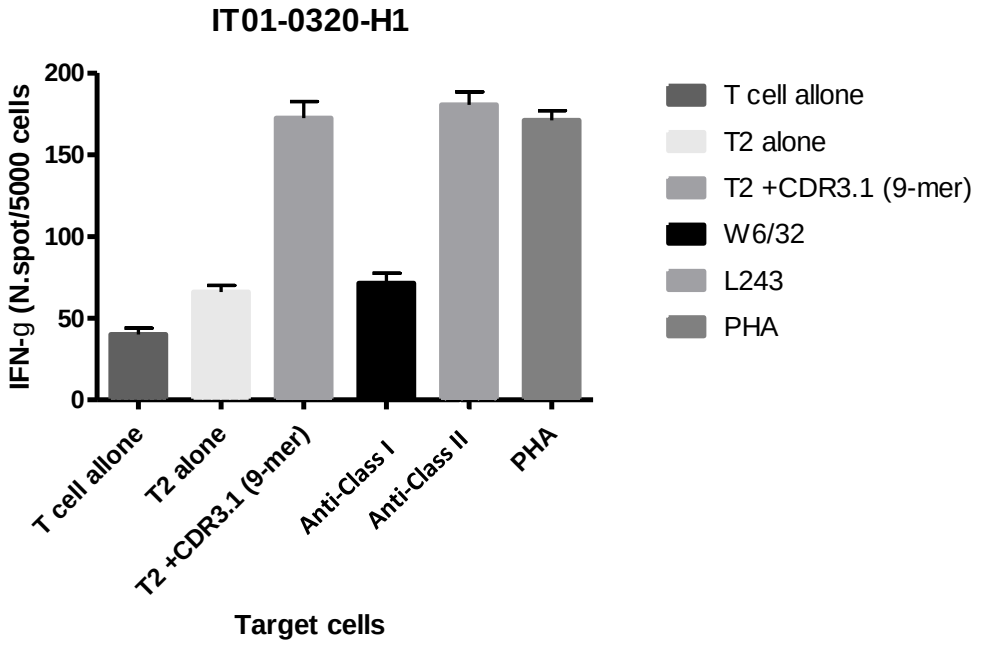

CDR3-derived epitopes can elicit T cell specific responses in patients with CLL *in vitro*

Rovida A, Macalli C et al, 2020 submitted

Stereotyped receptors in Eμ-TCL1 mice

Design of synthetic peptides

N=35 Eμ-TCL1 derived leukemic clones
Identity analysis of CDR3 sequences

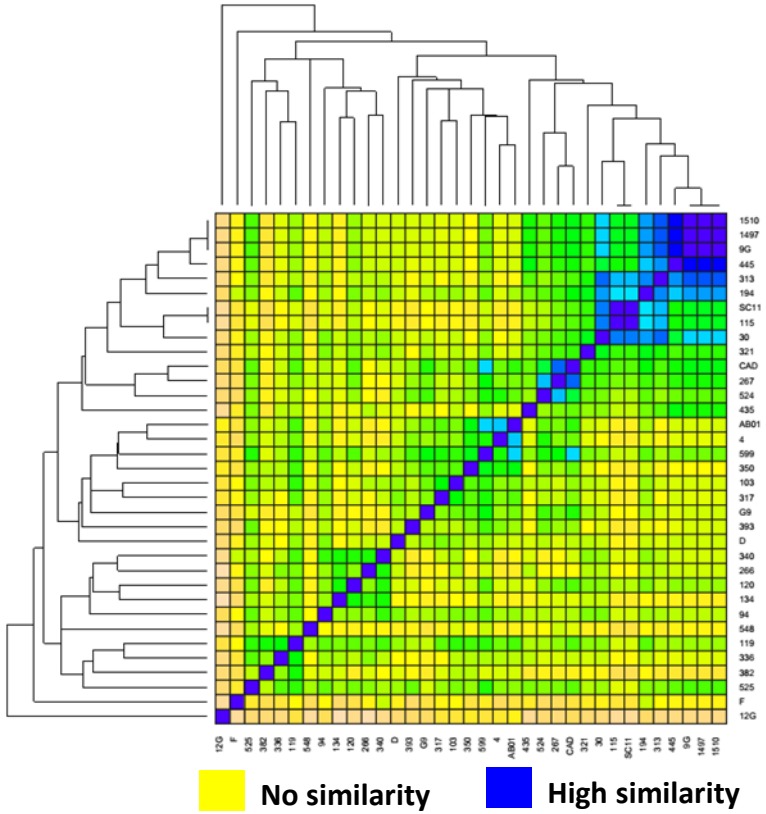

Monoclonal HCDR3 sequence (n=6):

CAGDYDGYWYFNVW

http://www.syfpeithi.de/

Peptide design and synthesis

G D Y D G Y W Y F

Rovida A, Macalli C et al, 2020 submitted

Experimental scheme

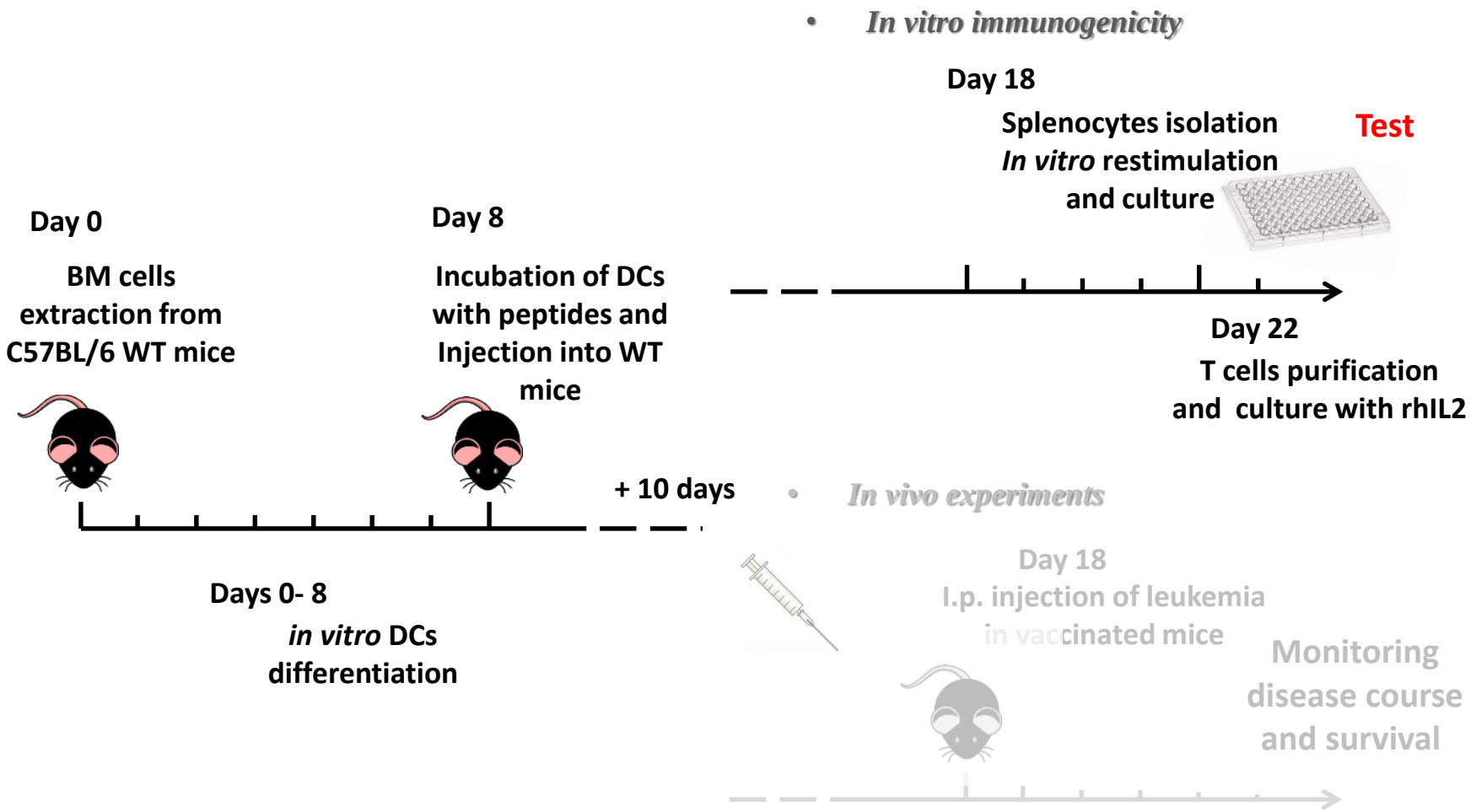

Rovida A, Macalli C et al, 2020 submitted

Experimental scheme

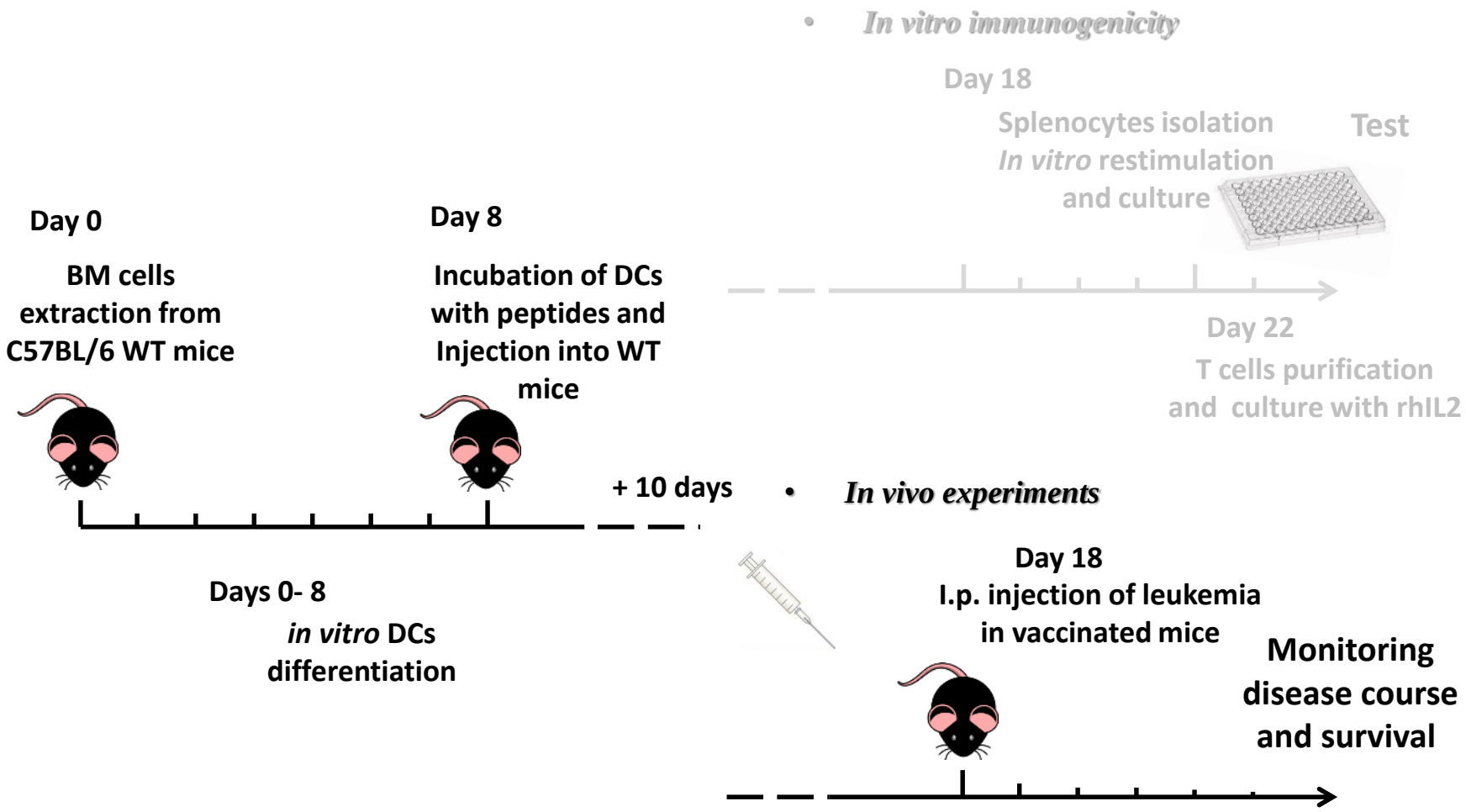

Rovida A, Macalli C et al, 2020 submitted

Stereotyped receptors in Eμ-TCL1 mice

Immunogenicity of synthetic peptides

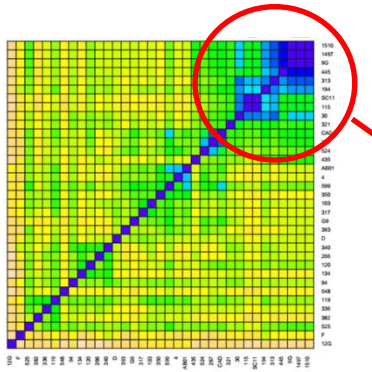

Mouse #	HCDR3 Sequence	Peptide	Peptide Sequence
#445	CAGDYDGYWYFNVW	p445	G D Y D G Y W Y F
#115	CAGDRWGYWYFDVW	-	G D R W G Y W Y F

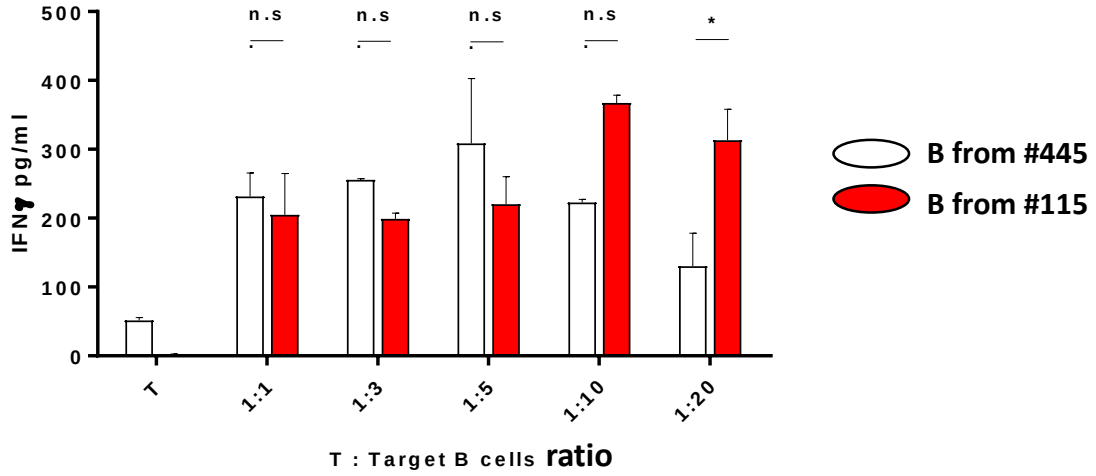

- **The response of T cells is analogous for 2 leukemic clones belonging to the same subset (similar HCDR3)**

Rovida A, Macalli C et al, 2020 submitted

In vivo prophylactic vaccine against murine CLL

Leukemia #350

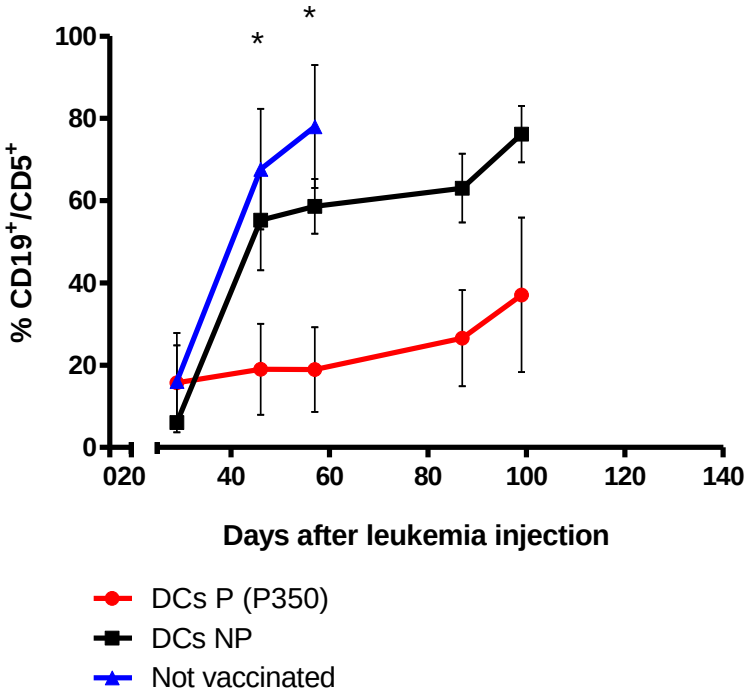

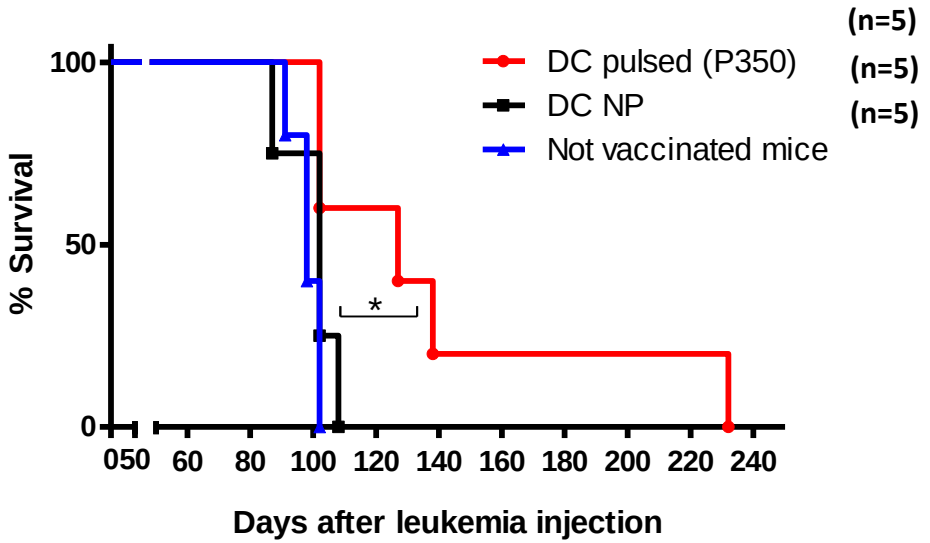

Median survival (days): **DCs P**: 127; **DC NP**: 102; **NV**: 98

The prophylactic vaccine inhibited the growth of leukemic CD19⁺/CD5⁺ clone in the PB of Eμ-TCL1 transplanted mice and increased the overall survival

Rovida A, Macalli C et al, 2020 submitted

In vivo prophylactic vaccine against murine CLL

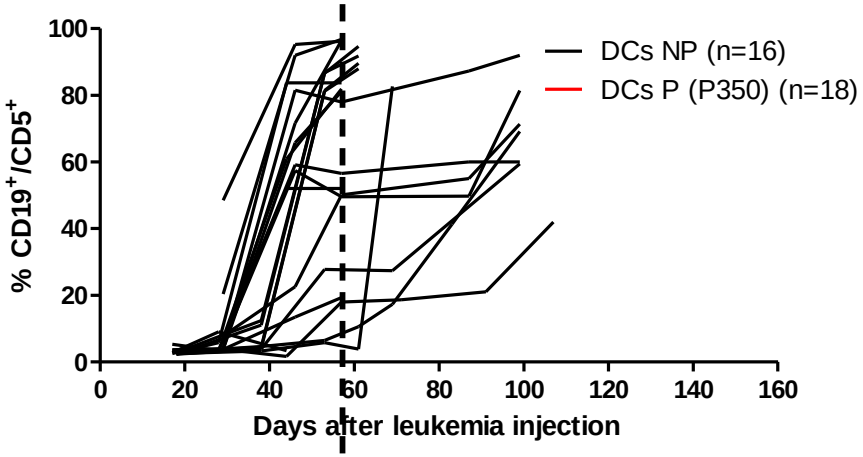

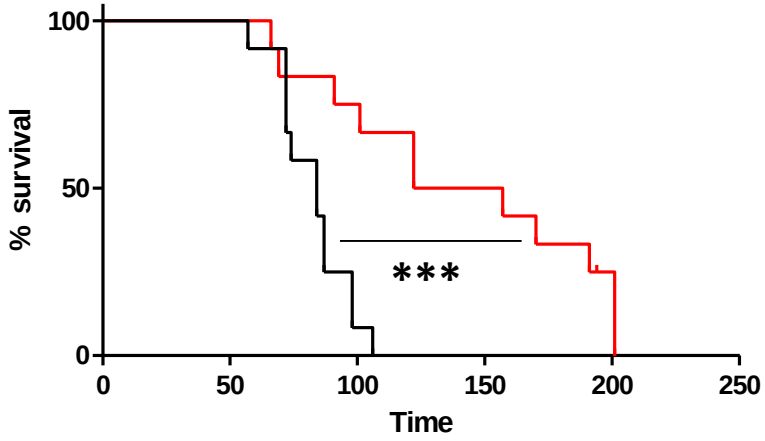

Median survival (days):
DCs P (P350) 139; DCs NP 84

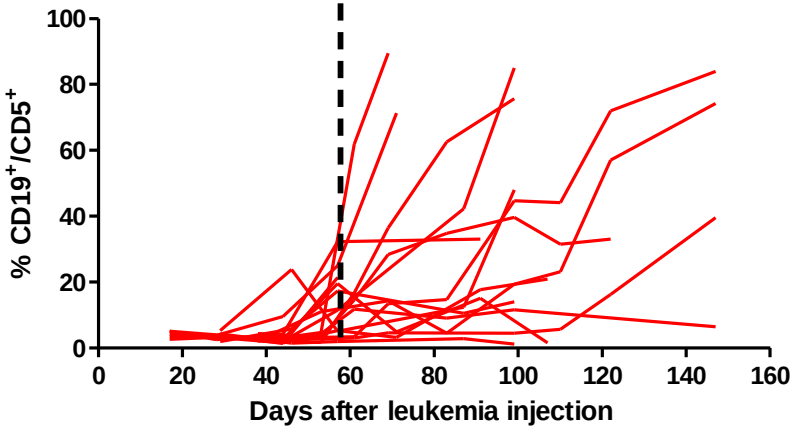

Leukemia #350

Rovida A, Macalli C et al, 2020 submitted

IMPROVE: Intensification in patients CLL who need it

Study design

- **Phase 2 single-arm** interventional study
- **Relapsed/refractory** patients with CLL, **naïve to BTK and BCL2 inhibitors** (previous treatment with **PI3Kδ inhibitors allowed**)
- **Primary objective: efficacy** of the addition of ibrutinib to venetoclax in terms of **MRD**

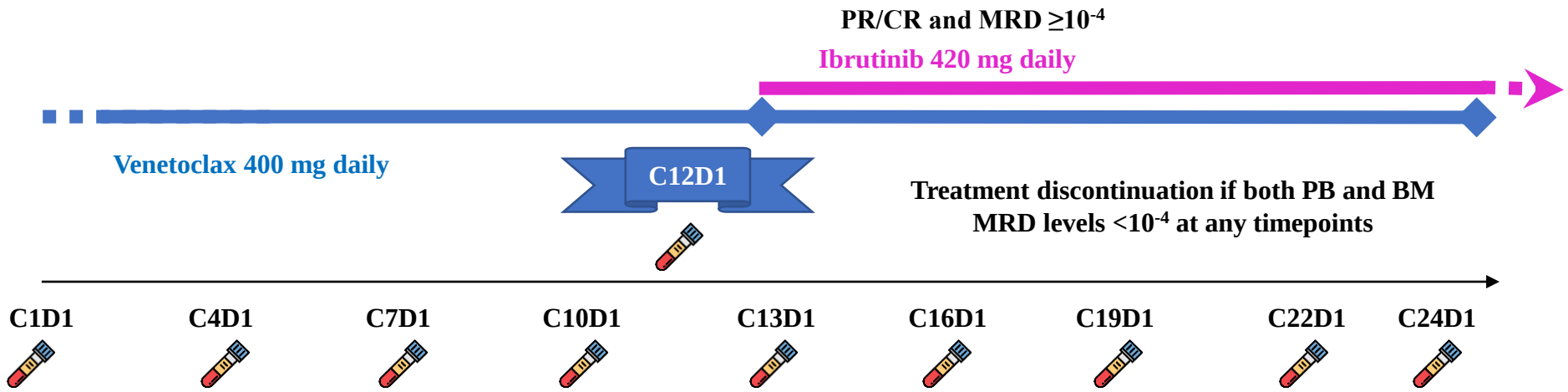

6-color flow cytometry ERIC panel including CD5/CD81/CD43/CD19/CD20/CD79b *Scarfò et al, iwCLL 2019*

Target CLL cells in the 3D model with Ibrutinib

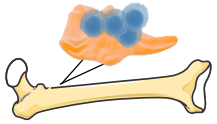

CLL cells inside the scaffold

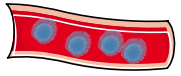

CLL cells outside the scaffold

Confocal microscopy

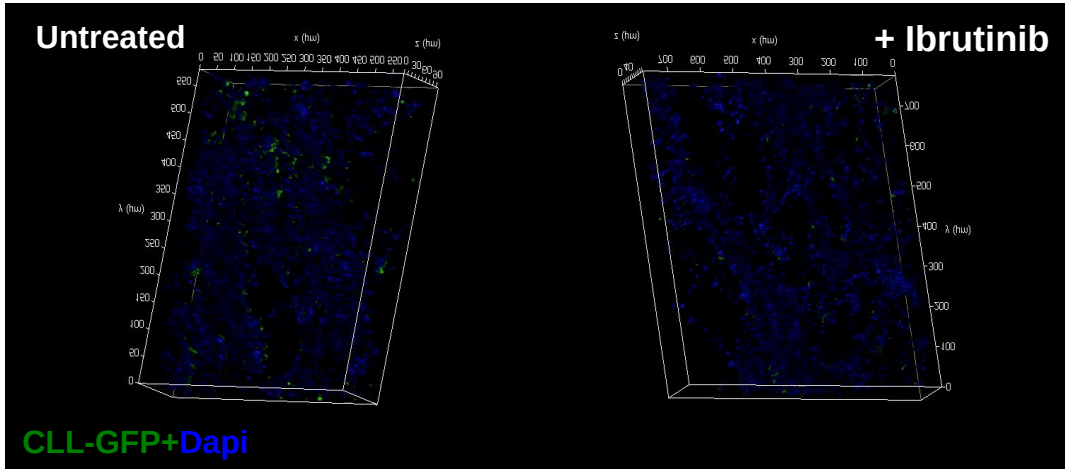

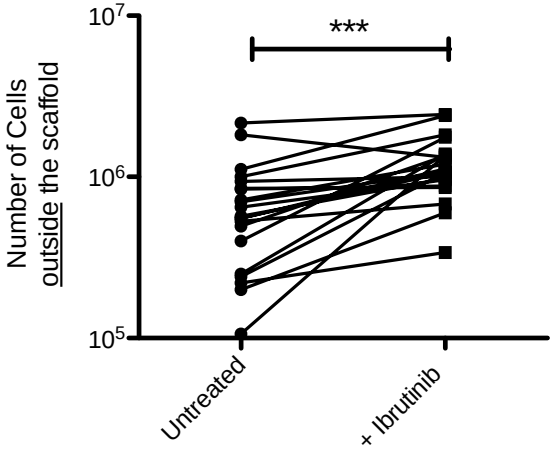

Barbaglio F, Belloni D […] Scielzo. Submitted

What about non-stereotyped BcR? The case of IGHV1-69

The most frequent gene (90% IG-unmutated)

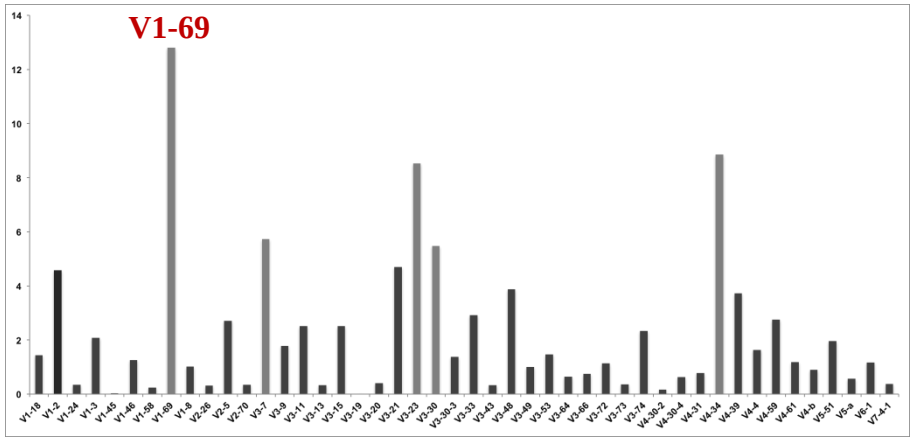

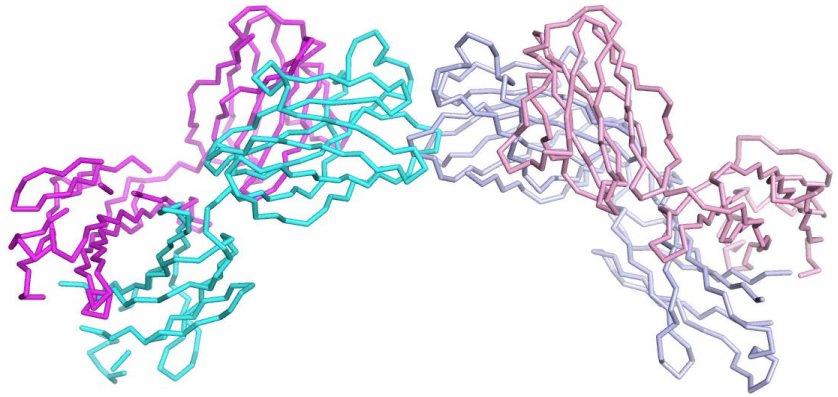

Aggressive outcome

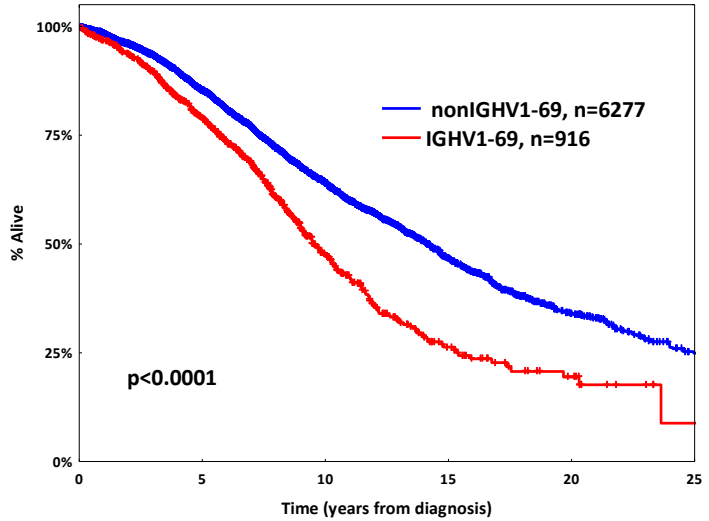

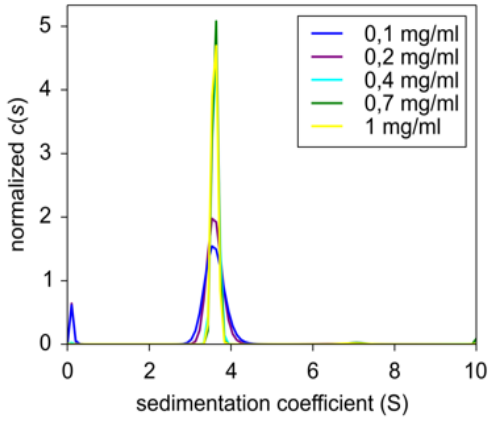

Johnson et al. J Immunol 1997 | Fais et al. J Clin Invest 1998
Widhopf et al. Blood 2004 | Agathangelidis et al. Blood 2012

Baliakas et al. Lancet Haematol 2014

Minici, Gounari et al, unpublished

A non-stereotyped CLL BcR

- **Homotypic interactions mediated by HCDR1 and FR3**

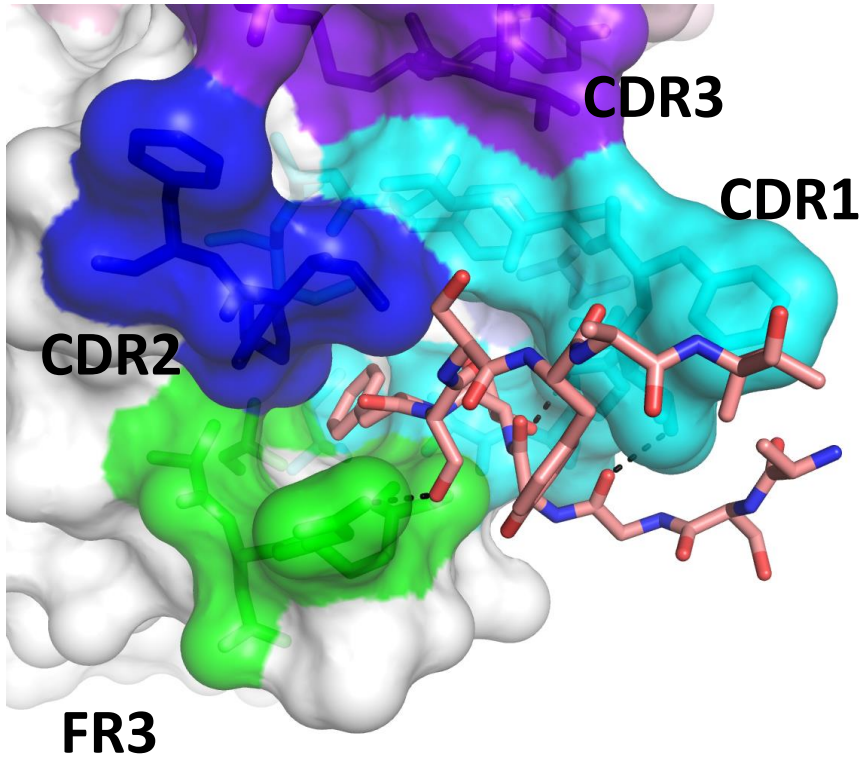

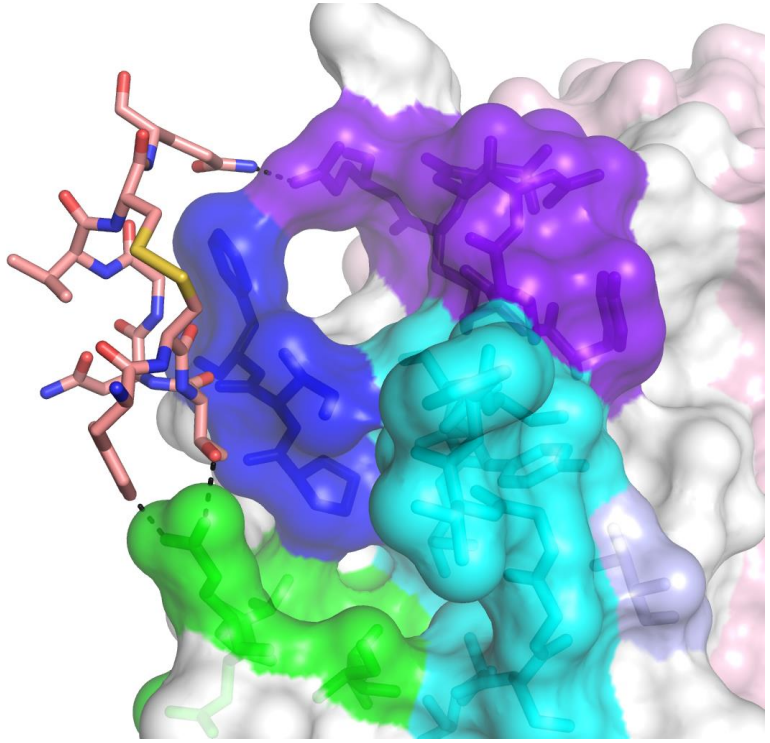

Minici, Gounari et al, unpublished

BcR anergy is modulated by TLR signalling

TLR triggering elicits responses

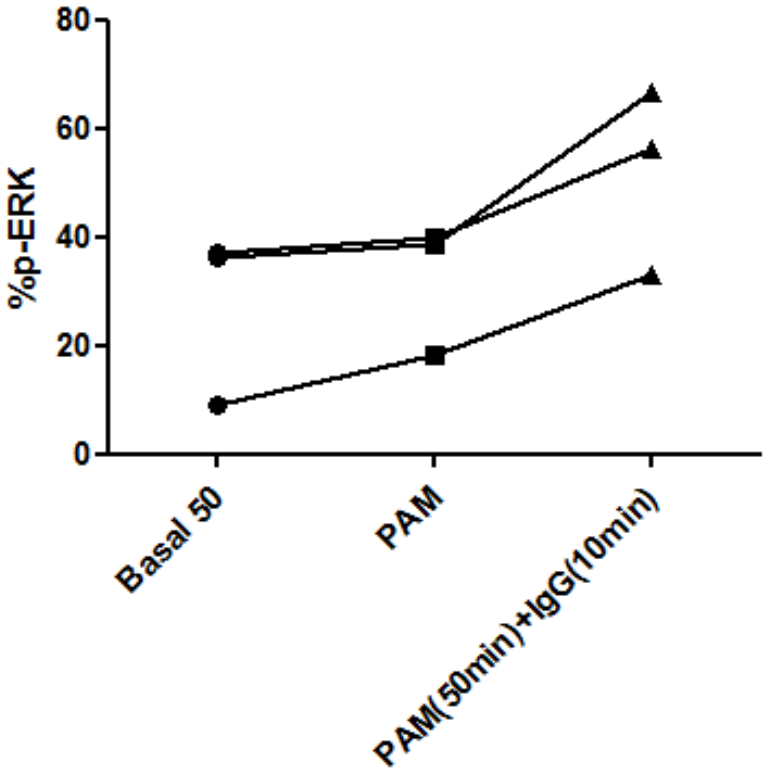

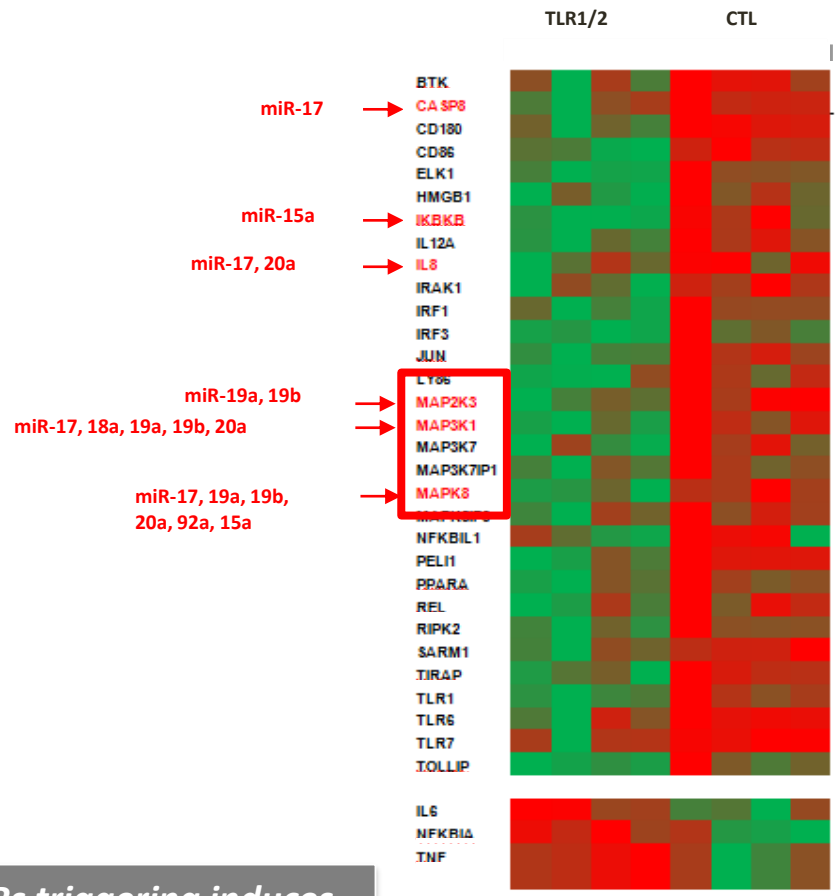

TLRs triggering induces a distinctive gene expression program miR-17~92 involvement

Ntoufa et al, J. Immunol 2016

BTK: essential effector of multiple B-cell processes

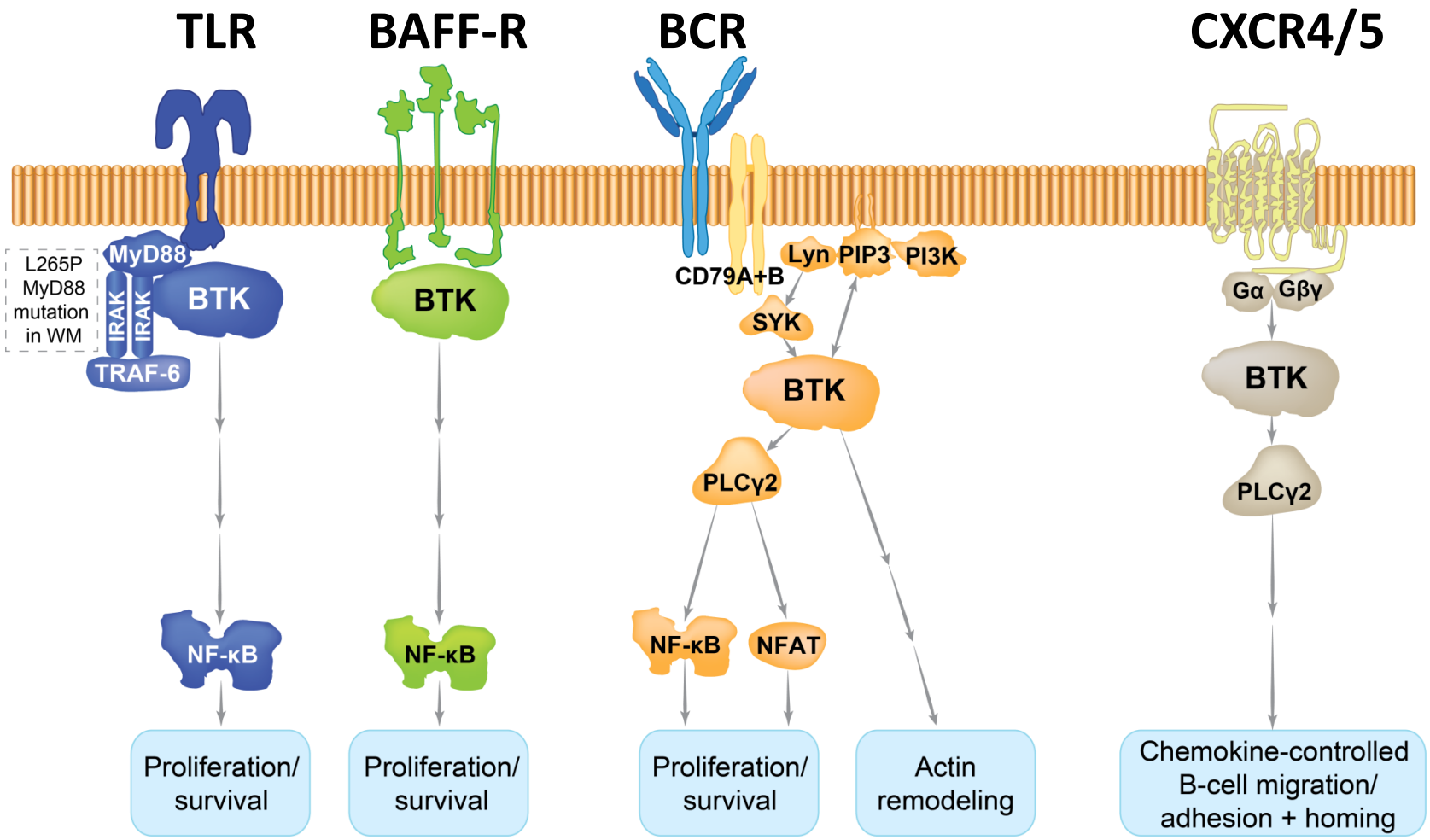

The phosphorylation status of MAP kinases (pERK, pJNK, pp38), pIKK, STATs, BTK and PLCγ2 decreased at 1 month of treatment.

pJNK

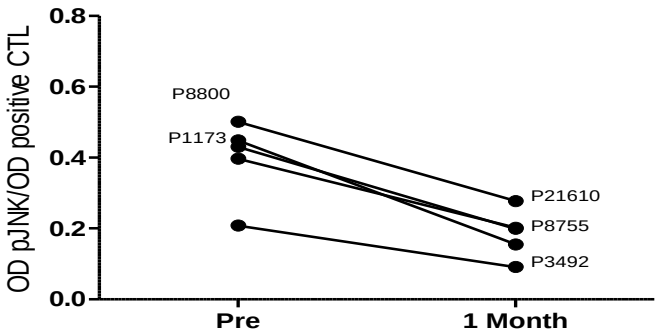

pp38

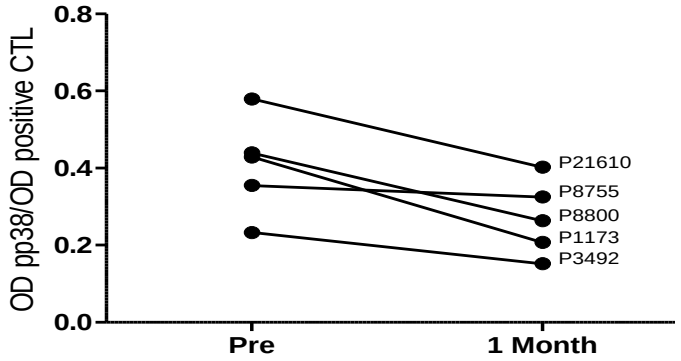

pSTAT1

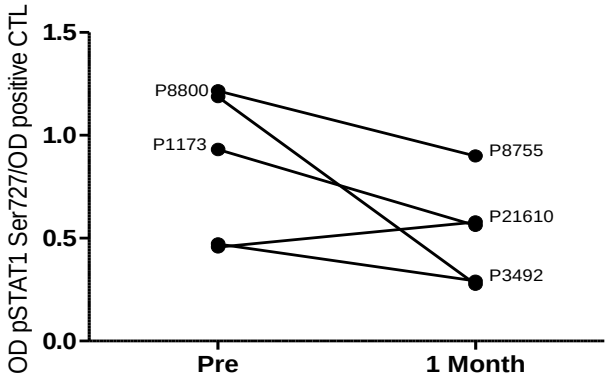

Gounari et al. Leukemia 2019

Significant decrease in BcR signaling capacity under treatment

Reduction of calcium flux upon BcR cross-linking

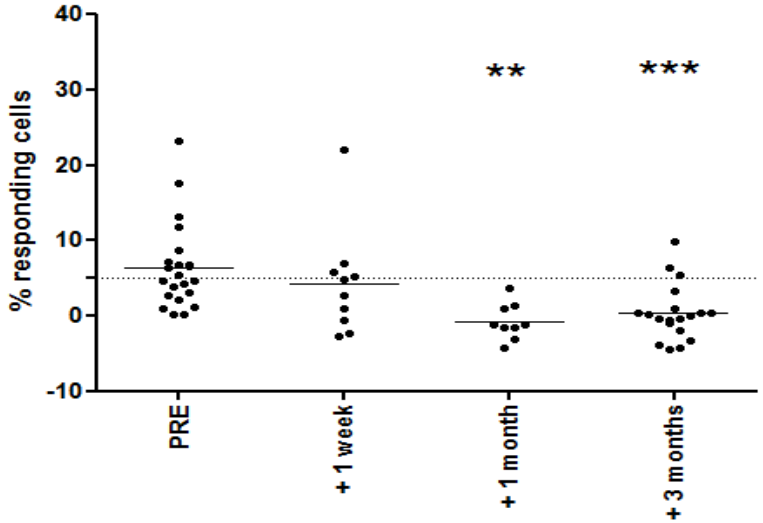

Inability to increase phosphorylation of signaling molecules

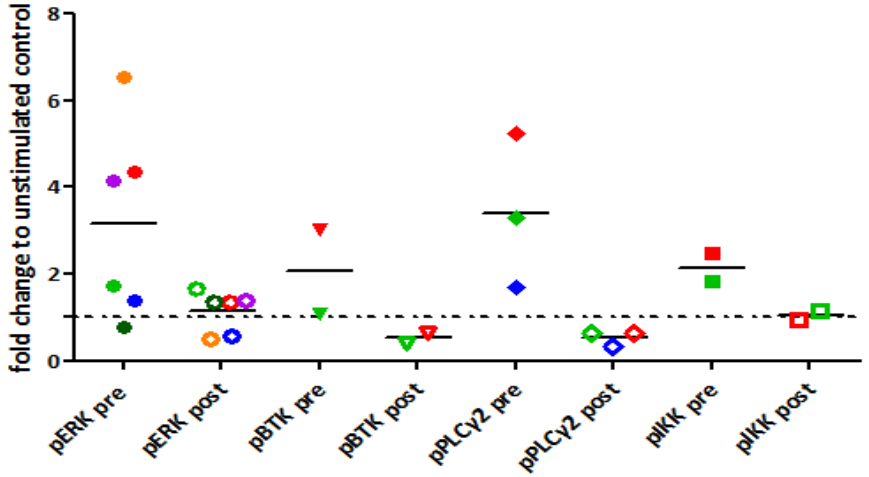

Gounari et al. Leukemia 2019

Differential responses to TLR stimulation

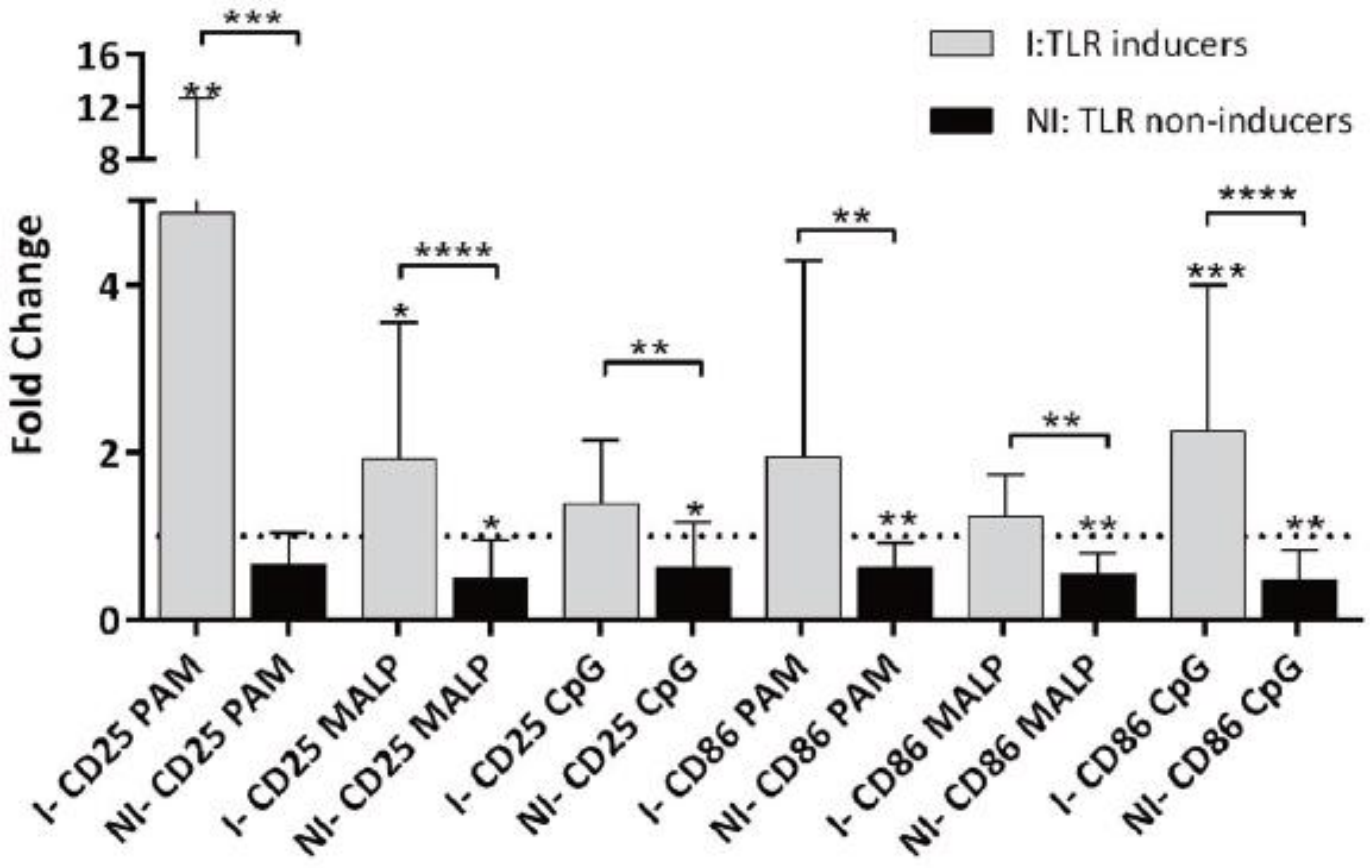

Gounari et al. Leukemia 2019

TLR signaling capacity under ibrutinib associates with outcome

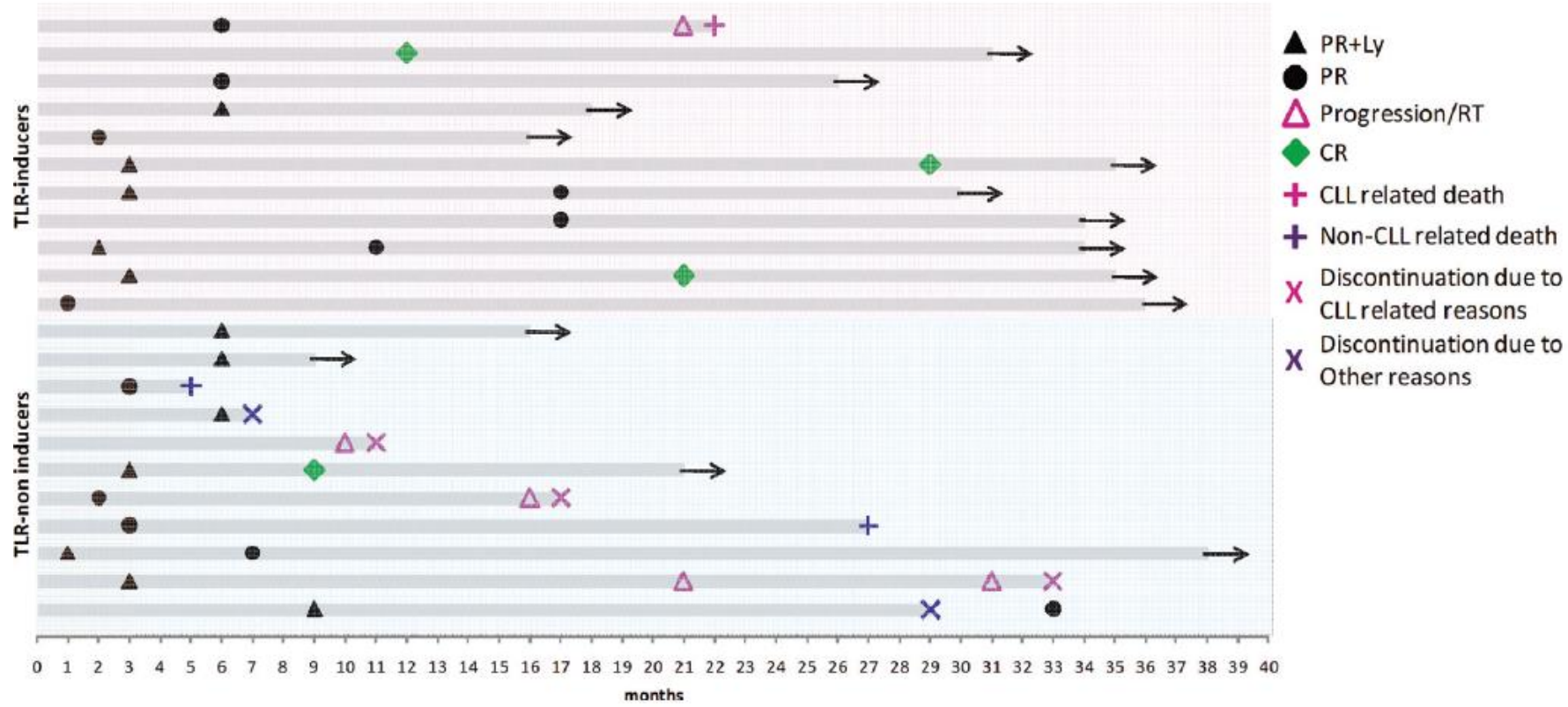

Gounari et al. Leukemia 2019

Subset 8

V gene	N1	D gene	N2	J gene

Subset 8:

- expresses IGHV4-39/IGKV1(D)-39 BcR IG
- is G-switched
- carry long and positively charged VH CDR3s
- AGGRESSIVE/BCR RESPONSIVE→ RICHTER SYNDROME

Subset 8 CLL are at higher risk of RS

Sample	Diagnosis	Subset	IGHV	IGHD	IGHJ	% homology	HCDR3 aa sequence
3542	RS	Murray 8	IGHV4-39*01	IGHD6-13*01	IGHJ5*02	100	CAASRGYSSGWYEGVNWFDPW
5675	RS	Murray 8	IGHV4-39*01	IGHD6-13*01	IGHJ5*02	100	CARIYGYSSSWYGGSNWFDPW
7342	RS	Murray 8	IGHV4-39*01	IGHD6-13*01	IGHJ5*02	99.10	CARSMGYSSSWYGGGNWFDPW
7599	RS	Murray 8	IGHV4-39*01	IGHD6-13*01	IGHJ5*02	100	CARRSGYSSSWYALKNWFDPW
7842	RS	Murray 8	IGHV4-39*01	IGHD6-13*01	IGHJ5*02	100	CARMTGYSSSWYKRD-WFDPW
5889	Non-transformed CLL	Murray 8	IGHV4-39*01	IGHD6-13*01	IGHJ5*02	100	CARRVGYSSSWYGQKNWFDPW
VG_770	Non-transformed CLL	Murray 8	IGHV4-39*01	IGHD6-13*01	IGHJ5*02	100	CARITGYSSSWFAS-NWFDPW

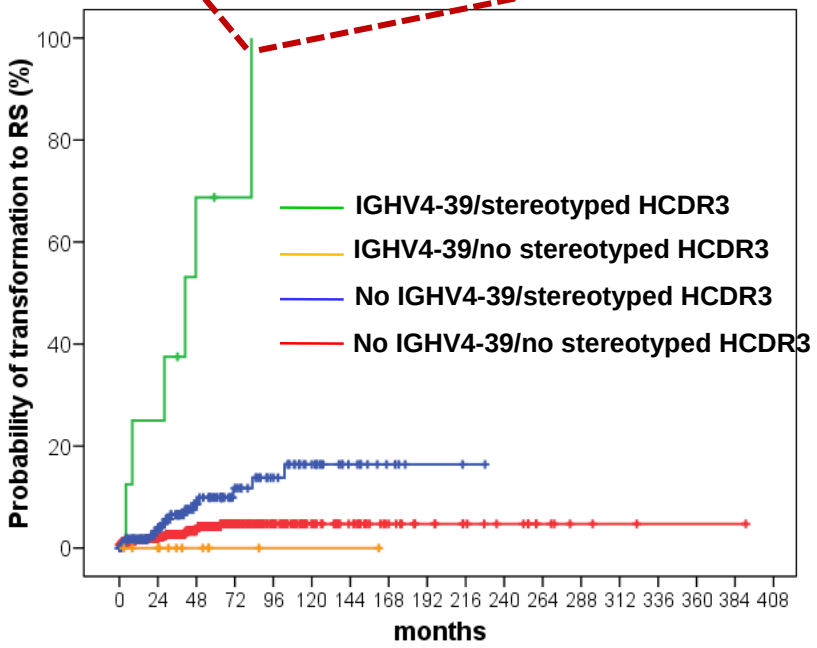

HR and 95% CI

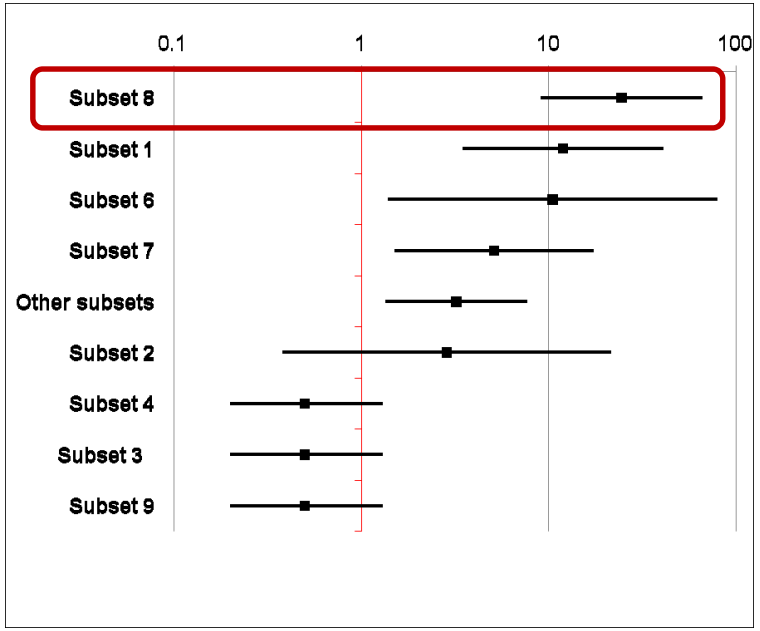

Rossi et al, Clin Cancer Res 2009

Subset #8 respond avidly via the BcR

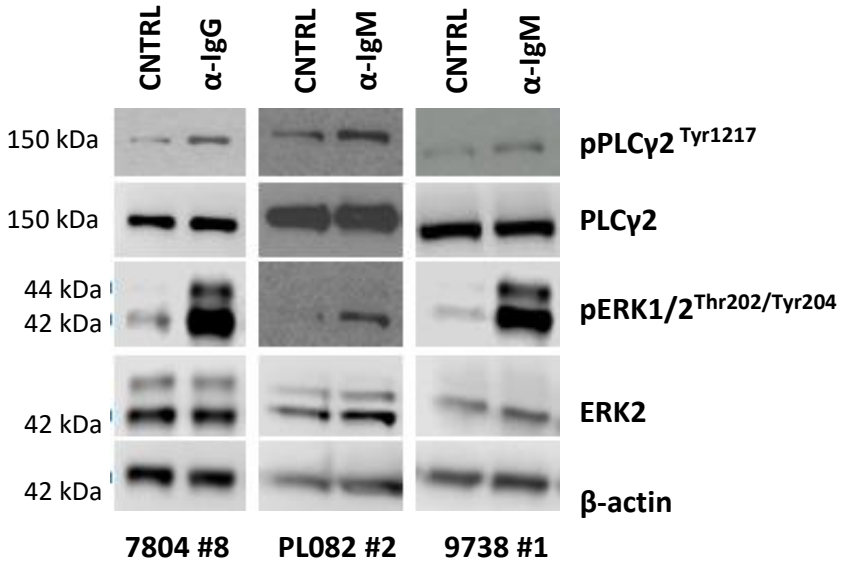

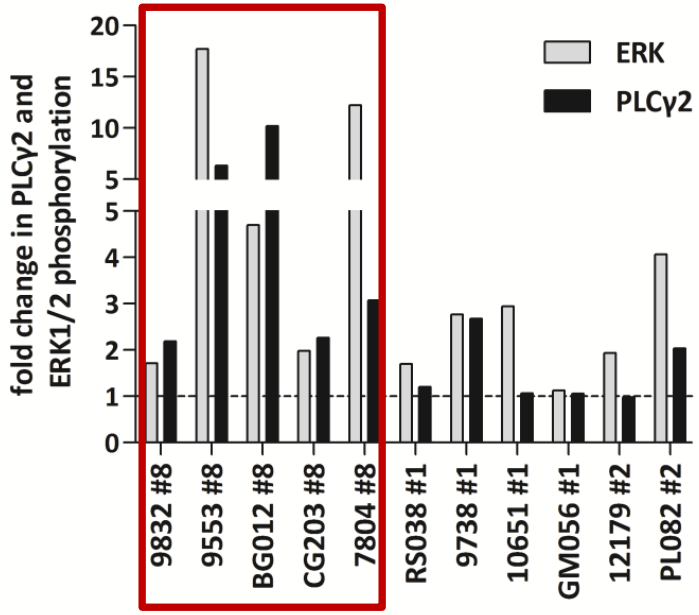

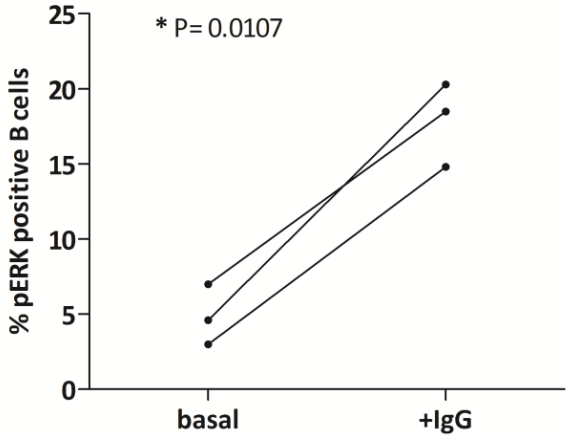

Subset #8 CLL mAbs bind microbial epitopes

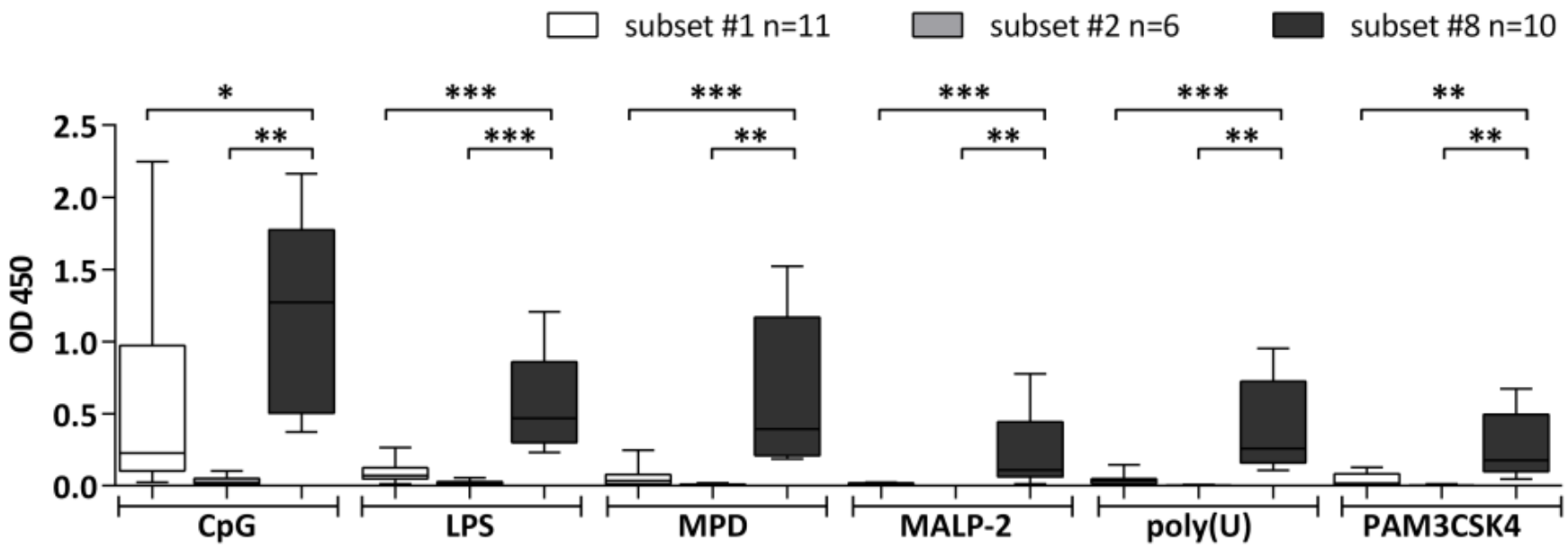

Gounari et al, Blood, 2015

#8 reacts against autoantigens and neoepitopes

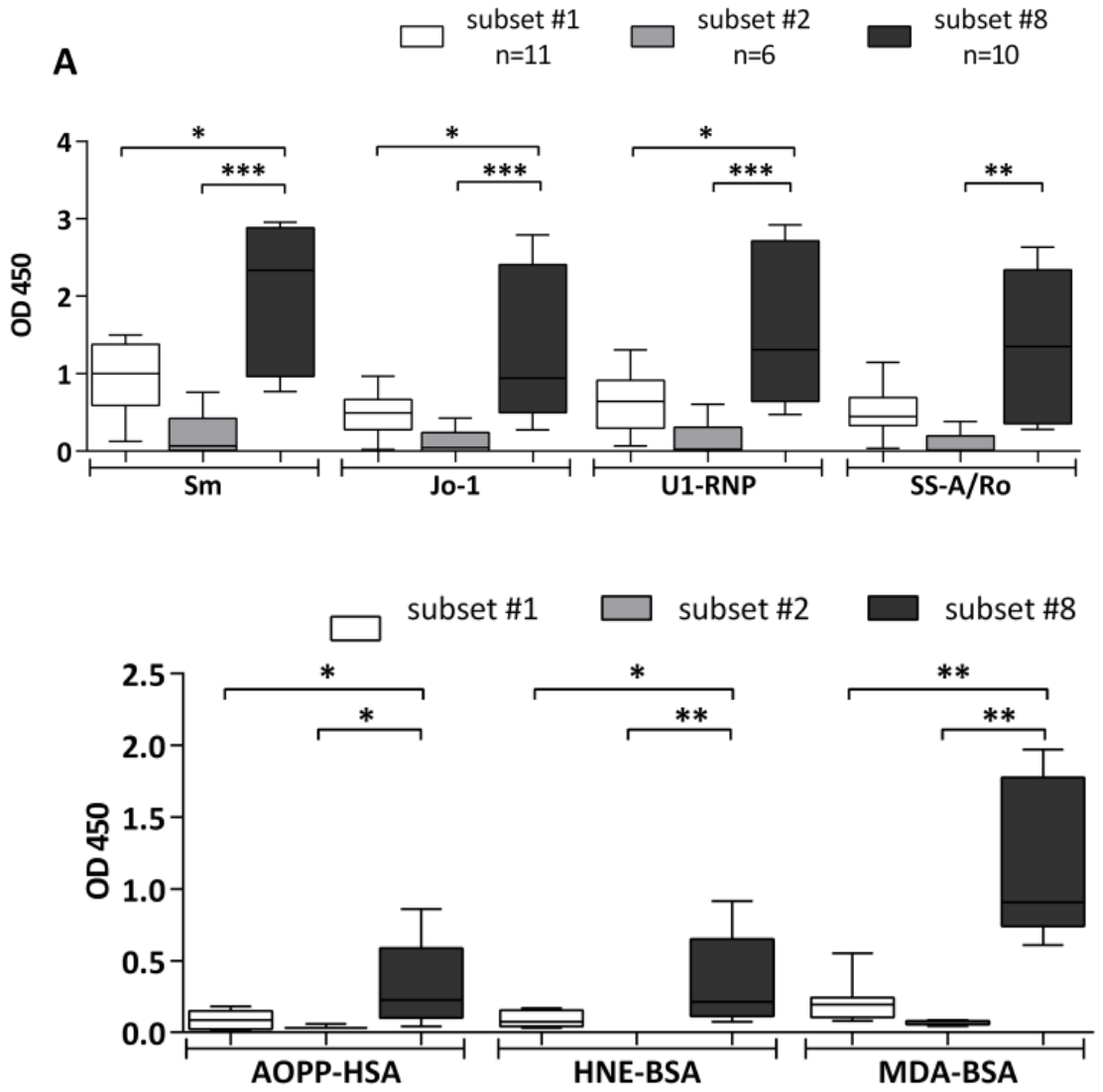

Gounari et al, Blood, 2015

Subset #8: self recognition of CLL Fab

p1615

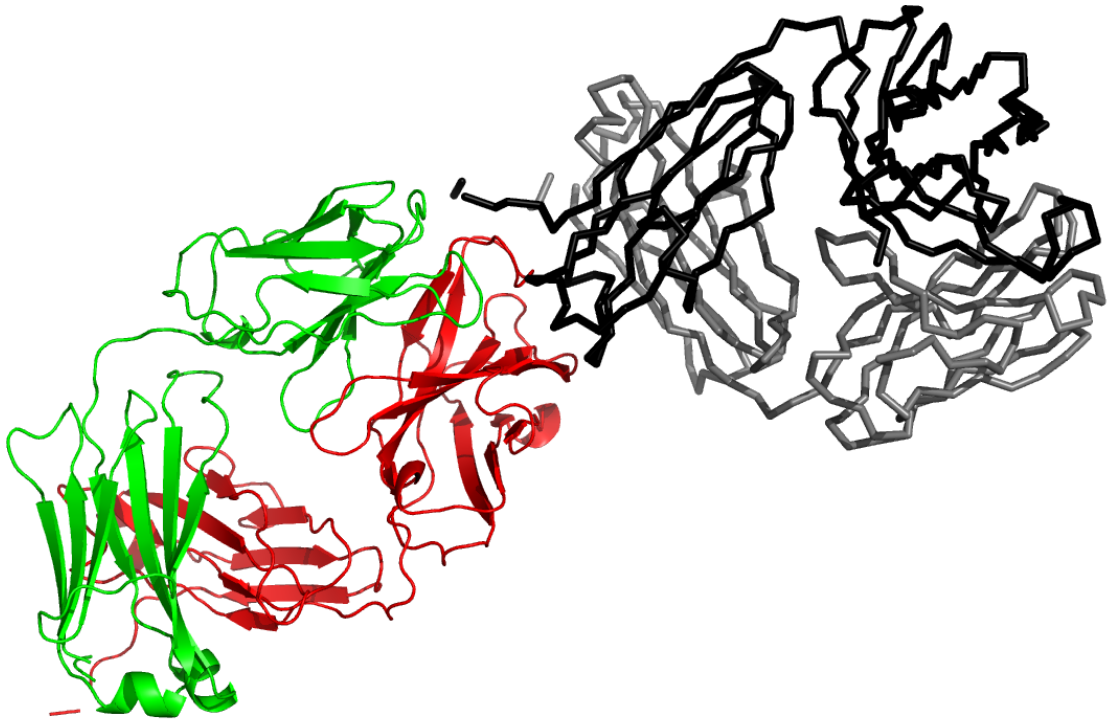

Interaction with the CL and C_{H1} domain of the “antigen” molecule

Minici, Gounari et al, unpublished, 2016

Subset #8: CLL p1615 sedimentation velocity

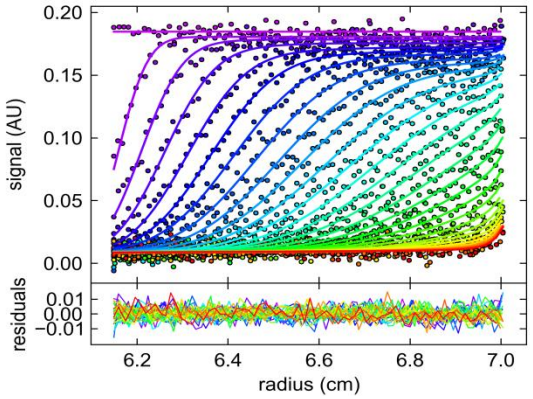

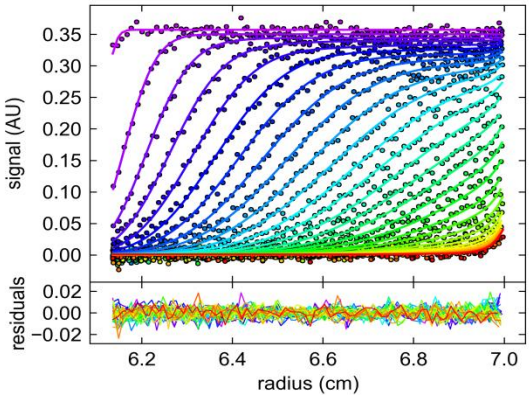

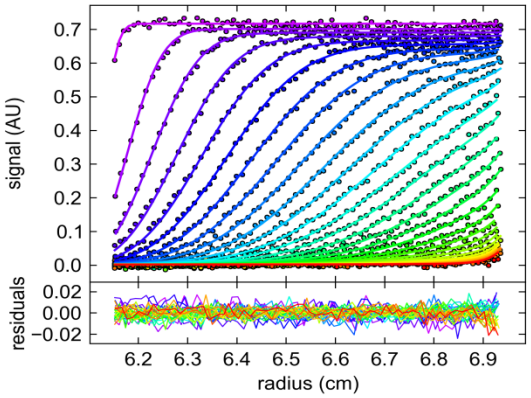

p1615

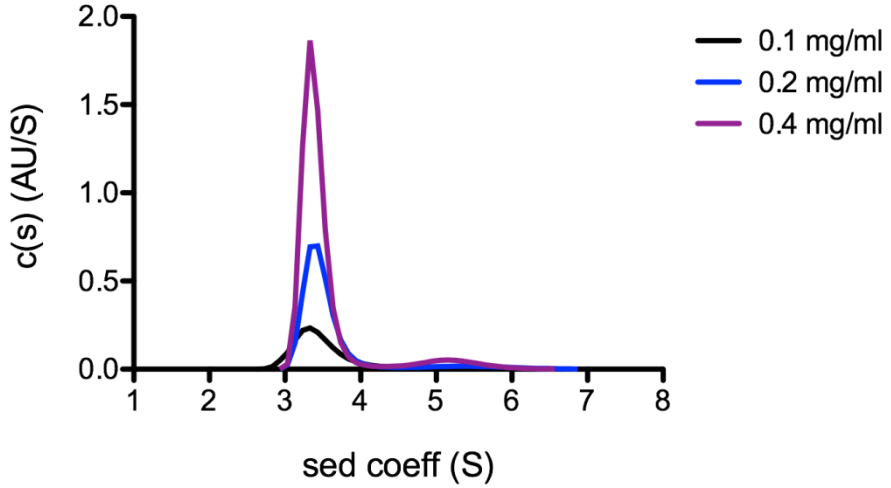

Single species at s=3.4
Appearance of a second species at s=5.1
Suggests fast and intermittent interactions

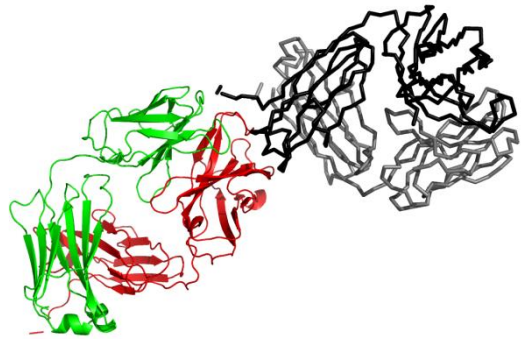

Minici, Gounari et al, unpublished, 2016

Anergic features in CLL

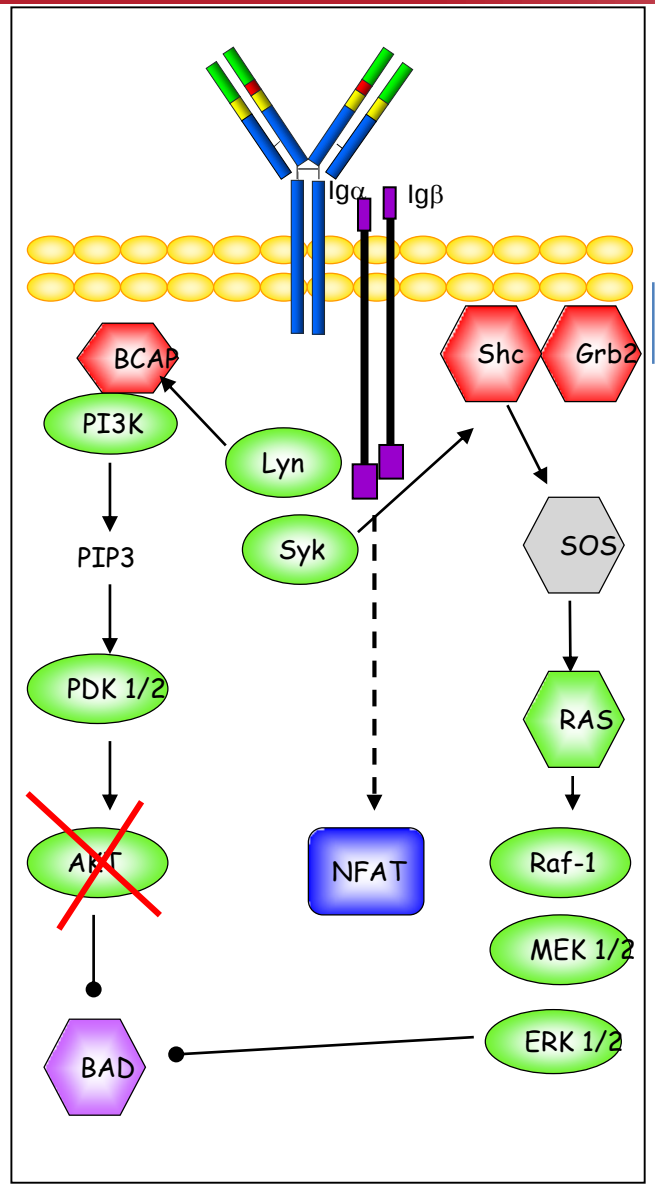

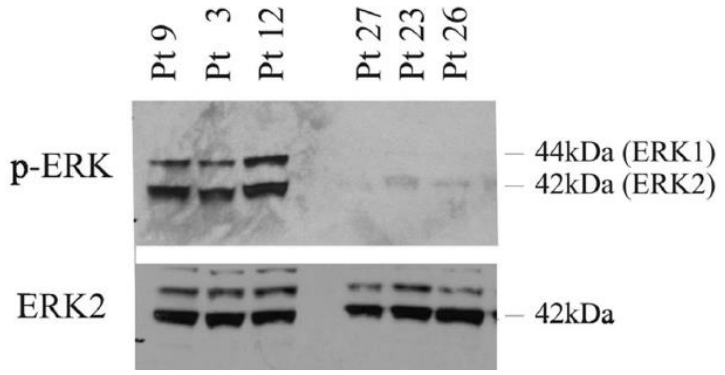

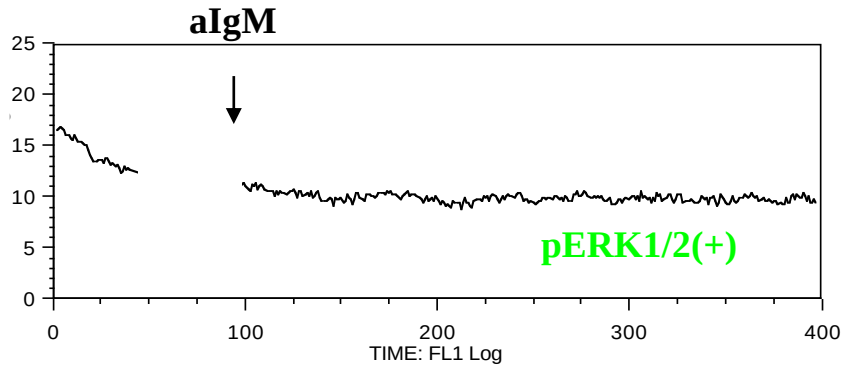

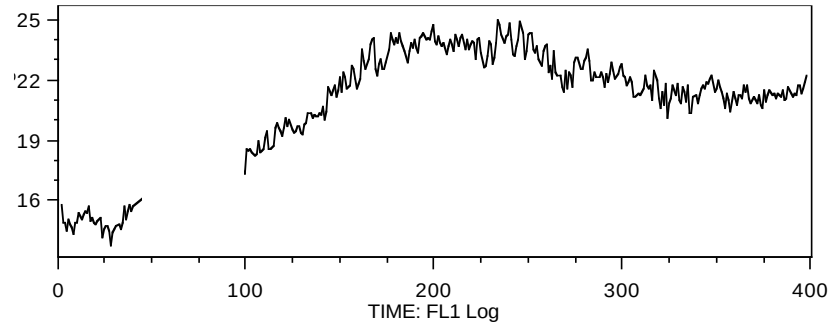

Muzio et al, Blood 2008, Apollonio et al, Blood 2013

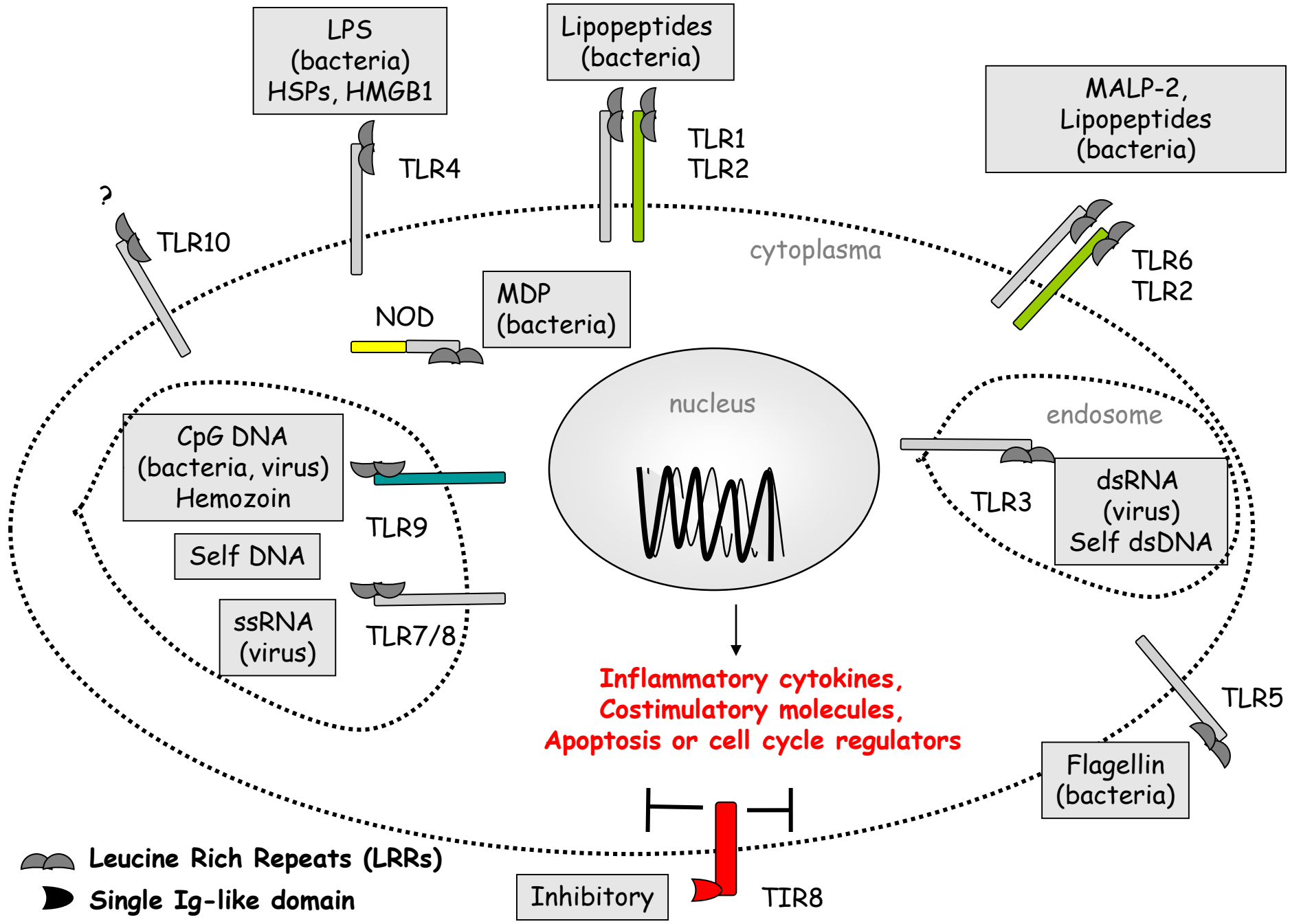
LPS
(bacteria)
HSPs, HMGB1
Lipopeptides
(bacteria)
MALP-2,
Lipopeptides
(bacteria)
TLR4
TLR1
TLR2
?
TLR10
cytoplasma
TLR6
TLR2
MDP
(bacteria)
NOD
nucleus
endosome
CpG DNA
(bacteria, virus)
Hemozoin
TLR9
Self DNA
TLR3
dsRNA
(virus)
Self dsDNA
ssRNA
(virus)
TLR7/8
Inflammatory cytokines,
Costimulatory molecules,
Apoptosis or cell cycle regulators
TLR5
Flagellin
(bacteria)
Leucine Rich Repeats (LRRs)
Single Ig-like domain
Inhibitory
TIR8

BcR is stimulated in LN-derived CLL cells

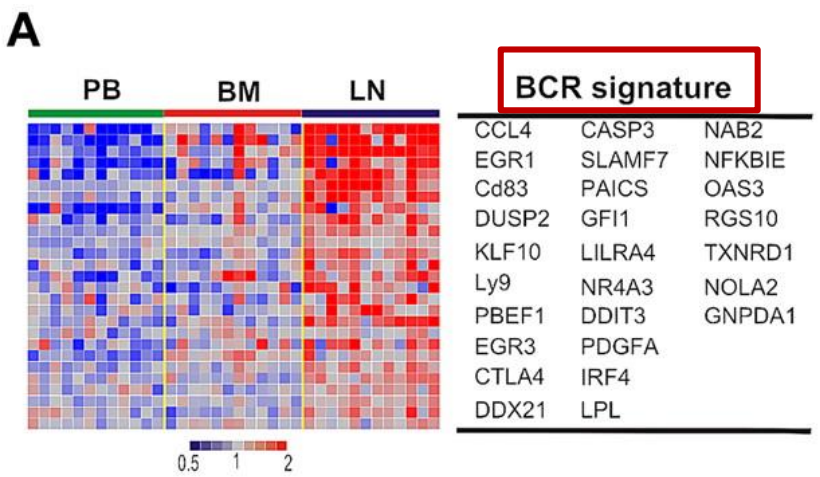

BCR signature

CCL4	CASP3	NAB2
EGR1	SLAMF7	NFKBIE
Cd83	PAICS	OAS3
DUSP2	GFI1	RGS10
KLF10	LILRA4	TXNRD1
Ly9	NR4A3	NOLA2
PBEF1	DDIT3	GNPDA1
EGR3	PDGFA	
CTLA4	IRF4	
DDX21	LPL	

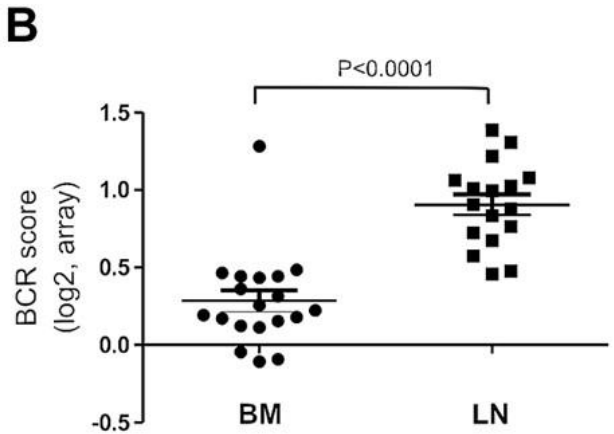

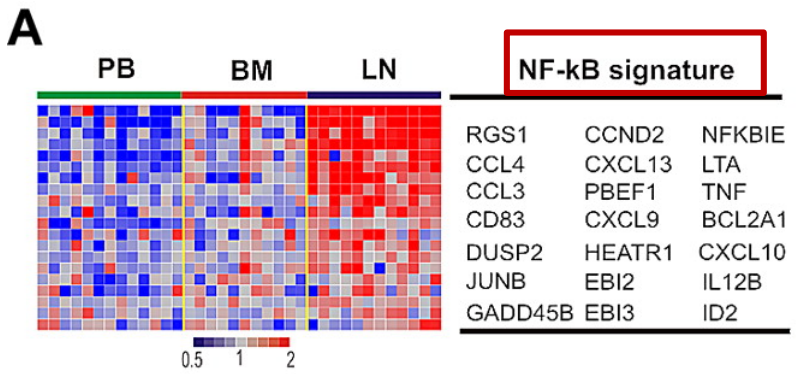

NF-kB signature

RGS1	CCND2	NFKBIE
CCL4	CXCL13	LTA
CCL3	PBEF1	TNF
CD83	CXCL9	BCL2A1
DUSP2	HEATR1	CXCL10
JUNB	EBI2	IL12B
GADD45B	EBI3	ID2

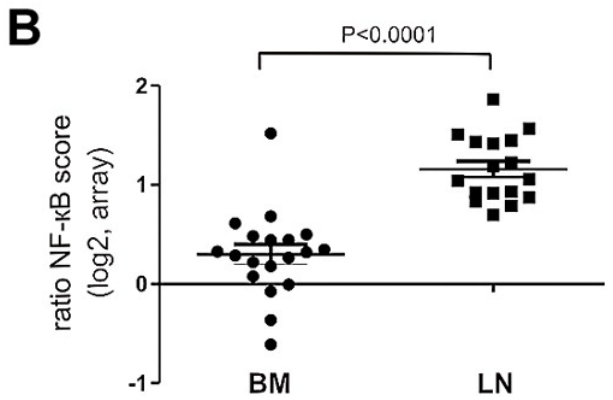

Herishanu Y et al. Blood 2011

Figure 1. CD23.CAR$^+$ T cells can be efficiently generated from samples obtained from CLL patients. (A) CD23.CAR expression in CLL-derived T cells (gray) and control not-transduced (NT) T cells (white). (B) Phenotype of NT (white bars), and CD23.CAR$^+$ (gray bars) T lymphocytes generated from CLL samples. T cells have been identified as described in the Methods. The data represent means (± SEM) from six different differentiations.

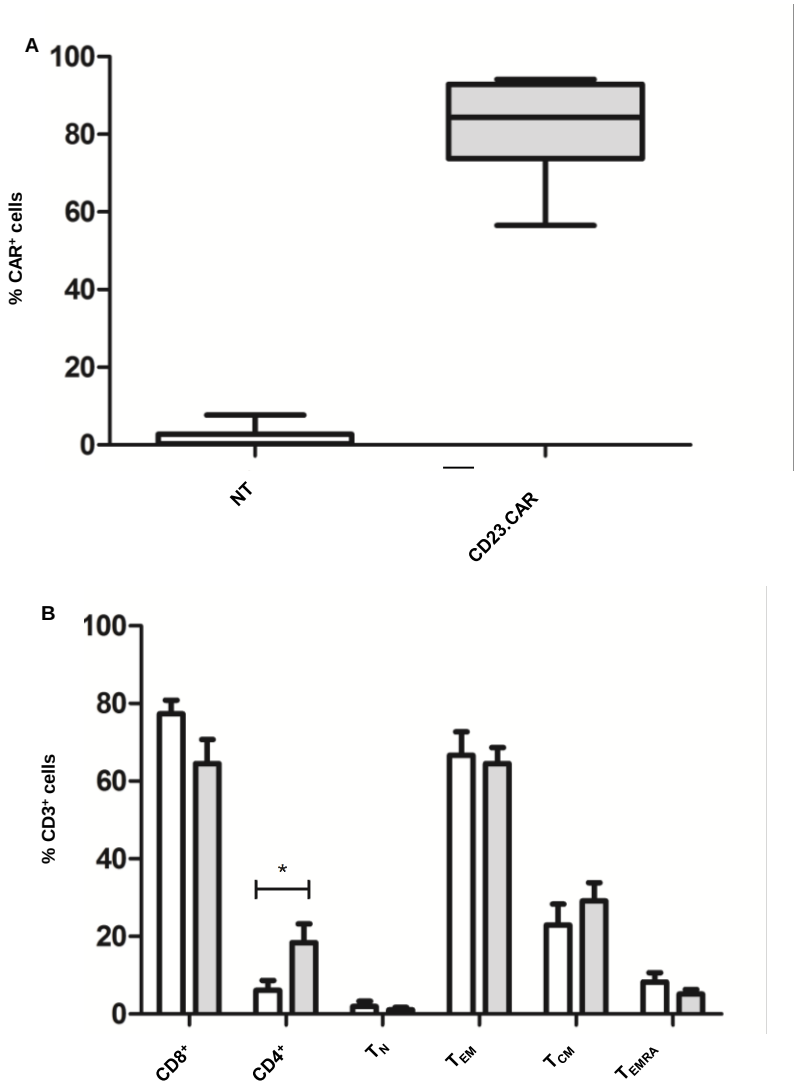

Figure 2. Lenalidomide improves IS formation and exerts a costimulatory effect on CD23.CAR$^+$ T cells against MEC1 cells. (A) For FACS-based synapse analysis, CellTracker PE-labeled MEC1 cells were cocultured with CellTracker FITC-labeled CD23.CAR$^+$ T cells (E:T ratio, 1:2) for 48 hours in presence or absence of lenalidomide. PE and FITC double-positive cells were quantified by flow cytometry (n=3, ***, p<0.001). (B) Gating strategy of PE/FITC double-positive cells in one representative experiment. (C-F) *In vitro* functional characterization of NT and CD23.CAR$^+$ T cells (untreated control or pretreated with lenalidomide) (n=4). The data represent means ± SEM, and unpaired *t*-test was used to compare NT and CD23.CAR$^+$ T cells. (C) Short-term cytotoxic assay, E:T ratio, 5:1. **p< 0.01 (D) Intracellular staining for Ki67 after 72h. E:T, 1:1. (E-F) Intracellular staining for IFN-γ and IL-2 after 5h. E:T, 1:3. The data represent means ± SEM, and unpaired *t*-test was used to compare NT and CD23.CAR$^+$ T cells.

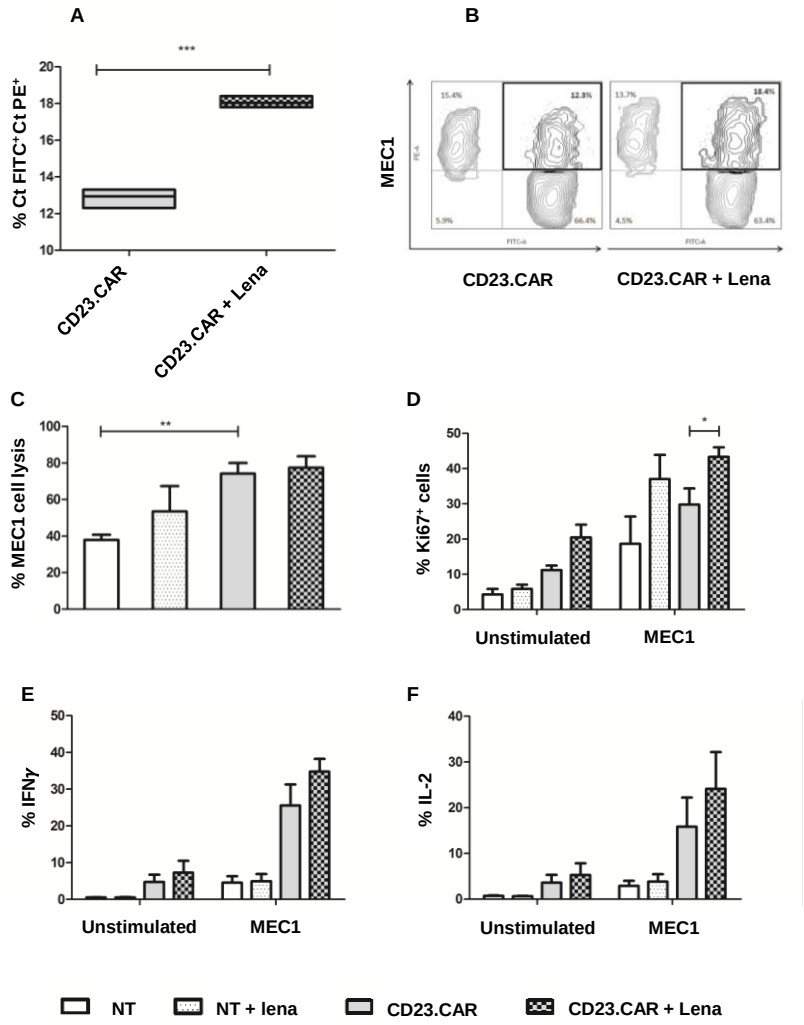

Figure 3

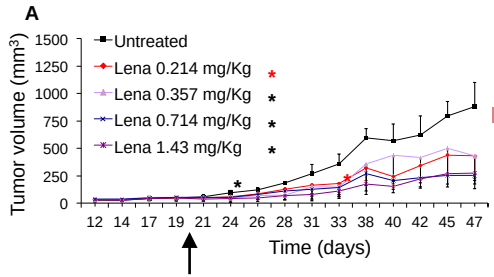

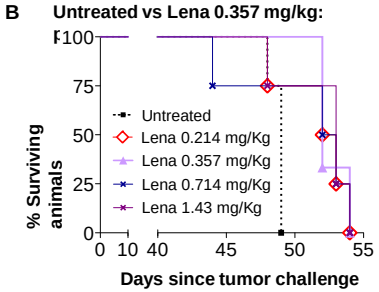

Figure 3. Anti-leukemic effect and survival benefit of lenalidomide in CLL xenotransplanted mice

(A) Tumor growth curves obtained in Rag2$^{-/-}\gamma_c^{-/-}$ female mice that received in the left flank a subcutaneous transplant of MEC1 cells (10 × 10^6). Twenty days later, when the tumors had reached a mean volume of 95 mm^3, lenalidomide was injected daily (arrow) following the dose schedule used in human clinical trials. Mice were randomly assigned to one of the following intraperitoneal treatments (4 mice/group): untreated (black squares), lenalidomide 15mg/day (0.214 mg/kg, red rhombi); lenalidomide 25mg/day (0.357mg/kg, violet triangles); lenalidomide 50mg/day (0.714 mg/kg, blue crosses); lenalidomide 100mg/day (1.43 mg/kg, purple stars). Each treatment was repeated daily from day 20 to day 47 and animals were monitored for tumor growth, by caliper measurements of perpendicular tumor diameters.

Animals were killed when the tumor volume reached 1000 mm^3. Measurements were stopped when 75% of originally treated mice were still surviving. *Statistically significant differences were calculated using the Student *t*-test: *P < 0.05. Black asterisk refers to Lena 0.357mg/kg, 0.714 mg/kg and 1.43 mg/kg compared to untreated control. Red asterisk refers to Lena 0.214 mg/Kg and untreated control comparison. Data are from one representative experiment of two.

(B) Kaplan-Meier survival curves for female Rag2$^{-/-}\gamma_c^{-/-}$ mice challenged subcutaneously in the left flank with MEC1 cells. Twenty days after MEC1 injections, mice bearing MEC1 tumors were randomly assigned to one of the following intraperitoneal treatments (4 mice/group): untreated (black squares), lenalidomide 0.214 mg/kg (red rhombi); lenalidomide 0.357mg/kg (violet triangles); lenalidomide 0.714 mg/kg (blue crosses); lenalidomide 1.43 mg/Kg (1.43 mg/kg, purple stars). Each treatment was repeated daily from day 20 to day 47. Tumor size was evaluated by caliper measurements of perpendicular tumor diameters. Animals were killed when the tumor volume reached 1000 mm^3. Data are from one representative experiment of two.

Figure 4

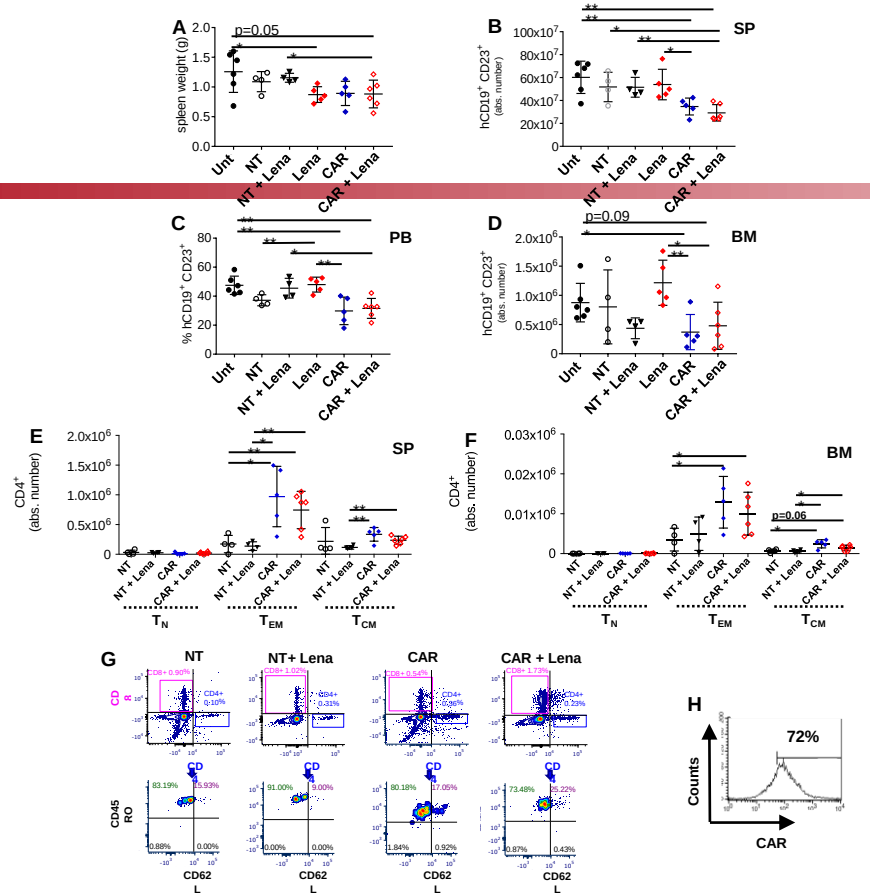

Figure 4. Lenalidomide improves the *in vivo* therapeutic efficacy of CD23.CAR$^+$ T lymphocytes from CLL patients.

(A-B-C-D-E-F-G) Rag2$^{-/-}\gamma_c^{-/-}$ mice transplanted i.v. with MEC1 cells on day 11 of the leukemic challenge were left untreated (Unt, black circles), injected with lenalidomide (Lena) as monotherapy (red rhombi), or adoptively transferred with NT T cells (empty circles), NT T cells with lenalidomide (black triangles), CD23.CAR$^+$ T cells (blue rhombi), CD23.CAR$^+$ T cells with lenalidomide (empty red rhombi). Mice received 0.214 mg/kg of intraperitoneal lenalidomide daily starting at day 8, except for the day of the adoptive transfer. NT and CD23.CAR$^+$ T lymphocytes were obtained from CLL donor #1. At day 23 after the transplantation, mice were evaluated by flow cytometry analysis for the presence of human CD19$^+$ CD23$^+$MEC1 cells in the lymphoid tissues. The graphs show: (A) spleen weight, (B) the mean value (± SD) of the relative contribution of hCD19$^+$ CD23$^+$cells (gated on CD19$^+$ cells) in SP, (C) the mean value (± SD) of the percentage of hCD19$^+$ CD23$^+$cells (gated on CD19$^+$ cells) in PB, (D) the mean value (± SD) of the relative contribution of hCD19$^+$ CD23$^+$cells (gated on CD19$^+$ cells) in BM, (E-F) the mean value (± SD) of the relative contributions of hCD4$^+$ T_N, T_{EM}, and T_{CM} in SP and BM, (G) Representative flow cytometry plots of human CD8$^+$ and CD4$^+$ T lymphocytes expressing CD45RO CD62L in the BM of mice adoptively transferred with NT or CD23.CAR$^+$ T cells (alone or in combination with lenalidomide) from CLL patient #1. *P < 0.05, **P < 0.01, Student's *t*-test .

(H) Expression of anti-CD23.CAR on the surface of T lymphocytes purified from the BM of xenotransplanted mice (day 30) treated with CD23.CAR$^+$ T cells in combination with lenalidomide (treatment schedule described in panel A) evaluated by flow cytometry with a Cy5-conjugated-anti-human-Fc antibody (CAR). NT and CD23.CAR$^+$ T lymphocytes were obtained from CLL donor #2.

Figure 5. Lenalidomide impacts immune cells of the microenvironment.
(A-B-C-D-E-F-G) Rag2$^{-/-}\gamma_c^{-/-}$ mice were transplanted with MEC1 cells and treated as described in Figure 4A-G. NT and CD23.CAR$^+$ T lymphocytes were obtained from CLL donor #1. At day 23 after the transplantation, murine neutrophils, monocytes and macrophages were evaluated by flow cytometry analysis in the PB and lymphoid tissues. The graphs show: (A) the mean value (± SD) of the relative contribution of CD11b$^+$ CSF1R$^-$ SSC^{high} neutrophils gated on CD45$^+$ in PB, (B) the mean value (± SD) of the absolute number of CD11b$^+$ CSF1R$^-$ SSC^{high} neutrophils gated on CD45$^+$ in SP, (C) the mean value (± SD) of the absolute number of CD11b$^+$ CSF1R$^-$ SSC^{high} IL-6$^+$ neutrophils gated on CD45$^+$ in SP, (D) the mean value (± SD) of the absolute number of CD11b$^+$ CSF1R$^+$ monocytes gated on CD45$^+$ in SP, (E) the mean value (± SD) of the absolute number of CD11b$^+$ CSF1R$^+$ IL-6$^+$ monocytes gated on CD45$^+$ in SP, (F) the mean value (± SD) of the absolute number of CD11b$^+$ F4/80$^+$ macrophages gated on CD45$^+$ in SP, (G) the mean value (± SD) of the absolute number of CD11b$^+$ F4/80$^+$ IL-6$^+$ macrophages gated on CD45$^+$ in SP. *P < 0.05, **P < 0.01, ***P < 0.001, Student's *t*-test.

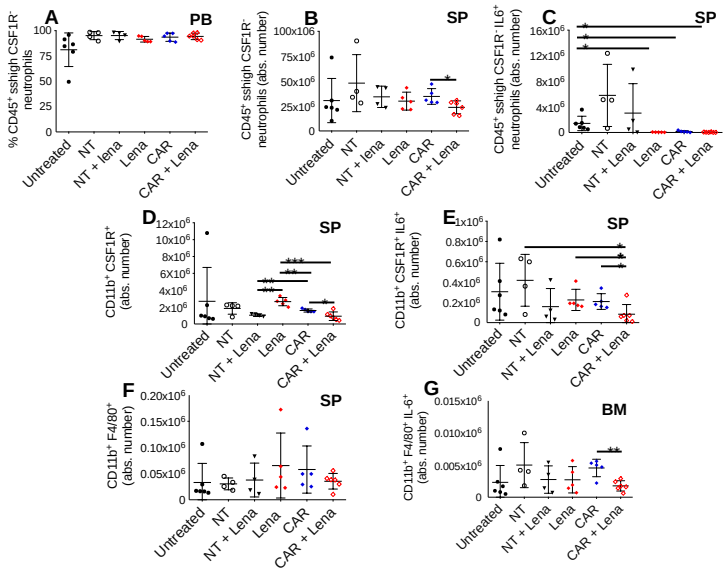

Figure 6. Combination therapy with lenalidomide and CD23.CAR T cells impacts the survival of CLL xenotransplanted mice.
(A) Expression of CD23.CAR on the surface of T lymphocytes derived from CLL patient #3 evaluated by flow cytometry with a Cy5-conjugated-anti-human-Fc antibody (CAR).
(B) Rag2$^{-/-}\gamma_c^{-/-}$ mice who received MEC1 cells intravenously on day 0 were left untreated (black circles) or given NT T lymphocytes (days 11 and 18) with rhIL-2 every other day, starting at day 12 (six administrations, empty rhombi); NT T lymphocytes (days 11 and 18) with daily lenalidomide from day 8 (black triangles); CD23.CAR$^+$ T lymphocytes (at days 11 and 18) with rhIL-2 every other day starting at day 12 (six administrations, full blue rhombi); or CD23.CAR$^+$ T lymphocytes (at days 11 and 18) with daily lenalidomide from day 8 (full red rhombi) and monitored for survival. NT and CD23.CAR$^+$ T lymphocytes were from CLL donor #3. mNT and mCAR refers to multiple adoptive transfer (days 11 and 18). Kaplan-Meier survival curve is represented; statistical analysis was performed using Log-Rank test and is indicated in Figure.

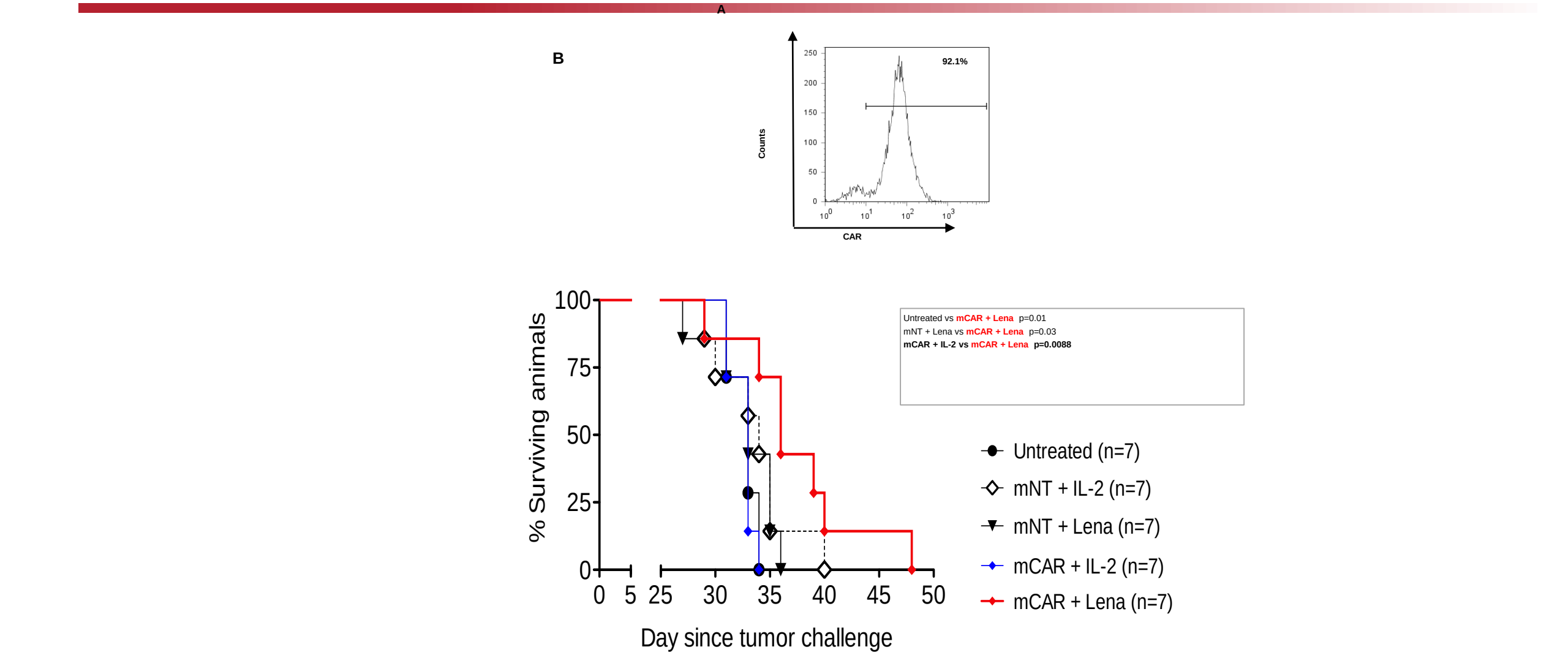

Figure 7. Lenalidomide elicits a tumor-specific cytotoxic activity of CD23.CAR⁺ T lymphocytes in CLL xenotransplanted mice.
(A) Expression of CD23.CAR on the surface of T lymphocytes derived from CLL patient #4 evaluated by flow cytometry with a Cy5-conjugated-anti-human-Fc antibody (CAR).
(B-C-D) Rag2$^{-/-}\gamma_c^{-/-}$ mice who received MEC1 cells intravenously (day 0) were left untreated (black circles) or adoptively transferred with NT T lymphocytes (day 11, white circles), NT T lymphocytes (day 11, black triangles) with daily lenalidomide starting at day 8, NT T lymphocytes (day 11) with rhIL-2 every other day starting at day 12 (six administrations, empty rhombi), CD23.CAR⁺ T lymphocytes (day 11) with rhIL-2 every other day starting at day 12 (six administrations, blue rhombi), CD23.CAR⁺ T lymphocytes (day 11) with daily lenalidomide starting at day 8 (red rhombi). NT and CD23.CAR⁺ T lymphocytes were obtained from CLL donor #4. (B) BM cells were flushed from mice femurs and tibiae; using MACS-microbeads for human CD3 positive selection NT and CD23.CAR⁺ T cells were isolated via magnetic separation. After 12h of *in vitro* culture without restimulation, NT (white bar) and CD23.CAR⁺ (black bar) T cell cytotoxic activity (from IL-2- and lenalidomide-treated mice, respectively) was evaluated against CD23⁺ MEC1 target, in a 4-hour assay at an E:T ratio of 3:1. The graphs show (C) the mean value (± SD) of the relative contribution of hCD19⁺ cells in BM, and (D) the mean value (± SD) of the relative contribution of hCD19⁺CD23⁺ cells in BM. *P < 0.05, **P < 0.01, Student's *t*-test.